Master of Science in Civil Engineering Theses   Department of Civil and Construction Engineering

Fall 11-16-2018

Laboratory Self-Weight Consolidation Testing of Dredged Material Analyzed Using a One-Dimensional Finite Strain Consolidation Method

Artine Azimi

Follow this and additional works at: https://digitalcommons.kennesaw.edu/msce_etd

Part of the Geotechnical Engineering Commons

Laboratory Self-Weight Consolidation Testing of Dredged Material Analyzed Using a One-Dimensional Finite Strain Consolidation Method

Artine Azimi

Bachelor of Science in Geology, Georgia State University

May 2013

A Thesis

Submitted in Partial Fulfillment of the Requirements for the Degree of

Master of Science in Civil Engineering (MSCE)

at the

Department of Civil and Construction Engineering

Southern Polytechnic College of Engineering and Engineering
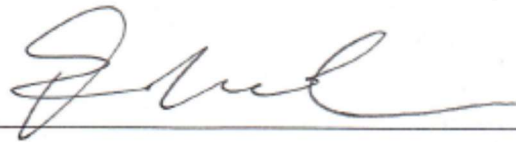
Technology

Kennesaw State University, Marietta Campus

December 2018

This thesis has been approved
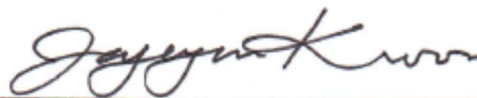
For the Department of Civil and Construction Engineering and the Graduate College by

_____

Dr. Fatih Oncul, Associate Professor, Department of Civil and Construction Engineering, Thesis Committee Chairperson

_____

Dr. M. A. Karim, Associate Professor, Department of Civil and Construction Engineering, Thesis Committee Chairperson

_____

Dr. Jayhyun Kwon, Associate Professor, Department of Civil and Construction Engineering, Thesis Committee Chairperson

Acknowledgment

First and foremost, I would like to thank my parents for their unconditional love and support throughout the years and my sister for her continued positivity and encouragement.

I would like to extend my deepest gratitude to Dr. Nader S. Rad for his guidance, patience and encouragement, this project would not have been possible without him. I would also like to thank Kenneth W. Cargill for all his assistance throughout the project and Moffatt & Nichol for allowing me to use their test samples for this research project.

I would like to express my appreciation to all my colleagues at Excel Geotechnical Testing for their assistance and support throughout the testing phase of this project. I would also like to thank all my previous professors at Georgia State University and Kennesaw State University for all the assistance and guidance throughout my academic journey. I would like to especially thank my Thesis advisor, Dr. Fatih Oncul, who always made time for me, his assistance has been paramount in this project.

I am very grateful to Dr. M. A. Karim and Dr. Jayhyun Kwon for effortlessly agreeing to serve on my thesis committee.

Lastly, I would like to acknowledge how thankful I am for all my friends and family. I am very fortunate to know such people.

This research project is dedicated to my parents, Nasrin and Safa Azimi, for their endless sacrifice, love, and support.

Artine Azimi

Abstract

Research has shown that the properties which govern the consolidation of dredged material are best determined using a one-dimensional finite strain consolidation theory. This method requires a complete relationship between void ratio and effective stress for all expected void ratios in a dredged layer, which can be determined from laboratory testing. The United States Army Corps of Engineers (USACE) suggests using a self-weight consolidation test apparatus to obtain void ratio/effective stress conditions for very low effective stresses. In this paper a modified laboratory testing method of a self-weight consolidation test is developed to obtain a range of void ratios and effective stress conditions at low effective stresses for material obtained from the Savannah River Harbor. Testing methods are discussed and data is analyzed using a selected one-dimensional finite strain consolidation method. Findings from the research conducted in this paper are as follows: a reliable relationship between vertical effective stress and permeability as function of void ratio can be obtained from the test methods described; there appears to be a unique void ratio/effective stress relationship and a unique void ratio/permeability relationship for the material tested; a three to four-month period is a satisfactory amount of time to obtain near 100 percent primary consolidation for materials with initial void ratios of 7.0 to 10.0; and test methods are repeatable and can produce homogeneous samples.

Table of Contents

Acronyms

ASTM - American Society for Testing and Materials

DMCA - Dredged Material Containment Area

LSCRS - Large Strain Controlled Rate of Strain

SHEP - Savannah Harbor Expansion Project

USACE - United States Army Corps of Engineers

USCS - Unified Soil Classification System

WES - Waterways Experiment Station

Table of Figures

List of Tables

1. Introduction

1.1 Problem Statement

As sediment accumulates in a riverbed, the overall depth is reduced. For sustained use of harbors and waterways by ships and other large vessels, periodic dredging must be performed. Large volumes of soft fine-grained sediment are hydraulically dredged from the bottom of rivers then transported and stored in Dredged Material Containment Areas (DMCAs). These confined disposal sites are engineered to provide required storage volumes over long periods of time, however, as disposal sites become less available with use, a central issue becomes how to design efficient and suitable containment areas for dredged material.

When material is initially placed in a containment area, it acts as uniform slurry and assumes a volume throughout the disposal area. With time the volume of dredged material decreases through means of settling of solids, pore water being expelled from soil matrix and decanting/desiccation. This decrease in volume allows potential for further storage of newly dredged sediment. Freshly dredged slurry initially exhibits settlement where the particle weight is supported by hydrodynamic forces only (Lin, 1983). As settlement progresses, particles begin to form a lattice type structure where the newly formed slurry can be described by traditional soil parameters. In this soil matrix, effective stresses develop, and the soil consolidates under its own weight. As consolidation occurs water is squeezed from the pores and the soil particles reorder themselves in a denser arrangement, thus decreasing the volume of the initial slurry. The

comparatively large void ratios exhibited by the soils allow for the development of large strains, sometimes greater than 50% (Stark et al., 2005). In the past geotechnical engineers have borrowed concepts developed in other disciplines to address the sedimentation phase of the settling slurry. Pioneering studies however, did not consider the phenomenon of self-weight consolidation of the soil structure.

The theory of one-dimensional consolidation has been well established in geotechnical engineering and is most commonly referred to as "Small Strain Theory", since expected strains are assumed to be infinite and small in magnitude. The application of traditional consolidation theory has proven to be too restrictive for predicting consolidation behavior of highly saturated soils that undergo large strains. Conventional theories of one-dimensional consolidation tend to under estimate the ultimate settlement and the time rate of consolidation (Cargill, 1983). For geotechnical engineers to properly predict the long-term consolidation behavior of dredged material, more general theories of consolidation must be considered. In this research project a one-dimensional finite strain consolidation theory originally developed by Gibson et al. (1967 & 1981) is used to analyze the consolidation behavior of soils that experience large strains when no external load is applied, and gravity is the only driving force that induces settlement.

The United States Army Corps of Engineers (USACE) outlines testing procedures for self-weight consolidation testing of soft, fine-grained dredged material. The primary purpose of the self-weight consolidation test is to measure void ratios at very low effective stresses, generally less than 10 psf (Cargill, 1983). When used in conjunction with oedometer testing, a wide range of void ratio/effective stress conditions can be established for a soil layer at different

void ratios. In this paper a modified test method based on the USACE method is developed and used in the testing of dredged slurry at various initial void ratios. Test results from self-weight tests, at different initial void ratios, provides a range of void ratio/effective stress conditions for low effective stresses. This paper presents the results of these tests, which are analyzed using a finite strain method as outlined by the USACE.

1.2 Significance of Research

The research goal of this paper is to provide guidelines for a simplified version of a self-weight consolidation test originally outlined by the USACE. Test samples were created at various initial void ratios, representative of newly dredged slurry, to obtain relationships between void ratio and effective stresses at effective stresses less than 10 psf. Void ratio/effective stress profiles are difficult to obtain at low effective stresses, the research presented in this paper intends to introduce a modified laboratory testing method for determining the physical and hydraulic properties of dredged slurries at low effective stresses.

Data obtained from self-weight consolidation testing can be combined with other laboratory tests (i.e. oedometer and/or Large Strain Controlled Rate of Strain Test (LSCRS)) to estimate a wide range of void ratio/effective stress conditions in a dredged fill layer. Using laboratory data from each of these tests, an estimated curve can be established. Figure 1.1 shows a mock curve (created for illustrative purposes only) with circles illustrating the laboratory tests that can be performed to obtain each range of void ratio/effective stress conditions. This paper

3

will focus on void ratio/effective stress relationships, for the lowest ends of effective stresses, obtained using self-weight consolidation tests.

If void ratios can properly be estimated for a given effective stress, over a wide range of effective stresses using a curve like the one shown in figure 1.1, the overall settlement and the time rate of the settlement of a layer of dredged material that is deposited in a DMCA can be estimated. Test results in this paper were analyzed using a finite strain method outlined by the USACE. Results can aid in predicting the consolidation behavior of dredged material from the Savannah River Harbor, which is in the process of undergoing a large dredging operation.
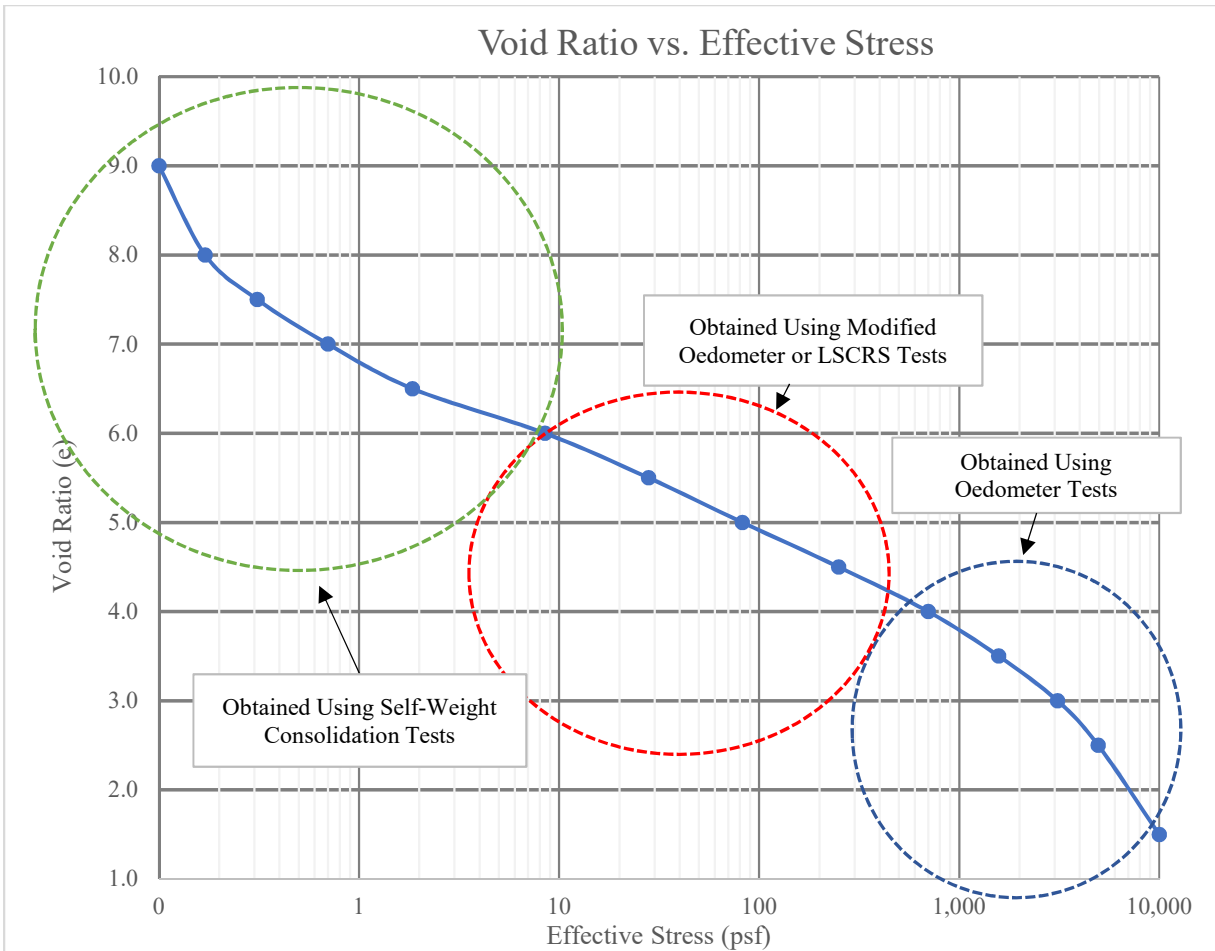
Figure 1.1: Mock Version of a Void Ratio/Effective Stress Curve Over a Full Range of Void Ratios Expected in a Dredged Fill Layer

1.3 Research Objectives

The primary objectives of this research project are as follows:

1. Develop self-weight consolidation equipment and test procedures.

2. Study the relationship between effective stress and the permeability as a function of void ratio and time for dredged material collected from the Savannah Harbor.

3. Use an available one-dimensional finite strain consolidation theory to analyze the test

   results

2. Background & Literature Review

2.1 Background

2.1.1   Dredging Operations in the United States

Navigable waterways and channels are maintained through dredging. Dredging is a process in which sediments are removed from the bottom of streams, rivers, lakes, and coastal waters; transported via ship, barge, or pipeline; and discharged to land or water (USACE, 1987). Dredging of inland and coastal waterways is crucial as they are a major means of commercial transportation. In the United Sates only a few of the ports, harbors, and waterways are naturally deep, without dredging, many navigable channels and waterways would be impassable to waterborne cargo and passenger ships (USACE, 2015).   The U.S. Army Corps of Engineers reported that from 2008 to 2012 the average annual quantity of material removed was approximately 212 million yd^3 (USACE, 2015). Material removed from dredging operations can be disposed of in several ways. A majority of dredged material is placed in aquatic disposal sites, and the remaining material is placed in near shore confined disposal facilities or near shore waters to create wetlands.

2.1.2 Dredged Material Containment Areas

In order to properly asses the storage capacity of disposal sites, engineers must be able to predict the long-term behavior of the material being dredged. Prior to 1970, containment facilities were sized using bulking factors of 1 to 2 to estimate the required volume of the facility; the assumption was that the excavated material will occupy more space in a fill than in-situ because of the mechanical disturbance of the dredging process and the removal of overburden pressure (Lin, 1983). This method proved to be unreliable and too dependent on the specific site characteristics, leading to storage capacity of facilities being significantly over or underestimated. The need for a more scientific approach led the U.S. Army Corps of Engineers to fund several research initiatives through its Waterways Experiment Station (WES). The work done by the WES contributed heavily to the current design and maintenance of DMCAs.

In the case of above land disposal, dredged material is usually placed in confined disposal sites that are engineered to provide required storage volume and to meet required effluent solids standards. Confined containment areas, sometimes referred to as diked containment areas, are designed such that they can retain dredged material being placed while simultaneously allowing the carrier water to be released. Storage capacity of a containment area is defined as the total volume available to hold dredged material and is equal to the total unoccupied volume minus the volume associated with ponding and freeboard requirements and since this material assumes its final configuration essentially as soon as it is deposited, there is a direct relationship between its volume before and after dredging (Cargill, 1983). The two main objectives for an ideal DMCA are to provide required storage capacity to meet dredging requirements and to attain the highest

possible efficiency in retaining solids during the dredging operation in order to meet effluent suspended solids requirements. These considerations are basically interrelated and depend upon effective design, operation, and management of the containment area (USACE, 1987).

Figure 2.1 provides a schematic representation of the typical components of a diked containment area. The hydraulically dredged mud is rapidly pumped into a confined surface area, where coarse material such as sand, clay clots, and/or gravel quickly settle at the inlet and form a mound, while the fine grain sediment assumes the remaining volume. A pond of water is maintained over the fine-grained section during disposal to facilitate sedimentation and promote a more uniform slurry distribution.
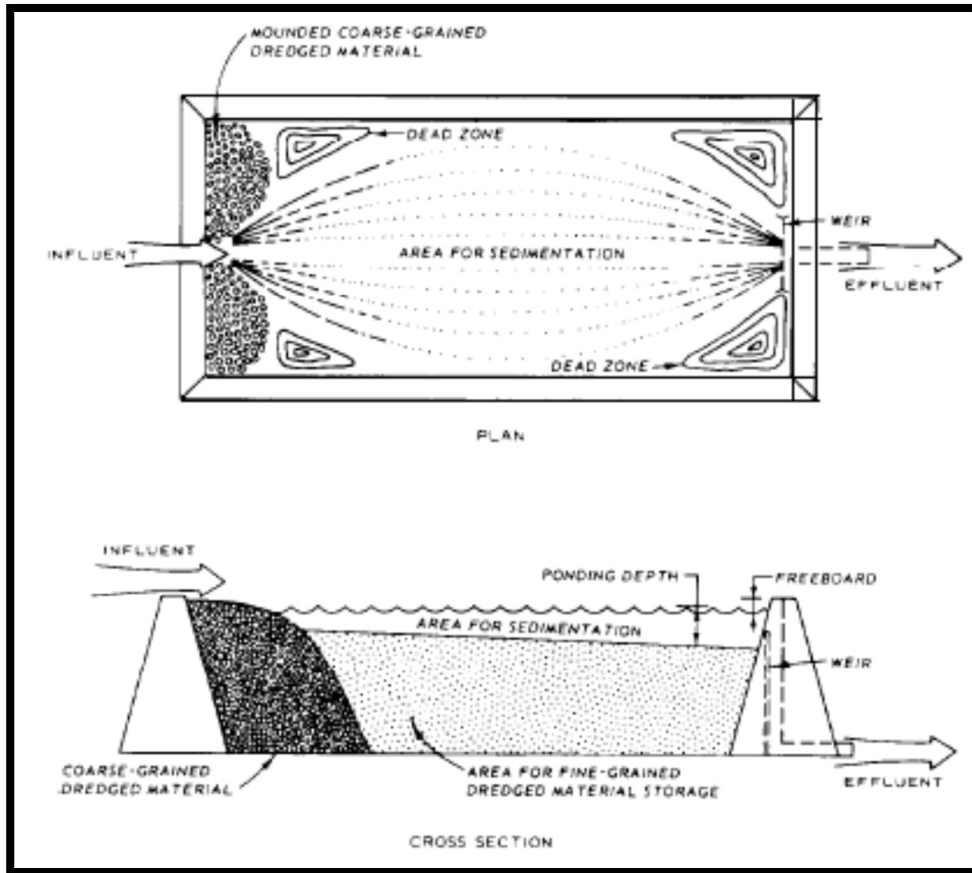
Figure 2.1: Diked containment area schematic (USACE, 1987)

2.1.3   Stages of Settlement During Disposal

Settling of solids dominates the initial sedimentation process in a freshly dredged material. Using criteria developed by Coe and Clevenger (1916) researchers at the WES defined four settling processes which would potentially be seen in a dredged slurry suspension over time. The type of settling is a function of the type of particles present and the concentration of particles at a given time. Thackston et al. (1988) describes the four types as follows:

I. <u>Discrete Settling</u> - The particles do not interact during settling. Each particle maintains its individuality and does not change in size, shape, or density while settling. Each particle settles as if it were alone and isolated.

II. <u>Flocculent Settling</u> - The particles flocculate and agglomerate during settling. As the particles grow in size, they decrease in density because of entrained water, but they usually settle faster.

III. <u>Zone Settling</u> - The concentration of particles is so great that they touch adjacent particles in all directions and maintain their spatial relationship, settling as a mass or open matrix. They usually exhibit a definite interface between the settling particles and the clarified liquid above. The particle matrix settles more slowly than the individual particles of the same size and density because the quantity of water being displaced by the settling particles is so great that the resulting upward velocities of the displaced water reduce the effective downward velocity of the particle mass.

IV. <u>Compression Settling</u> - The concentration is so great that the particles rest on each other and mechanically support each other. The weight of the particles above slowly compresses the lower layers, increasing the pore pressure and squeezing out the water. This is also sometimes called thickening. In treatment plants, the settling is sometimes aided by slow stirring to break up the bridging action of the particles.

2.1.4 Consolidation of Dredged Material

When a slurry mass enters the zone settling and compression settling phases described in the previous section, it can essentially to be treated as a consolidating mass. While sedimentation of solid particles has been studied in other disciplines such as mining and metallurgic engineering, chemical engineering and sanitary engineering, these studies exclusively considered the particle weight being supported by hydrodynamic forces and do not consider forces from effective stress. As settling particles come into contact to form a three-dimensional, interconnected lattice, effective stresses are developed, and sedimentation models fail (Lin, 1983). Once settling of particles is complete, the soil becomes a homogenous mass and forms an interface where the water is being expelled from the top of the slurry. The buoyant weights of the solid particles create effective stresses and the soil begins to consolidate under its own weight. Consolidation of the layers continues for long periods following disposal, causing a decrease in the volume occupied by the layers and a corresponding increase in storage capacity for future disposal. As a result, a need to analyze the consolidation behavior of the soil becomes apparent.

2.1.5 Finite Strain Consolidation Theory

The traditional one-dimensional theory of consolidation, commonly referred to as "Small Strain Theory", is the most common and accepted method among engineers when predicting consolidation behavior of soil layers. Small strain theory assumes infinitesimal strains, constant soil parameters and liner stress-strain relationships. These assumptions have proven to be unsuitable for very soft, fine-grained material that exhibits large strains. Using a more general

theoretical basis developed by Gibson et al. (1967; 1981), Cargill (1982; 1983; 1986) published

comprehensive technical reports for the U.S. Army Corps of Engineers applying the theory to the

real-world testing and analysis of soft, fine-grained materials that exhibit large strains. These

methods are still used today.

2.1.6 *Laboratory Self-Weight Consolidation Testing of Dredged Material*

When predicting consolidation properties of dredged material, a fundamental requirement

is having an accurate void ratio/effective stress relationship for a very wide range of effective

stresses that are expected in the fill layer. The larger effective stresses can be simulated with

traditional oedometer tests, while the lower values of effective stresses must be found using a

self-weight consolidation test. Cargill (1986) suggests using a special settlement apparatus to

perform self-weight consolidation testing. The relatively complex Plexiglas apparatus suggested

and endorsed by the USACE is composed of several inner rings, which can be removed to

sample slurry layers, and one large outer ring holding the inner rings in place. A modified,

simplified version of this self-weight consolidation test is developed, the results, which are

analyzed using finite strain methods, are reported and discussed in this paper.

2.2 Literature Review

2.2.1 Dredged Material Containment Area Design History

Prior to the 1970s, the volume of dredged material that would occupy a containment facility was estimated largely by rule of thumb. Depending on the type of sediment being dredged, a bulking factor was multiplied by the volume of sediment to predict the volume that the sediment would occupy. Later a settlement factor was combined with the bulking factor to account for shrinkage of dredged material due to long term settlement (Lin, 1983). These methods were strictly empirical. Lacasse et al. (1977) improved the bulking factor sizing method that was being used at the time by accounting for sediment properties, dredged material behavior once it was placed, and the components of the dredging operations that may affect dredged sediment volume. More sophisticated methods were initially reported by Montgomery (1978), who provided the first major research into the settling properties of suspensions having solids concentrations in the range of dredged material slurries. Montgomery (1978) detailed column settling test procedures to obtain settlement properties of dredged materials. However, the report solely considered particle settlement and solids concentration in design considerations and depended on sedimentation theories for analysis. Guidelines for predicting the settlement of the slurry layers once they have entered the consolidation phase were not present. Bartos (1977) conducted comprehensive research into the engineering properties of dredged material. The index properties, compaction properties, shear strength, and compressibility were all analyzed. The study concluded that dewatered dredged material, typical of material formed once the sedimentation phase in a newly dredged slurry layer is completed, is a soil and can be analyzed

14

as a soil (Bartos, 1977). Cargill (1983) mentions that the design of confined disposal areas for fine-grained dredged material during and immediately after a single disposal operation is a relatively simple and straightforward exercise utilizing the results of column sedimentation tests as described in Montgomery (1978) and Palermo et al. (1978), however these reports did not adequately provide a method of predicting long-term behavior due to consolidation. Although, Palermo et al. (1978) did recognized that the proper design of areas where several disposal operations occur intermittently over a period of years requires consideration of the settlement due to the self-weight consolidation of the newly placed dredged material and due to the consolidation compression of foundation soils. However, the authors suggested using classical theories of consolidation when considering long-term consolidation behavior of a slurry layer when it enters the consolidation phase, after the sedimentation phase is complete. Cargill (1982) suggested that dredged material that has entered the consolidation phase, be analyzed using a finite strain theory of consolidation, where soil properties are non-constant. The following sections will review the literature as it pertains to a specific one-dimensional finite strain theory of consolidation, which is used by the USACE when analyzing consolidation properties of dredged material.

2.2.2   *One Dimensional Finite Strain Consolidation Theory*

2.2.2.1 Derivation of Finite Strain Consolidation Theory

The governing equation for small strain consolidation theory is based on the continuity of fluid flow in a differential soil element, Darcy's law, a linear stress-strain relationship for the soil

matrix, and the effective stress equation (Cargill, 1983). Mikasa (1965) was among the first to recognize the need for a more general equation of consolidation, for highly saturated clays that exhibit large strains, while performing a field consolidation test at a reclaimed site in the Harbor of Osaka in the spring of 1960. The purpose of the project was to consolidate and stabilize soft dredged fill clay by draining from an overlying sand mat. Using consolidation data obtained from soft fill clay in the Osaka port, Mikasa (1965) concluded that the assumptions associated with the traditional theory of one-dimensional consolidation, which include constant permeability and compressibility throughout the soil layer during the consolidation process, were too restrictive and that soil permeability and compressibility were variable. He discovered that if the permeability k and compressibility a_v vary proportionally, their relationship to the strain ε in the soil layer follows the equation

$$\frac{\partial \varepsilon}{\partial t} = c_v \frac{\partial^2 \varepsilon}{\partial z^2} \tag{2.1}$$

where z is coordinate position and the coefficient of consolidation c_v remains constant and is

$$c_v = \frac{k}{a_v \gamma_w} \tag{2.2}$$

where γ_w is the unit weight of water. An equation which accounts for self-weight of the clay in a non-stationary state is given by Mikasa (1965) to be

$$\frac{\partial C}{\partial t} = c_v C^2 \left\{ \frac{\partial^2 C}{\partial z_o^2} - \frac{d}{dC}(m_v \gamma') \frac{\partial C}{\partial z_0} \right\} \tag{2.3}$$

where C' is the consolidation ratio, which is equal to ($1+e_o/1+e$) where e_o is the initial void ratio and e is the final void ratio, m_v is the coefficient of volume change, and γ' is the effective unit weight of the clay material. When observed settlement rates from the field were compared against theoretical settlement rates using calculated values, traditional calculation methods under estimated the rate of settlement, while values obtained using equation 2.3 gave satisfactory results. Mikasa (1965) also observed a non-linear distribution of the effective stress and the pore water pressure, caused by the reduced permeability in the lower part of the clay layer due to consolidation. Results of this study were deemed acceptable for the particular project, but the research was done on a very specific area and was performed against a time schedule. More research was needed to adequately conclude the observations made.

Gibson et al. (1967) developed a governing equation for the consolidation behavior of soft, fine-grained saturated clays. In his theory it is assumed that Darcy's law is valid, however it is modified to a form where it is the relative velocity of the soil skeleton and the pore fluid that is related to the excess pore fluid pressure gradient (Gibson et al., 1967). The theoretical basis developed by Gibson et al. (1967) for soft, fine-grained soils that exhibit large strains will hereafter be referred to as one-dimensional finite strain consolidation theory. The basic assumptions necessary for the development of one dimensional finite strain consolidation theory are: the material is homogenous, the soil system is fully saturated and consists of a compressible soil matrix where the fluids and individual solid particles are incompressible, pore fluid velocities are small and governed by Darcy's law, there is a unique relationship between the permeability and the void ratio, and there is a unique relationship between the vertical effective

stress and the void ratio. Additionally, the usual assumption made in small strain theory restricting the magnitude of the strain is not made for finite strain theory (Cargill, 1982). The principals and equations behind the finite strain consolidation theory will be derived in the following sections.

2.2.2.2 Selection of a Proper Coordinate System

A prerequisite for analysis of a differential soil element requires selecting an appropriate material coordinate system. When considering the consolidation behavior of soil masses that exhibit large strains, a Lagrangian coordinate system is most convenient. The Eulerian coordinate system, which is most common in geotechnical engineering applications, stands at a disadvantage since the boundaries remain constant in space while soil particles and pore fluid flow through. In a Lagrangian coordinate system the boundaries constantly encapsulate the same solid particles, allowing for moving boundary conditions. In conventional theory, where strains are small, making a distinction between these two types of coordinate systems may be unnecessary, but in cases where large strains are expected this distinction becomes important (Gibson et al., 1967). Figure 2.2a shows a soil skeleton at $t = 0$ with the space coordinate a that describes a plane of particles original distance from the datum. The upper boundary of the layer remains as $a = a_o$ and the datum plane remains constant at $a = 0$. A soil element (A_o, B_o, C_o, D_o) is defined by its position in space with respect to a. Additionally, δ_a describes the thickness of the soil element, making the coordinates of the top and bottom layers of the soil element $(a+\delta_a)$ and a, respectively. When $t \neq 0$ a new coordinate ε is defined, which is referred to as the convective coordinate, figure 2.2b. Convective coordinates are a function of the Lagrangian

coordinates and time. Expressing the dependent variables in terms of ε and t is inconvenient since ε in and of itself is a function of t. Therefore, expressing the variables in terms of a and t simplifies the mathematics of finite strain consolidation theory (Gibson et al., 1967). Time dependent events can be described using either Lagrangian coordinates (a, t) or convective coordinates (ε, t), where the Lagrangian coordinate system refers all events back to t = 0.
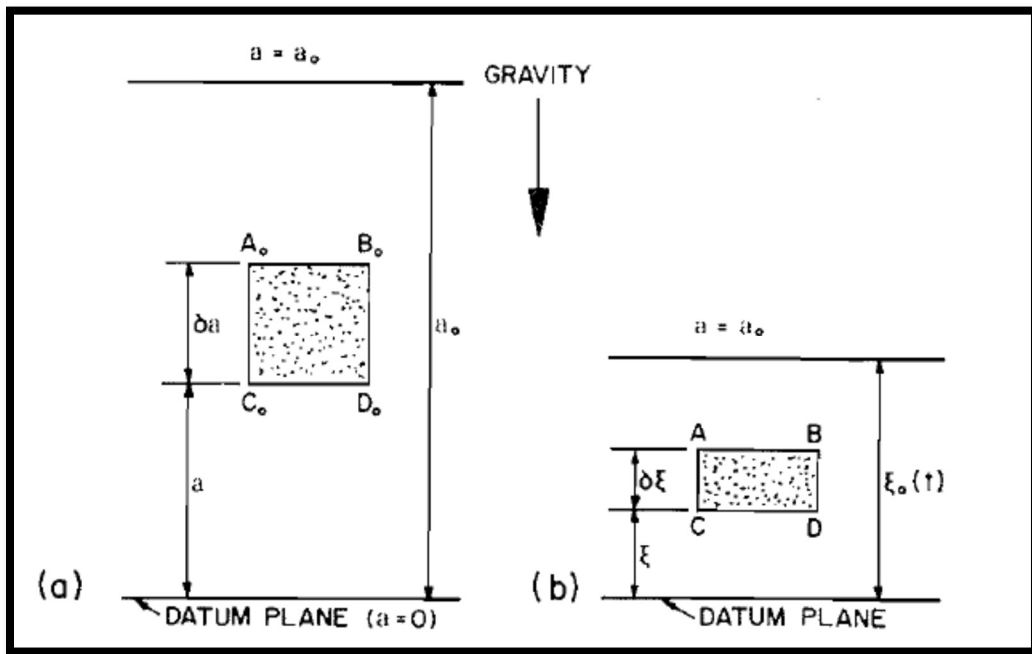
Figure 2.2: (a) Lagrangian coordinates at t=0. (b) Convective coordinates at t ≠ 0. (Gibson et al., 1981).

19

2.2.2.3 Equations of Continuity and Equilibrium

The new position (A, B, C, D), figure 2.2b, must satisfy the following equation of equilibrium to maintain vertical equilibrium of solids and fluids in the soil skeleton

$$\frac{\partial \sigma}{\partial a} \pm \left(n\gamma_f + (1-n)\,\gamma_s \right)\frac{\partial \varepsilon}{\partial a} = 0 \qquad (2.4)$$

where n is the porosity, σ is the total vertical stress, and the unit weight of the fluid and solids is γ_f and γ_s, respectively. Since the soil skeleton is a closed system, equations of continuity of solids and fluids must be satisfied. Given that the Lagrangian coordinates allow boundary conditions to constantly encapsulate the same solids particles (Gibson et al., 1967), the equation for solid continuity becomes

$$\gamma_s(a,0)[1 - n\gamma_s] = \gamma_s(1-n)\frac{\partial \varepsilon}{\partial a} \qquad (2.5)$$

Equation 2.5 shows that the initial concentration of solids must be equal to the concentration of solids at any location of ε in the soil element (A, B, C, D). Since fluid flow in the soil element is governed by Darcy's Law, the rate of fluid inflow and fluid outflow must be considered. Equation 2.6 shows the rate of weight inflow of the element (Gibson et al., 1967). The equation accounts for both velocity of fluids, v_f, and the velocity of solids, v_s.

$$\text{Rate of Weight Inflow} = n(v_f - v_s)\gamma_f \qquad (2.6)$$

The rate of fluid flowing out of the element is a modified version of equation 2.6, where it becomes a differential equation that considers element thickness, δ_a, making the rate of weight outflow according to Gibson et al. (1967)

$$\text{Rate of Weight Outflow} = \frac{\partial}{\partial a}[n\gamma_s(v_f - v_s)]\delta_a \tag{2.7}$$

For the fluid in the element to maintain equilibrium, the rate of fluid change in the element must equal the outflow, such that

$$\frac{\partial}{\partial a}[n\gamma_s(v_f - v_s)] + \frac{\partial}{\partial t}\left[n\gamma_f\frac{\partial\varepsilon}{\partial a}\right] = 0 \tag{2.8}$$

Finally, a generalized version of Darcy's Law can be used when describing the movement of pore fluid in the element (Gibson et al., 1967)

$$n(v_f - v_s) = -\frac{k}{\gamma_f}\frac{\partial u}{\partial\varepsilon} \tag{2.9}$$

where k is the hydraulic conductivity of the soil element and u is the excess pore pressure. The excess pore pressure gradient is expressed as

$$\frac{\partial u}{\partial\varepsilon} = \frac{\partial p}{\partial\varepsilon} \pm \gamma_f \tag{2.10}$$

where p is fluid pressure.

2.2.2.4 Reduced Material Coordinates

Since Lagrangian and convective coordinates are both measurements of the soil system, including solid particles and pore fluid (Stark et al., 2005), it becomes useful to define material coordinates in terms of the volume of solids between a given point and the datum plane. This coordinate is referred to as z, which, like a, is independent of time and is expressed as

$$z(a) = \int_0^a [1 - n(a',0)]da' \qquad (2.11)$$

Instead of porosity n, equations using the material coordinate z are worked in terms of void ratio e, where

$$e = \frac{n}{1-n} \qquad (2.12)$$

Gibson et al. (1981) gives the reduced coordinate relationship as

$$z(a) = \int_0^a \frac{da'}{1+e(a',0)} \qquad (2.13a)$$

or

$$\frac{dz}{da} = \frac{1}{(1+e_0)} \qquad (2.13b)$$

where e_0 is the void ratio at t = 0. Using the reduced coordinates derived above, where values of porosity n and coordinate a are replaced with void ratio e and coordinate z, respectively, equations 2.4, 2.8, 2.9, and 2.10 respectively become

$$\frac{\partial \sigma}{\partial z} \pm (e\gamma_f + \gamma_s) = 0 \tag{2.14}$$

$$\frac{\partial}{\partial z}\left[\frac{e(v_f - v_s)}{1+e}\right] + \frac{\partial}{\partial t} = 0 \tag{2.15}$$

$$\frac{e(vf-vs)}{k} \pm (1+e) + \frac{1}{\gamma f}\frac{\partial p}{\partial z} = 0 \tag{2.16}$$

$$\frac{\partial p}{\partial z} - \frac{\partial u}{\partial z} \pm \gamma_f \frac{\partial \varepsilon}{\partial z} = 0 \tag{2.17}$$

2.2.2.5 The Governing Equation

The permeability k in the reduced coordinate version of Darcy's Law, equation 2.6, is anticipated to depend on void ratio alone if the soil skeleton is homogenous, possesses no creep effects and exhibits monotonic consolidation (Gibson et al., 1981). This relationship becomes

$$k = k(e) \tag{2.18}$$

where the vertical effective stress

$$\sigma' = \sigma - p \tag{2.19}$$

governs the void ratio

$$\sigma' = \sigma'(e) \tag{2.20}$$

Equations 2.18 and 2.20 illustrate the concept of a unique relationship between void ratio and permeability as well as void ratio and effective stress, which was mentioned previously as a fundamental assumption of finite strain theory.

Finally, the governing equation for one dimensional finite strain consolidation developed by Gibson et al. (1967) combines equations 2.14, 2.15, and 2.16 to ultimately result in

$$\pm \left(\frac{\gamma_s}{\gamma_f} - 1 \right) \frac{d}{de} \left[\frac{k}{1+e} \right] \frac{\partial e}{\partial z} + \frac{\partial}{\partial z} \left[\frac{k}{(1+e)\gamma_f} \frac{d\sigma'}{de} \frac{\partial e}{\partial z} \right] + \frac{\partial e}{\partial t} = 0 \tag{2.21}$$

As outlined in previously, equation 2.21 is based on the continuity of fluid flow in a differential soil element, Darcy's law, and the effective stress principle similar to small strain theory. Additionally, finite strain theory considers vertical equilibrium of the soil mass and places no restriction on the form of the stress-strain relationship (Cargill, 1983). Furthermore, the governing equation 2.21 derived by Gibson et al. (1967) is highly nonlinear and does not consider the effect of self-weight of the soil.

2.2.2.6 Refinement of Original Theory

The original equation developed by Gibson et al. (1967) was found for a thin homogenous clay layer where self-weight effects are negligible. Gibson et al. (1981) considered the self-weight effect of overlying soils and refined the original theory for a thick homogenous clay layer where self-weight effects considered. Additionally, Gibson et al. (1981) showed that the highly non-linear formula, equation 2.21, can be made linear and its solutions can be simplified with the use of non-dimensional variables, while retaining the non-linearity of the permeability and compressibility, by considering material properties.

In conventional consolidation theory, the coefficient of consolidation c_v contains the material properties that govern consolidation and is expressed as

$$c_v = -\frac{k}{\gamma_f}\frac{1+e_0}{a_v} \tag{2.22}$$

where a_v is the coefficient of compressibility. Gibson et al. (1967) developed a coefficient of consolidation g for the finite strain theory of consolidation, where the stress-strain relationship is combined with the permeability to give

$$g = -\frac{k}{\gamma_f(1+e)}\frac{d\sigma'}{de} \tag{2.23}$$

It is suggested that assuming g to be constant is reasonable since it is likely to be much less sensitive than its constituent terms (Gibson et al., 1981). If g is constant, equation 2.21 becomes

$$\frac{\partial^2 e}{\partial z^2} \pm (\gamma_s - \gamma_f) \frac{d}{de}\left(\frac{de}{d\sigma'}\right)\frac{\partial e}{\partial z} = \frac{1}{g}\frac{\partial e}{\partial t} \qquad (2.24)$$

which can also be expressed as

$$\frac{\partial e}{\partial t} = g \frac{\partial^2 e}{\partial z^2} \qquad (2.25)$$

resembling the one-dimensional consolidation equation developed by Terzaghi (as cited in McCarthy, 1977).

$$\frac{\partial u}{\partial t} = c_v \frac{\partial^2 u}{\partial z^2} \qquad (2.26)$$

Gibson et al. (1981) gives a reasonable formulaic approximation between the relationship of g and c_v to be

$$g = \frac{c_v}{(1+e)^2} \qquad (2.27)$$

Equation 2.25 presents a formulaic relationship between void ratio and effective stress. Although there is valid reasoning to allow g to remain constant, the presence of a variable coefficient λ

$$\lambda(e) = \frac{d}{de}\left(\frac{de}{d\sigma'}\right) \qquad (2.28)$$

26

makes equation 2.25 non-linear (Gibson et al., 1981). To allow linearity, the assumption that λ remains constant is made. When this is the case, the relationship between void ratio and effective stress can be evaluated as the following exponential equation

$$e = (e_{00} - e_{\infty})\exp(-\lambda\sigma') + e_{\infty} \qquad (2.29)$$

where e_{00} is the void ratio under zero effective stress and e_{∞} is the void ratio at the end of consolidation. Gibson et al. (1981) concludes that the form of equation 2.29 is compatible with the general shape of the void ratio/effective stress relationship encountered with conventional soils. Additionally, Gibson et al. (1981) presents equation 2.29 as a substitute for equation 2.30, which is commonly used to describe oedometer test results for normally consolidated soil

$$e = e_o - C_c log_{10}\left(\frac{\sigma'}{\sigma'_o}\right) \qquad (2.30)$$

where e_o and σ'_o are the reference void ratio and effective stress, respectively, and C_c is the compression index.

2.2.2.7 Theoretical Settlement and Degree of Consolidation

To predict settlement as a function of time, the change in thickness of a soil element is first considered. The change in thickness of the soil element δS at any time t is given as

$$\delta S = (1 - \frac{\partial \varepsilon}{\partial a})da \qquad (2.31)$$

Therefore, making the settlement S of the entire layer being considered

$$S(t) = \int_0^{h(0)} \left(1 - \frac{\partial \varepsilon}{\partial a}\right)da \qquad (2.32)$$

This equation can also be expressed in terms of the reduced material coordinate z as

$$S(t) = \int_0^l [e(z,0) - e(z,t)]dz \qquad (2.33)$$

Making the expression for degree of consolidation

$$U(t) = \frac{S(t)}{S(\infty)} = \frac{\int_0^l [e(z,0) - e(z,t)]dz}{\int_0^l [e(z,0) - e(z,\infty)]dz} \qquad (2.34)$$

2.2.2.8 Non-Dimensional Variables

To simplify numerical analysis, Gibson et al. (1981) developed the following non-dimensional variables, which consider the materials properties

$$E(z,t) = e(z,t)/e(0,0) \tag{2.35}$$

$$Z = z/l \tag{2.36}$$

$$T = g/l^2 \tag{2.37}$$

$$N = \lambda l(\gamma_s - \gamma_f) \tag{2.38}$$

$$B = e_\infty/e(0,0) \tag{2.39}$$

$$R = e(0,t)/e(0,0) \tag{2.40}$$

Making the equation 2.34 for the degree of consolidation in non-dimensional form

$$U(t) = \frac{S(t)}{S(\infty)} = \frac{\int_0^l [E(Z,0) - E(Z,T)]\,dz}{\int_0^l [E(Z,0) - E(Z,\infty)]\,dz} \tag{2.41}$$

Using the non-dimensional parameter N and T, the degree of consolidation U can be estimated, where U is dependent on the normalized parameter N (Gibson et al., 1981). Figure 2.3 shows an example of the degree of consolidation U vs time factor T relationship for a series of N values.
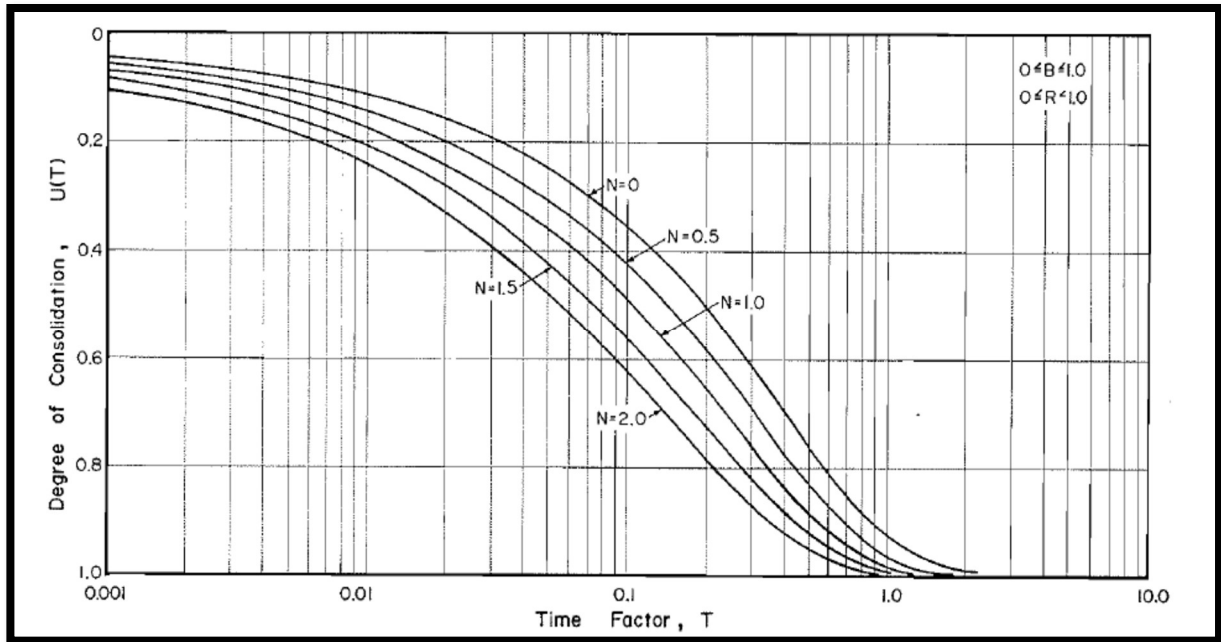
Figure 2.3: Degree of consolidation plotted in non-dimensional variables. (Gibson et al., 1981)

2.2.2.9 Application of Finite Strain Theory

To test the theoretical basis that had been developed up to this point, Gibson et al. (1981) used soil property data originally reported by Mikasa (1965) to make calculations based on the newly developed theories. The results suggested that conventional theory can greatly overestimate the time of consolidation and can underestimate the amount of excess pore pressure at any given time; the latter situation can lead to overestimating the shear strength of a soil deposit (Gibson et al., 1981). Whereas the newly developed method of finite strain consolidation theory gave satisfactory results when compared with field measurements. The work provided by Gibson et al. (1981) gives a complete theoretical approach to analyzing consolidation behavior of highly saturated soils that exhibit large strains. However, the assumption that the finite strain coefficient of consolidation g remains constant during the consolidation process is erroneous

30

when considering how soils actually behave (Gibson et al., 1981). Additionally, the assumption that soils exhibiting large strains are free from the effects of skeleton creep is also unlikely when considering real world behavior.

2.2.3   Practical Use of One-Dimensional Finite Strain Consolidation Theory

2.2.3.1 Real World Application

Using the theoretical basis developed by Gibson et al. (1967; 1981), Cargill (1982; 1983; 1986) published a series of extensive technical reports through the United States Army Corps of Engineers, which outlined an applied approach, using finite strain consolidation principles, to estimate one-dimensional consolidation of very soft, fine-grained dredged material. Many of the concepts and formulations are still used and accepted today by the USACE. Before the work of Cargill (1982; 1983; 1986), the long-term storage capacity of DMCA's was based on the work of Palermo et al. (1978), where settlement of homogenous clay layers is calculated using small strain consolidation theory, not a finite strain theory. Cargill (1982) showed the more general finite strain consolidation theory to be a superior method to the already well-established small strain theory of consolidation for analyzing the consolidation properties of dredged material. At the time of publication many figures relating the percent consolidation U to the non-dimensional time factor T for small strain theory had been well established, however similar theories based on finite strain theory were not available and had to be developed, i.e. figure 2.3. Solutions were developed and compared to actual field data, which provided good agreement.

The work presented by Cargill (1982; 1983; 1986) drew heavily from the theoretical foundation developed by Gibson et al. (1967; 1981), where soil properties are non-linear. The purpose of the report was to present working engineers with practical solutions, that can be utilized in real life field applications, for the ultimate settlement and time rate of settlement of a consolidating dredged layer. Proper analysis requires a full range of void ratio/effective stress conditions to be determined from laboratory tests. Low effective stress conditions must be determined from a self-weight consolidation test, while higher values of effective stress are found using oedometer tests, combining the two can provide a range of effective stresses expected in the field. Cargill (1986) published a report providing the guidelines for a Large Strain Controlled Rate of Strain (LSCRS) device, which is useful for medium ranges of effective stress where large strains are still expected, however these values can also be obtained by making certain modifications to conventional oedometer equipment. The report also included the description of a special apparatus for self-weight consolidation testing. The apparatus is essentially a settling column with several removable rings of equal thickness that can be sequentially removed to sample soil layers for water content with increasing depth. The data obtained can be used to find the void ratio and effective stresses in each layer. This information can be combined with oedometer tests to provide a wide range of void ratios expected over the life of multiple consolidating layers. The self-weight consolidation testing apparatus is essential, as it is the most accurate way to adequately obtain void ratio/effective stress relationships at the lowest levels of effective stresses, which are characteristic of a newly dredged fill layer. The following methods were used in this research paper to determine the physical and hydraulic properties of the dredged material being tested at low levels of effective stress.
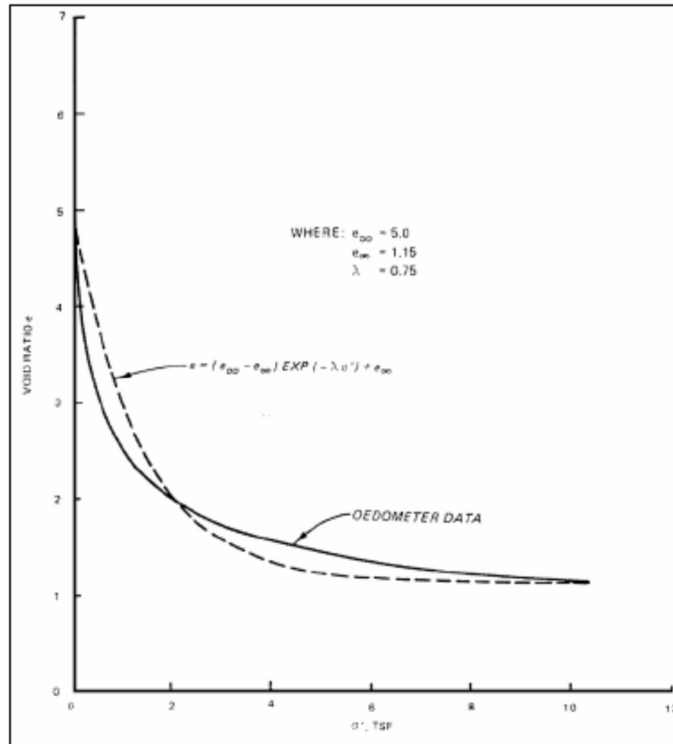
Figure 2.4: Exponential Void Ratio-Effective Stress Relationship Compared to Laboratory Oedometer Data.

(USACE, 2015)

2.2.3.2 The Exponential Void Ratio/Effective Stress Relationship

The exponential form, equation 2.29, of the original governing equation for finite strain consolidation, equation 2.22, is integral to making hand calculations from laboratory data. The application of a simplified procedure presented by Cargill (1983) is based on two fundamental assumptions reported by Gibson et al. (1981), which are that the coefficient of consolidation g and the variable coefficient λ remain constant in the soil layer. These two assumptions allow for the use of equation 2.29, when making hand calculations. Numerical values for void ratio vs.

33

effective stress can be determined from laboratory tests. A best apparent fit curve, created using

equation 2.29, can then be fitted over laboratory data to establish an exponential void

ratio/effective stress relationship. This exercise involves choosing appropriate constants λ, e_{oo},

and e_∞ until a satisfactory curve is created. An example is shown in figure 2.4. Using void ratios

calculated from the exponential form, equation 2.29, settlement calculations can then be made.

2.2.3.3 Ultimate Settlement Using Finite Strain Method

The ultimate settlement of a consolidating fine-grained layer is defined as settlement that

has occurred after all excess pore pressure has dissipated. Within the layer, the material assumes

a void ratio distribution due to the buoyant weight of material above plus any surcharge, and this

void ratio is related to the effective stress by the material's e-log-σ' curve as determined by

laboratory testing (Cargill, 1986). The ultimate settlement of a dredged layer is analyzed in

reduced coordinates. Equation 2.42 gives the layer thickness in reduced coordinates l as

$$l = \frac{h}{1+e_{00}} \qquad (2.42)$$

where h is the initial layer thickness as deposited and e_{oo} is the initial void ratio. A consolidating

layer can then be divided into sublayers l_i, which can be found by dividing the initial layer into m

number of sublayers using

$$l_i = \sum_{i=1}^{m} \frac{h_i}{1+e_i} \qquad (2.43)$$

where h_i is the initial sublayer height and e_i is the average void ratio in a sublayer. The void ratio for a given sublayer is found using the exponential e-log-σ′ curve created using laboratory test data. This method allows the settlement in each sublayer to be individually analyzed. The effective stress that is created in each sublayer is estimated using

$$\sigma_i' = \frac{1}{2} l_i (\gamma_s - \gamma_w) \tag{2.44}$$

Once all predicted effective stress values have been calculated for each sublayer, a corresponding void ratio can be found from the curve created using equation 2.29. Ultimate settlement δ can then be calculated using

$$\delta(\infty) = \sum_{i=1}^{m} (e_{i,0} - e_{i,\infty}) l_i \tag{2.45}$$

where $e_{i,\,o}$ and $e_{i,\,\infty}$ are the average initial and final void ratios of each sublayer, respectively and l_i is the initial sublayer height.

2.2.3.4 Time Rate of Consolidation Using Finite Strain Method

Laboratory data can be used to estimate settlement as a function of time using finite strain consolidation theory. Once ultimate settlement is calculated based on the procedure described above, percent consolidation U can be related to ultimate settlement to calculate settlement at a given time using the following equation

$$\delta(T) = \delta_\infty U(T) \tag{2.46}$$

Figure 2.5 shows curves relating the time factor for finite strain consolidation T_{fs} to percent consolidation U for a singly drained layer of dredged fill. Each curve represents a different value of the nondimensional variable N, which can be calculated from equation 2.38. Laboratory test curves plotting slurry deformation against time can be used to estimate 100 percent primary consolidation, settlement and time at a given degree of consolidation U, and average void ratio at a given degree of consolidation U.
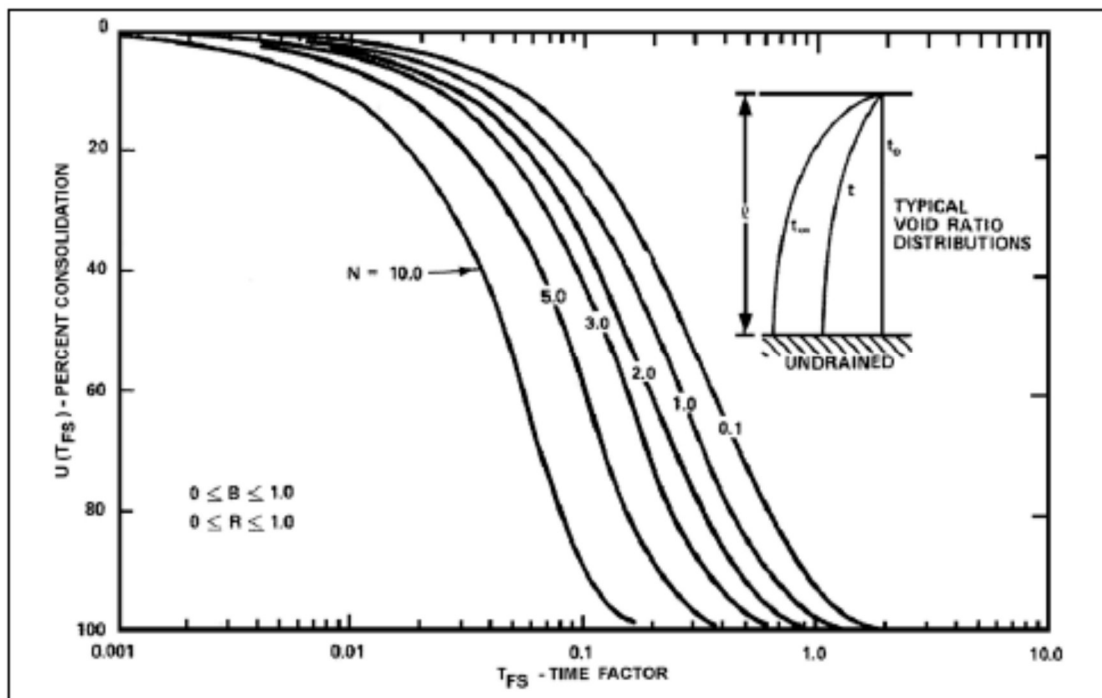
Figure 2.5: Degree of Consolidation as a Function of the Time Factor for Dredged Fill for Singly Drained Layers by Linear Finite Strain Theory. (USACE, 2015)

With a chosen degree of consolidation U and a value N calculated from laboratory data, the appropriate time factor T_{fs} can be determined. With the non-dimensional time factor T_{fs} known, equation 2.47 can be used to calculate the finite strain coefficient of consolidation g from laboratory data, which is

$$g = \frac{H_s{}^2 T_{fs}}{t} \tag{2.47}$$

where t is real time and H_s is the height of solids. The coefficient of consolidation g calculated from laboratory tests can be used to calculate permeability with equation 2.23, allowing a void ratio/permeability relationship, for a range of void ratios observed in laboratory tests, to be estimated. This relationship can then be used to estimate permeability for a given void ratio in field problems. A new coefficient of consolidation g can then be estimated from equation 2.23, for a given void ratio. Real time calculations can then be made using equation 2.47.

2.2.3.5 Conclusion on Finite Strain Theory

Cargill (1983) concludes that predicting ultimate settlement and time rate of settlement resulting from self-weight consolidation is possible by the procedures described in the report but depend heavily on a reliable void ratio/effective stress relationship which accurately reflects the material state at lower effective stresses. In all field problems considered by Cargill (1983), the calculated ultimate settlements were favorable to field measurements when using finite strain consolidation methods. Additionally, Cargill (1983) compared measured field values against calculated values using traditional small strain consolidation theory. The results showed that

conventional methods of estimating consolidation predict settlements much smaller than what was observed in the field and predict longer time rates of consolidation. Therefore, it is suggested, based on the finding of the report, that the selected finite strain theory of consolidation be used when predicting settlement of soft, fine-grained dredged fill layers subjected to self-weight loading.

2.2.4 *Other Studies on the Physical & Hydraulic Properties of Slurry Material*

Monte and Krizek (1976) developed a mathematical model to characterize the large strain consolidation of soft clays. In their study, the simplifying assumptions necessary in small strain consolidation theory, linear coefficient of compressibility and permeability, were shown to be non-linear. The authors developed a laboratory permeability testing procedure, where a slurry can be consolidated under very low effective stresses. Based on the results, the authors postulate that the coefficient of permeability will depend on whether the pore fluid passes through a fixed matrix of solids or is squeezed through a deforming matrix of solids.

Carrier and Keshian (1979) developed a 30-day settling test to define low effective stress conditions in a slurry layer. The test consists of allowing diluted dredged slurry to consolidate under its own self-weight for 30 days. After the 30-day period is over, an average void ratio is calculated, as well as the effective stress at the mid-point of the settling column. This allows a single point on a compressibility curve to be established. This process is repeated several times at different initial conditions to create several points on a compressibility curve for low effective stresses. Although the authors may have been acting in the interest of time by creating multiple

38

samples at different void ratios to establish a void ratio/effective stress relationship, this approach could have been potentially simplified by sampling layers of increasing depth of one settlement test that could run for a longer period.

Using sedimentation tests, Katagiri and Imai (1980) found the consolidation characteristics, such as compressibility, permeability and settlement, of highly saturated clays depend on the initial average water content of the soil. The authors tested several samples, made with the same soil, at increasing water contents and found that samples with average water contents greater than 500% showed very steep increases in their compression index C_c and generally followed a non-linear trend, whereas samples with average water contents of 300% or less showed very similar compression index values. The authors also found the coefficient of consolidation c_v and permeability k vary with increasing effective stress and void ratio, samples with higher initial average water contents generally showed higher values for c_v and permeability and decreased as the void ratios decreased with depth and time. The authors attribute these variabilities to the different soil skeleton structures formed during flocculation.

Imai (1980) found that settling rate for sedimentation testing of clays is not only influenced by the initial water content of the slurry mix, but also by the number of solid particles in the slurry. Imai (1980) concludes that the larger the total solid weight, the lower the critical initial water content, the higher the settling rate, and the lower the average water content at the end of the settling stage. In other words, a sample would settle faster, at the same initial water content, if a larger amount was tested.

Sridharan and Parkash (2003) used self-weight consolidation tests to study void ratio/effective stress relationships for soft soils having different clay mineral compositions. Samples were distinguished based on their clay mineralogy. The authors used glass jars with internal diameters of 61.1 mm to conduct the tests on four remolded soil samples containing principal clay particles composed of either Kaolinaite or Montmorrillonite. Samples with higher void ratios were classified as segregated samples, whereas samples with lower void ratios were classified as homogeneous. Samples were allowed to settle for a period of 15 to 60 days and were sampled using a spatula with a horizontal end to "slice" layers for void ratio calculation with depth. The authors found that samples with higher initial water contents (i.e. void ratio) showed steeper curves when plotted as void ratio versus the effective stress on a log axis. Homogenous samples with lower water contents were found to experience very little variation in void ratio with depth. The authors conclude that segregated samples exhibit steeper void ratio vs effective stress curves due to grain size sorting, while homogenous samples undergo self-weight consolidation to achieve their void ratio/effective stress relationship. Sridharan and Parkash (2003) base their water content adjustments on the soil's liquid limit. Homogenous samples were all made at 1.5 times the soils natural liquid limit, while the segregated samples were made anywhere between 2.75 to 4.5 times the soil liquids limit. These adjustments yielded initial void ratios as between 3 and 7. Natural sediments deposited in marine environments or created from dredging operations would potentially exhibit much larger initial void ratios. The author's use of 61.1 mm settling columns may have had adverse effects the homogenous samples that had lower initial water contents, which were denser at any given point. Samples with relatively dense layers tend to be affected more by wall friction then samples that are simply settling as flocs or individual particles (Been and Sills, 1981). The authors may have considered columns with

larger internal diameters. The study fails to report the height that the samples were made at, thus not making their work readily reproducible. In the case for the homogenous samples, height becomes an important distinction when considering the effective stress of sample since all stresses are developed from the self-weight of the solids present in the sample. The samples were allowed to settle for a maximum of 60 days. Most of the e-log-σ' curves reported in this particular study tend to curve in one direction, in other words they do not exhibit an "S" shape curve that would distinguish primary consolidation from secondary consolidation. The authors may have considered longer settling periods since it is well established that consolidation of clay layers can take very large amounts of time to complete. Some of the homogenous samples with relatively flat curves may require more time to truly consolidate.

Li et al. (2013) developed a relatively simple method to measure the physical and hydraulic properties of slurried deposits that are allowed to consolidate under their own weight. The authors created a sedimentation cylinder to where material height and pore pressure measurements can be made, while pore water pressure drains in one direction, from the top. Using this testing apparatus, the authors were able to measure various physical and hydraulic parameters at any given time, including the hydraulic gradient, fluid flow velocity, hydraulic conductivity, settlement, total density, void ratio, excess pore water pressure, and vertical effective stress. Experimental results agreed favorably with equations developed to describe the aforementioned parameters. The authors conclude their simple testing apparatus is an efficient way to measure the evolution of several physical and hydraulic properties of slurried deposits. The reported results were based on one layer deposition. The authors point out that in practice slurried deposits are usually placed in several layers. Additionally, the authors conducted the

tests with the tops of the sedimentation tube open, allowing evaporation of expelled water, which may have adverse effects on the measurements.

Gao et al. (2016) studied the effects of column diameter on settling behavior of dredged slurries in sedimentation experiments. Using dredged slurry collected from a disposal pond in Jiangsu province of China, the authors prepared several settling column samples at various column internal diameters and water contents to test the sample sensitivity to column diameter. Gao et al. (2016) found that the effect of settling column wall on the sample settling decreases with increasing column diameter and these effects can ultimately be ignored when the settling column is larger than 14.5 cm. This information was taken into consideration when selecting the appropriate size cylinders for this research paper.

3. Materials & Methods

3.1 Background of Study Area

Samples were collected as part of the Savannah Harbor Expansion Project (SHEP). The Savannah Harbor is a deep-draft harbor located on the South Atlantic coast of the United Sates, 75 miles south of Charleston Harbor in South Carolina, and 120 miles north of Jacksonville Harbor in Florida. The harbor comprises the lower 21.3 miles of the Savannah River and 11.4 miles of channel across the bar to the Atlantic Ocean (USACE, 2012). The goal of the expansion project is to deepen the harbor and shipping channel from its current authorized depth of 42 feet to a new authorized depth of 47 feet. Figure 3.1 shows the location of the general area of study. Deepening the harbor will let newer, larger cargo vessels to pass with fewer tidal restrictions and heavier loads. The deepening will let Savannah remain one of the nation's busiest container ports. It currently ranks as the fourth busiest in the nation and the second busiest on the East Coast (USACE, 2017).

Figure 3.1: Map view of the Savannah River and the general study area (USACE, 2015)

3.2 Material Index Properties

Undisturbed and disturbed samples from various locations along the Savannah River were composited in a 50-gallon drum barrel and mixed with site water to create a "parent" slurry. All subsequently tested specimens were formed from this composited slurry. Engineering index tests were conducted per ASTM standards on the "parent" composite. Index tests, along with the associated ASTM standard included: Atterberg limits (ASTM D 4318), moisture content (ASTM

D 2216), sieve analysis (ASTM D 6913), hydrometer analysis (ASTM D 7928), specific gravity (ASTM D 854), USCS classification (ASTM D 2487), and organic content (ASTM D 2974). Table 3.1 provides an overview of the materials engineering properties. The Atterberg limits for the composite plot above the "A" line, which puts it into the CH region, indicating a highly plastic clay, which can be seen in Table 3.2. Based on USCS classification the soil is a fat clay.

Gravel (%)	0.0
Sand (%)	4.1
Fines (%)	95.9
Silt (%)	17.8
Clay (%)	78.1
Liquid Limit	149
Plastic Limit	54
Plasticity Index	95
Specific Gravity	2.641
Organic Content (%)	8.2
USCS Classification	CH - Fat clay

Table 3.1: Index properties for Dredged Slurry Composite
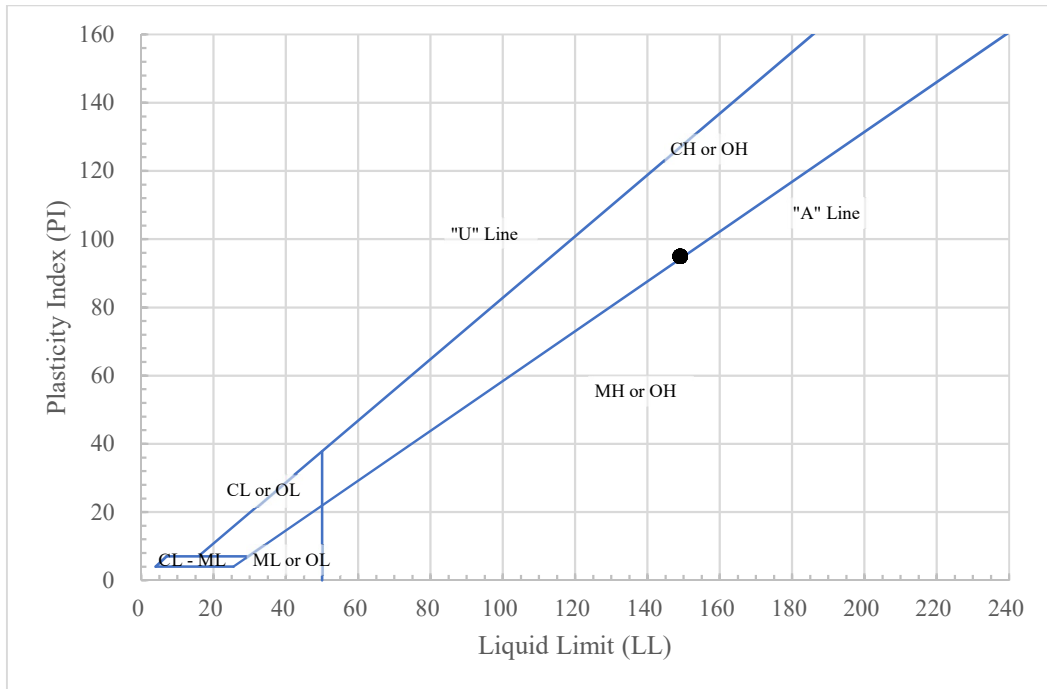
Figure 3.2: Atterberg Limits for Dredged Composite

3.3 Comparison of Test Methodologies

3.3.1   USACE Method Summary

A self-weight consolidation test procedure developed by the United States Army Corps of Engineers will be described in this section and will serve as a basis for comparison to the modified test method further developed in this paper.

The USACE method, originally reported by Cargill (1986) allows the sampling of a 6-inch diameter remolded sample. Figure 3.3 shows the device prepared with test slurry and figure 3.4 shows an exploded view of the apparatus. The device is made of Plexiglas and consists of a

large outer ring that covers 18 individual ½ inch inner rings, each 6 inches in diameter, that

allow for the sampling of individual layers with increasing depth at a constant layer height. Each

ring must be lightly coated with silicon vacuum grease in order insure that the device is

watertight. Once the test is complete, all removed layers are taken for moisture content

determination, thus providing a way to calculate a relationship between void ratio and vertical

position in the sample, which can be used to determine effective stress.
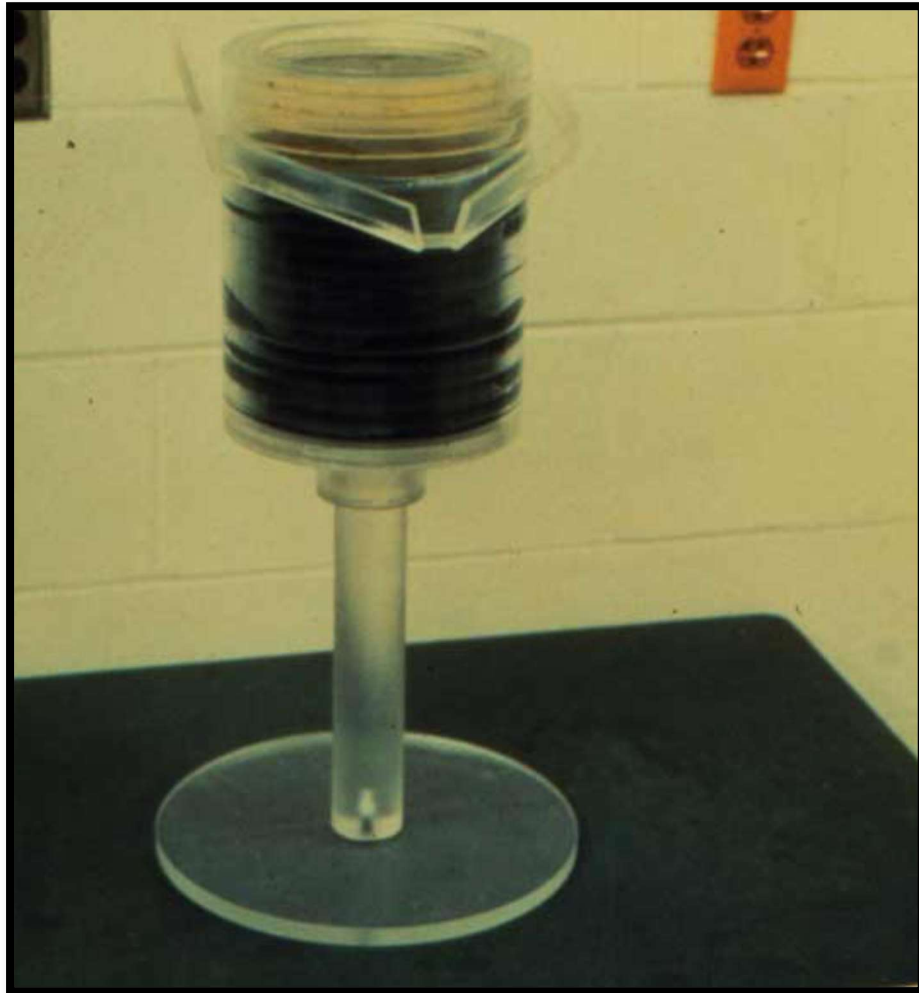
Figure 3.3: Self weight consolidation apparatus developed by the USACE, filled with test slurry. (USACE, 2015)
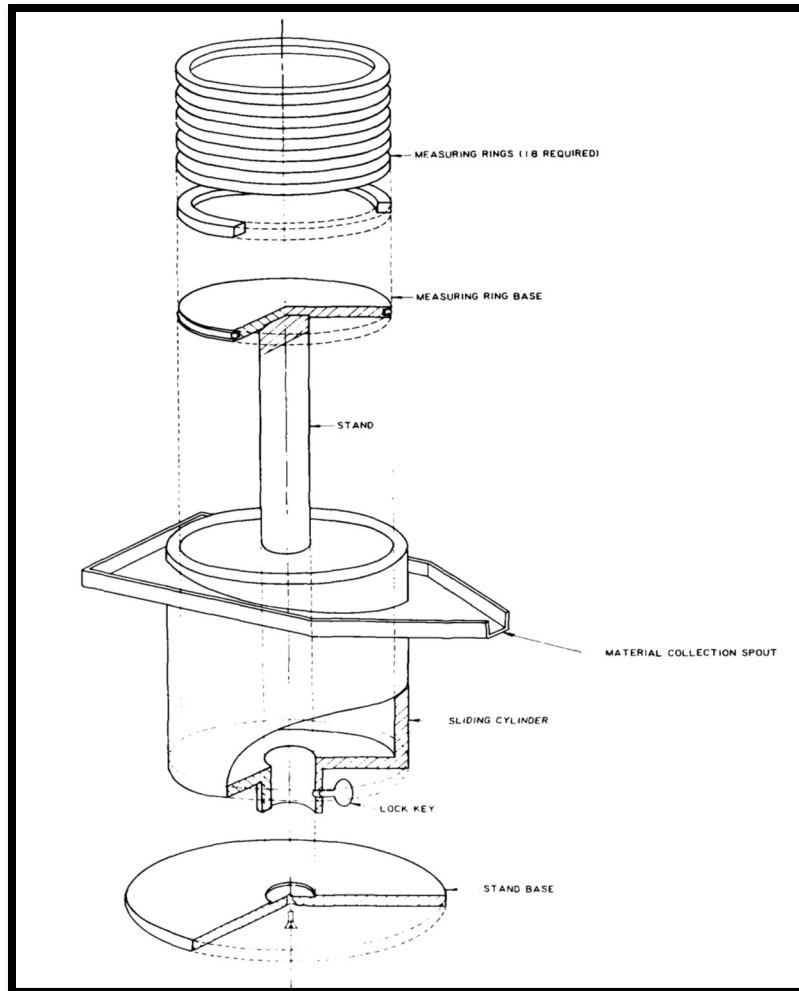
Figure 3.4: Exploded view of the self-weight apparatus (Cargill, 1983)

The device is filled with a completely remolded sample that is comprised primarily of

fine-grained sediment, which most closely resembles the actual site material being dredged and

pumped through the pipelines (Cargill, 1986). Initial conditions should be known, so sample

water content can be adjusted to the desired void ratio before beginning the test. Once the

sample is prepared it should be thoroughly agitated and mechanically mixed to obtain a

homogenous mixture while making sure not to entrap unwanted amounts of air. If multiple samples are to be made, Cargill (1986) suggests pouring the slurry into an arc shaped device, with an inlet at the top, which would allow the slurry to be randomly and evenly distributed to two separate chambers. This step insures homogeneity. Samples are prepared by filling the device with slurry to a desired height, while maintaining ½ inch freeboard. The device should be covered with plastic wrap to prevent evaporation of free water. Once the sample is placed, the test is self-conducting. The sample is to be left undisturbed with periodic measurements to the material height. These measurements should be plotted on a semilogarithmic plot of the material settlement versus time. This procedure allows the user to identify when primary consolidation is complete. Once primary consolidation is completed, or the user has deemed the appropriate amount of time of testing to be complete, excess water should be removed from the top of the sample prior to sampling individual layers. The first layer should be sampled at a depth less than a ¼ inch with a flat spatula. The sampling of subsequent layers involves lowering the outer cylinder of the device in ½ inch intervals, thus exposing the inner rings. Rings can readily be slid horizontally allowing the material to spill into a collection tare. This process is repeated at ½ inch intervals until the full depth of the sample has been reached. Each layer should then be placed in a constant temperature oven for moisture content determination, which is used to calculate void ratio and effective stress of the solid material in the sample.

3.3.2   *Modified Method Summary and Comparison*

The modified method for the self-weight consolidation test developed in this paper will be outlined in subsequent sections. This section will focus on comparing the two test methods.

The modified method presented in this paper differs mainly in the type of equipment

used. The USACE method employs a fairly complex Plexiglas apparatus which must be

manmade and is not readily available from any type of supplier, whereas the modified method

simply uses glass cylinders that can be found at many arts and crafts or home goods stores, figure

3.3. This provides an advantage when the equipment or expertise required to create the USACE

apparatus aren't readily available. Another advantage of the modified test is the fact that glass

cylinders will produce less friction than individually placed rings. The rough surface created by

stacking rings will produce more sidewall friction, which can affect settlement, than a smooth

continuous glass surface. Additionally, the potential for leaks in the equipment is much higher

for the USACE method. Although, Cargill (1986) points out that any leaks observed are mostly

self-healing. Any leakage will none the less cause an additional drainage path in the sample,

which can cause localized consolidation and can produce adverse test results. The main

disadvantage of the modified method is the quality of the test results depends on the user

sampling the specimen. While the USACE method has fixed rings at a fixed height that are

simply lid off, the modified method depends on the accuracy of the user sampling each layer, if

care is not taken not to disturb the underlying layers, results can be skewed.

Test set up for the two methods are basically identical, where a remolded sample at a pre-

selected void ratio is poured into the testing apparatus and allowed to consolidate under its own

weight, with periodic readings taken on the material height. Both test methods require removing

the free-standing water that has been expelled from the soil matrix before sampling. The

USACE method requires no more than a ¼ inch of the top soil layer to be removed with a

spatula. This step eliminates the top most layer of the sample. This step is taken since it is

nearly impossible to distinguish the water that belongs in the topmost slurry layer from any

residual water after decanting. Not performing this step may lead to inaccurate values of void

ratio for the very top layer. This step was not performed for the modified method and the effects

must be considered when analyzing results. Further sampling of the USACE method requires

simply removing the ½ inch rings. This provides layers of equal height but unequal weight,

since the water and solid content are changing with depth. The modified method requires the

calculation of the sample's unit weight per unit length. This requires calculating the net weight

of slurry once all free water has been removed and dividing by the total length at the end of the

test. This gives layers of equal weight, and increasing volume of solids, since the void ratio of

the slurry decreases with depth of the test sample as water is pushed out from the pores. Layers

are sampled carefully with a 90° spatula to ensure the next layer is not disturbed and as much

material as possible is placed into the sampling tare. With the data obtained from the layer

sampling of both tests, calculations of void ratio and effective stress can be made.

3.4 Testing Procedure

3.4.1   Test Equipment

The following equipment was used to perform the modified self-weight consolidation tests:

1) Settling cylinders - glass cylinders with an internal diameter of 5.8 inches (14.6 cm)
   and 9.5 inches (24.1cm) in height were used. Test cylinders were fashioned with
   measuring tape, reading to the nearest millimeter, to obtain settlement readings.

Empty cylinders were weighted before testing in order to readily calculate the net weight of slurry at the end of the test.

2) High speed hand held electric mixer - used to thoroughly mix samples with water to create a uniform slurry. Mixing blades were made of thick Plexiglas with dull corners to ensure particle segregation and not particle degradation.

3) Fifty-gallon plastic drum with lid - used to mix disturbed and undisturbed samples with site water to obtain a "parent" slurry from which all subsequent samples were made.

4) Ladle - used to pour slurry into cylinders during test specimen preparation.

5) Plastic wrap - to cover the top of the test cylinder to prevent evaporation of expelled water.

6) Rubber gaskets – placed under each test cylinder to maintain balance of the cylinder.

7) Thermometer - used to take temperature readings, to ensure temperature did not create any adverse effects. Kept next to samples.

8) Vacuum pump – consisting of a vacuum motor, water chamber, and hose with control valve. Used to remove free water at the end of each test.

9) Metal spatula - bent to a 90° angle and used to sample each layer without disturbing subsequent layers.

10) Silicon spatula - used during sampling to clean slurry from the sides of the cylinder after each layer.

11) Aluminum tares - for sampling moisture content.

12) Constant temperature oven - used for moisture content determination. Maintained at 110°C±5°C.
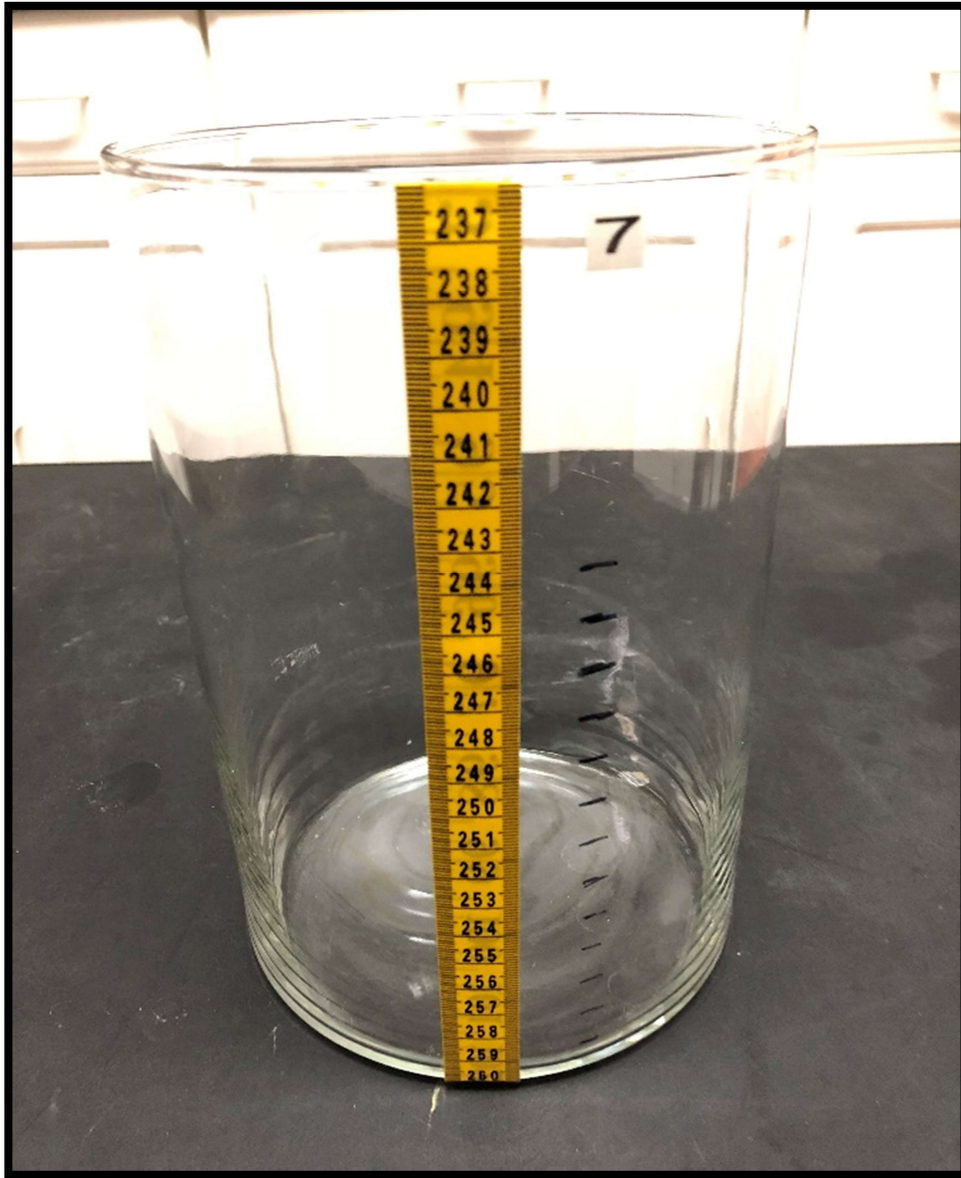
Figure 3.5: Settling Cylinder Used in the Modified Method

Figure 3.6: Spatulas Used to Sample Slurry from Settling Cylinder

Figure 3.7: Vacuum pump set-up for decanting free water after testing period is over.

3.4.2   Test Specimen Creation

Undisturbed and disturbed samples from various locations along the Savannah River were composited to create a "parent" slurry. Samples were combined into a 50-gallon plastic drum barrel and mixed with site water to create a slurry characteristic of material found in dredging operations in the Savannah River Harbor, figure 3.8. The slurry was mixed daily using a high-speed electronic blender for a period of roughly 6 weeks, until the slurry was observed to be completely homogenous with no visible clay clots. From the "parent" slurry, test samples were made in four groups of three. Each group contained one sample with a void ratio of 7.0, one sample with a void ratio of 8.5, and one sample with a void ratio of 10.0, allowing three different void ratios to be sampled every month for four months. These void ratios were selected in an attempt to create samples that were low enough in water content such that they would immediately be in the consolidation phase of settlement, as opposed to samples that may exhibit sedimentation at higher water contents. However, these void ratios were selected such that the water was high enough to allow samples to consolidation under their own weight. Samples were placed in their respective settling cylinders at the desired void ratio using a ladle. Each void ratio group was made at the same time to ensure homogeneity between test samples. To make each void ratio group, a portion of the "parent" slurry was mixed with additional water to obtain the desired void ratio. The newly made slurry was then placed layer by layer, in a serpentine pattern, between four test cylinders to complete one void ratio group. During this process the slurry was continuously mixed with a high-speed blender to guarantee no premature particle settlement could occur. All cylinders were filled to approximately 7.70 inches (19.5 cm) with slurry. Table 3.2 provides a list of the testing program, including specimen initial conditions.

Figure 3.8: "Parent" slurry being mixed with high speed electric mixer in 50-gallon drum barrel.

Specimen Number	Target Void ratio	Measured Moisture Content	Initial Measured Height	Length of Test
(-)	(-)	(%)	(inches)	(days)
C1	7	266.0	7.87	28
C2	7	266.0	7.72	53
C3	7	266.0	7.76	84
C4	7	266.0	7.72	112
C6	8.5	326.5	7.72	28
C7	8.5	326.5	7.56	53
C8	8.5	326.5	7.68	84
C9	8.5	326.5	7.64	112
C11	10	382.1	7.60	28
C12	10	382.1	7.60	53
C13	10	382.1	7.64	84
C14	10	382.1	7.52	112

Table 3.2: Specimen Test Program

3.4.3 Specimen Testing

Once the testing cylinders were prepared, testing was self-conducting with only periodic measurements to the water/slurry interface. Readings were taken at 0, 5, 10, 30, 60, 120, 240 minutes and then twice daily thereafter. Room temperature was recorded along with all interface readings. Observations were also made on the consistency of the slurry, cloudiness of the expelled water and on any signs of flocculation in the slurry. One group was sampled every four weeks for sixteen weeks for a total of twelve tests, each group containing one specimen at a void ratio of 7.0, 8.5, and 10.0.

Figure 3.9: Group of Settling Cylinders During Testing

3.4.4   Specimen Removal

One test specimen from each void ratio group was sampled every four weeks for sixteen weeks. A final measurement to the slurry/water interface was taken before decanting the free water using a vacuum pump and measuring the amount of water removed. The test specimen was then sampled in approximately equal layers using a metal spatula bent to a 90° angle to remove each layer, careful not to disturb the underlying layer. Figure 3.10 shows a test cylinder

being sampled. Layers of equivalent weight were determined by calculating the unit weight per

unit length W of the test specimen using the following equation

$$W = \frac{w_s - w_c}{h_f} \tag{3.1}$$

where w_s is the total weight of the cylinder containing the slurry with all of the free-standing

water removed, w_c is the weight of the clean empty test cylinder and h_f is the final height of the

slurry at the end of the test. Using this equation, a unit weight per ½ inch layer was used in

sampling the specimens, ½ inch layers were selected based on the USACE procedure. Once the

entire depth of the test specimen was sampled, all removed layers were weighted and placed in a

constant temperature oven at 110°C±5°C oven for moisture content determination per ASTM D

2216. Test data obtained from moisture content tests provided numerical values for all

subsequent calculations of the specimen's physical and hydraulic properties.

Figure 3.10: Test Specimen During Sampling

3.5 Equations Used in Study

3.5.1   Void Ratio

All void ratio e calculations were based on the following relationship

$$e = \frac{V_a + V_w}{V_s} \qquad (3.2)$$

where V_a is the volume of air, V_w is the volume of water and V_s is the volume of solids. A principal assumption of finite strain consolidation theory is that the soil being analyzed is fully saturated. Therefore, the volume of voids V_v, where $V_v = V_a + V_w$, was simply taken to be equivalent to the volume of water. Thus, making equation 3.2 a simple ratio of water volume to solids volume

$$e = \frac{V_w}{V_s} \qquad (3.3)$$

The total weight of the solids and water in each layer was determined from moisture content tests. To calculate void ratio, all weights were converted to volume. For simplicity, the unit weight γ_w of the water present in a slurry was assumed to be 1 g/cc, allowing one unit mass of water to equal one unit volume of water. Using the specific gravity G_s determined from ASTM D 854, the mass of solids M_s was converted to volume of solids V_s using the following relationship

$$V_s = \frac{M_s}{\gamma_w G_s} \qquad (3.4)$$

3.5.2   Solids Height

The volume of the solids V_s in each layer was used to calculate the height of solids H_s in each layer using the following equation

$$H_s = \frac{V_s}{A} \qquad (3.5)$$

where A is the circular area of the test cylinder.

3.5.3   Effective Stress

Effective stress for each layer was calculated by first finding the buoyant weight γ_b of the solids present in the removed layer using the following relationship

$$\gamma_b = M_s - V_s \gamma_w \qquad (3.6)$$

Effective stress σ' can then be found by equation

$$\sigma' = \frac{\gamma_b}{A} \qquad (3.7)$$

where A is the cross-sectional area of the test cylinder.

3.5.4   Final Strain

Final strain ε for each test cylinder was calculated using equation 3.8 where l_o is the initial measured height of the test cylinder and l_f is the final measured height of the cylinder

$$\varepsilon = \frac{l_o - l_f}{l_o} \; x \; 100 \tag{3.8}$$

3.5.5   Determination of λ

Equation 2.28 introduced what is referred to as the variable coefficient λ, this equation is used in linearizing the governing equation for the finite strain formulation and implies an exponential relationship between void ratio and effective stress, equation 2.29 (Cargill, 1983). Essentially λ can be considered a linearization constant.

In order to make time rate of settlement calculations, it is necessary to calculate the non-dimensional variable N using equation 2.38, which requires a value for the variable coefficient λ. The variable coefficient λ was obtained from laboratory data. Using a program written in Microsoft Excel, a best apparent fit curve was plotted over the laboratory test data curve using equation 2.29 by choosing appropriate constants λ, e_{oo}, and e_{∞} for each test sample. This iterative process involved selecting logical values, based on laboratory measurements, of e_{oo}, and

e_∞, then choosing an appropriate value for λ until a best fit curve was created. This process was repeated until the areas between the two curves on either side of the point of intersection were approximately equal, an example can be seen in figure 2.4. These curves provided the exponential void ratio/effective stress relationships for each test, which were used in subsequent calculations. Individual curves for each test are provided in Appendix A.

3.5.6   Ultimate Settlement Based on the USACE Method

Laboratory tests provided values for initial sample height, final sample height and specific gravity. Using equations 2.42, 2.43, and 2.44, the reduced height of the sample layer, reduced height of each sublayer, and the effective stress expected for each sublayer were calculated, respectively. Using the exponential test curves from section 3.5.5, void ratios corresponding to the effective stress calculated from equation 2.44 were assigned to each sublayer. Equation 2.45 was then used to find the calculated ultimate settlement of each test sample. Tabulated calculation can be found in Appendix A.

3.5.7   Coefficient of Consolidation

Equation 2.47 was used to calculate the finite strain coefficient of consolidation g. The finite strain time factor T_{fs} was found from figure 2.5. The appropriate curve was selected by calculating the non-dimensional variable N using equation 2.38, given the height of the samples the curve corresponding to an N= 0.1 was used for all tests. Using figure 2.5 a value for g was

calculated for degrees of consolidation of 20, 50, and 90 percent, for each test sample, to study

the change of permeability k with time.

3.5.8   Permeability

Using the coefficient of consolidation g found in section 3.5.7. Permeability of each test

sample was calculated using equation 2.23, to establish a relationship between void ratio and

permeability. A fundamental assumption of finite strain consolidation theory is that permeability

k is a function of void ratio e, equation 2.18. Thus, making the average permeability for each

test a function of the average void ratio at a given time. As the average void ratio in each test

sample changed with time, permeability was expected to change as well. Void ratio e for

equation 2.23 was taken as the average void ratio e_{avg} in the test cylinder at a time corresponding

to the degree of consolidation that the permeability is being calculated for. Average void ratio in

a test cylinder at a given time is calculated from laboratory data as

$$e_{avg} = \left(\frac{l_i - \Delta l}{H_s}\right) - 1 \tag{3.9}$$

where l_i is the initial length of the test sample and Δl is the amount of settlement in the test

cylinder at a given time. Settlement readings were found using settlement vs. log time plots

obtained from water/slurry interface readings. Equation 2.23 contains a previously undefined

variable, the coefficient of compression dσ'/de, which can be found by taking the slope of each

individual point from the best fit curves created with equation 2.29 (see section 3.5.5). The

coefficient of compression dσ'/de was plotted against the exponential void ratio ratios determined

from curves in section 3.5.5 to determine the appropriate coefficient of compression for the

average void ratio e_{avg} being used in calculations. Individual test curves for the coefficient

compression can be found in Appendix A

4. Results & Discussion

4.1 Self-Weight Consolidation Test Results

Test results from twelve modified self-weight consolidation test samples tested at various initial void ratios for different lengths of time will be discussed in this section. Testing and calculation methods outlined in the previous section were used.

4.1.1 Settlement vs. Time

The settlement of the remolded dredged test specimen was measured by the movement of the water/slurry interface, on a millimeter scale, against time. Figures 4.1, 4.2, 4.3, and 4.4 show settlement vs. log time and were used to identify when primary consolidation of the sample was complete. These figures were also used to obtain settlement vs. time readings for permeability calculations, see section 3.5.8. The end of primary consolidation was determined by drawing a straight line through the final points of the curve and another straight line though the steepest part of the curve, the intersection of the two lines, with respect to the y-axis, was taken to be the amount settlement at the end of primary consolidation. Curves plotted in figures 4.1 and 4.2 do not show a well-defined distinction between the final points and the steepest points, indicating more time was necessary to complete primary consolidation. In these cases, for the purpose of making calculations, the end of primary consolidation was assumed to be the final point on the curves.

All samples showed little to no settlement within the first 24 hours. After 24 hours all samples began to settle at different rates and slowly fan away from each other, continuing to do so with time. Samples with initial void ratios of 7.0 (C-1, C-2, C-3, C-4) show the least amount of settlement at any given time. Additionally, no further settlement is observed from month three to month four (C-3 to C-4), both settlement readings ended at 23 mm. Samples with initial void ratios of 10.0 (C-11, C-12, C-13, C-14) exhibit the most settlement. Again, both tests C-13 and C-14 show 54 mm of settlement, indicating no further settlement between month three and four. Samples with initial void ratios of 8.5 (C-6, C-7, C-8, C-9) exhibit intermediate settlements. From month three to month four, again no additional settlement was measured between tests C-8 and C-9, which both ended at 42 mm of settlement.

In all curves, the samples with initial void ratios of 8.5 and 10.0 generally exhibit parallel slopes, while the samples with initial void ratios of 7.0 show smaller slopes. After approximately one to two months, all samples begin to show a hump where it looks as if primary consolidation is completed but then begins again at approximately the same rate, as indicated by the slope of the line. This observation may be able to be explained by considering the side wall friction produced by the glass cylinders. Been and Sills (1981) found that samples with relatively dense layers tend to be affected more by wall friction than samples that are simply settling as flocs or individual particles. While the samples never experienced any flocculent or individual particle settling, it is logical to assume that the density reached a critical point where the wall friction had a greater effect for a short time before continuing to consolidate under its own weight. The work presented by Gao et al. (2016), concludes that cylinder diameter has little

effect on self-weight consolidation of slurry samples if the cylinders diameter is larger than 14.5 cm. Cylinders used in this study were approximately 14.6 cm internal diameter. Differences in soil composition could influence the minimum diameter suggested by Gao et al. (2016).

The shape of the curves in figure 4.3 suggest that primary consolidation can be assumed complete at about 80 to 90 days. This can be seen from the breaks in the curve's slopes at the end of the testing period. This is confirmed from the curves in figure 4.4, which begin to completely flatten. It should be noted that in this research study readings were taken to the nearest millimeter. The flat ends of curves in figure 4.4 do not suggest that settlement did not occur at all during this time, only that the magnitudes of settlement were too small to properly measure with the scale used. None the less, the amount of time the readings remained at the same millimeter reading suggest that all primary consolidation had been completed.
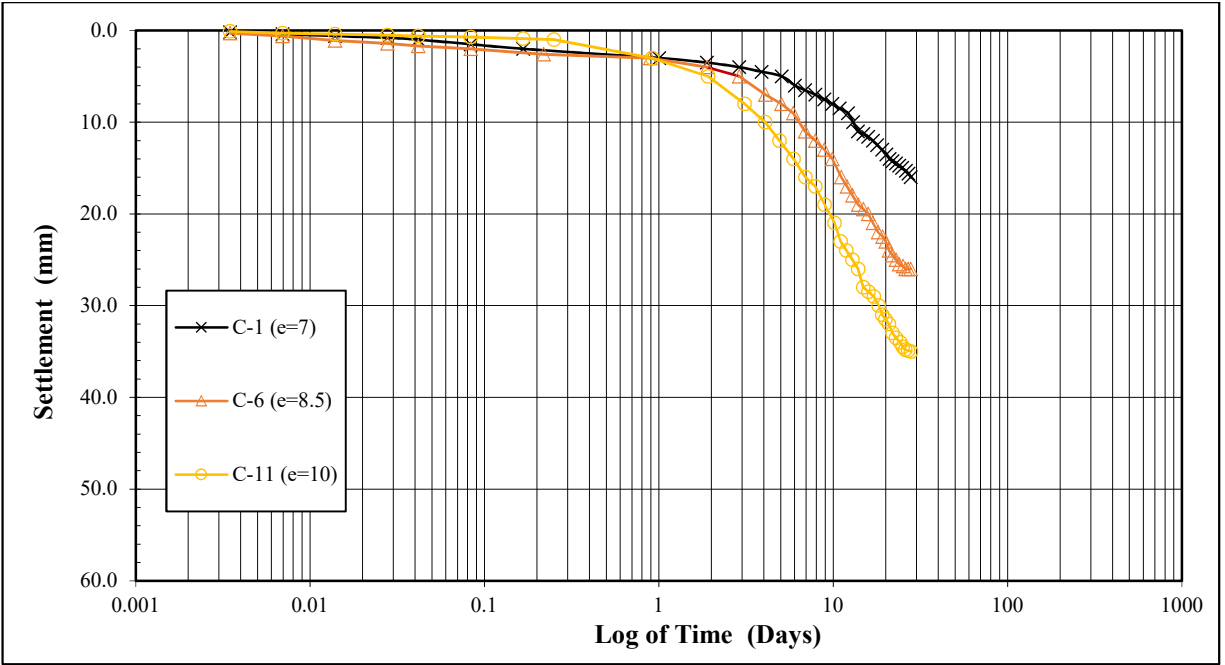
Figure 4.1: Settlement vs. Time Measurements for 4 Week Samples
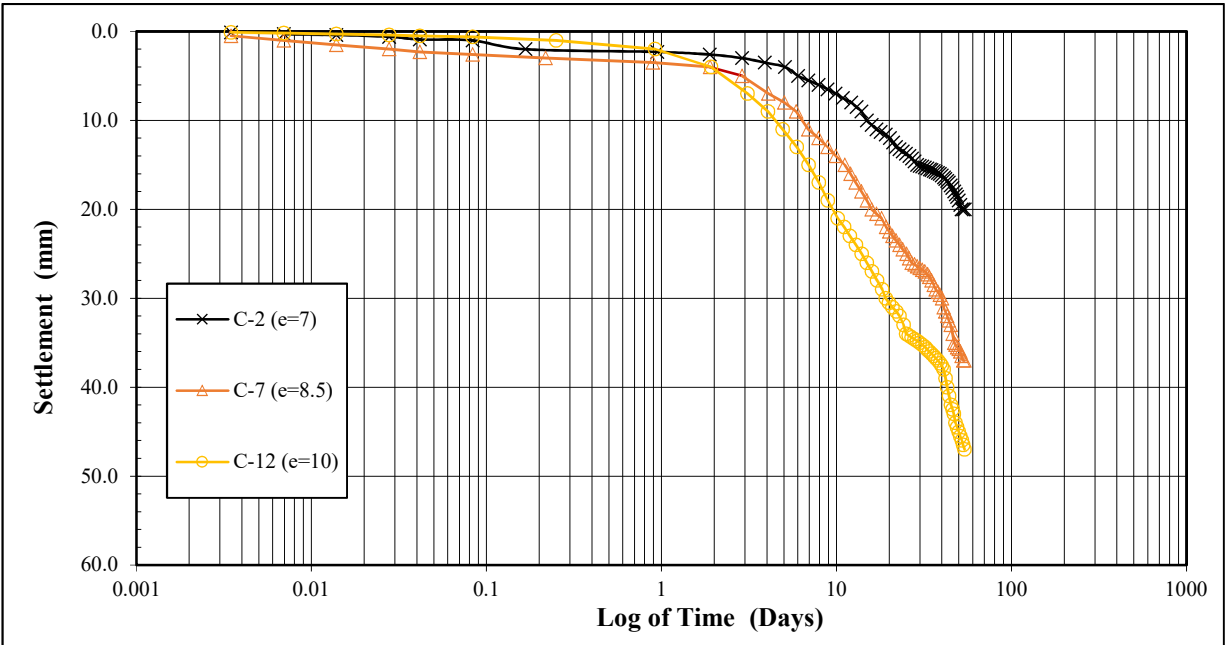
Figure 4.2: Settlement vs. Time Measurements for 8 Week Samples

71
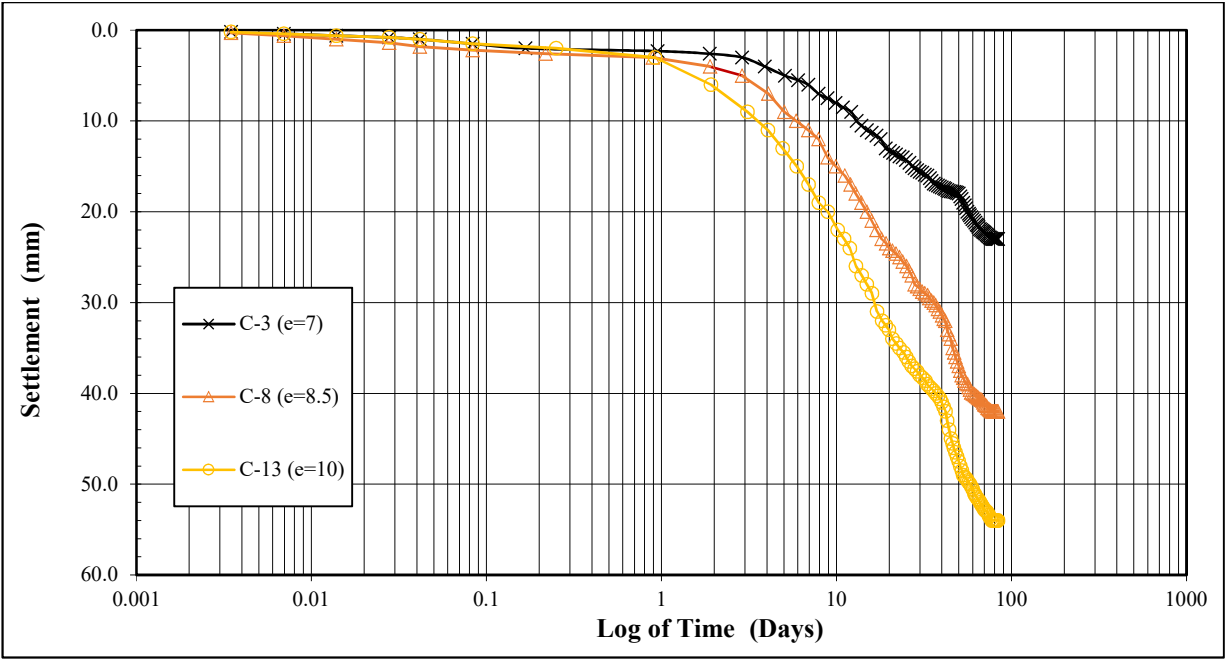
Figure 4.3: Settlement vs. Time Measurements for 12 Week Samples
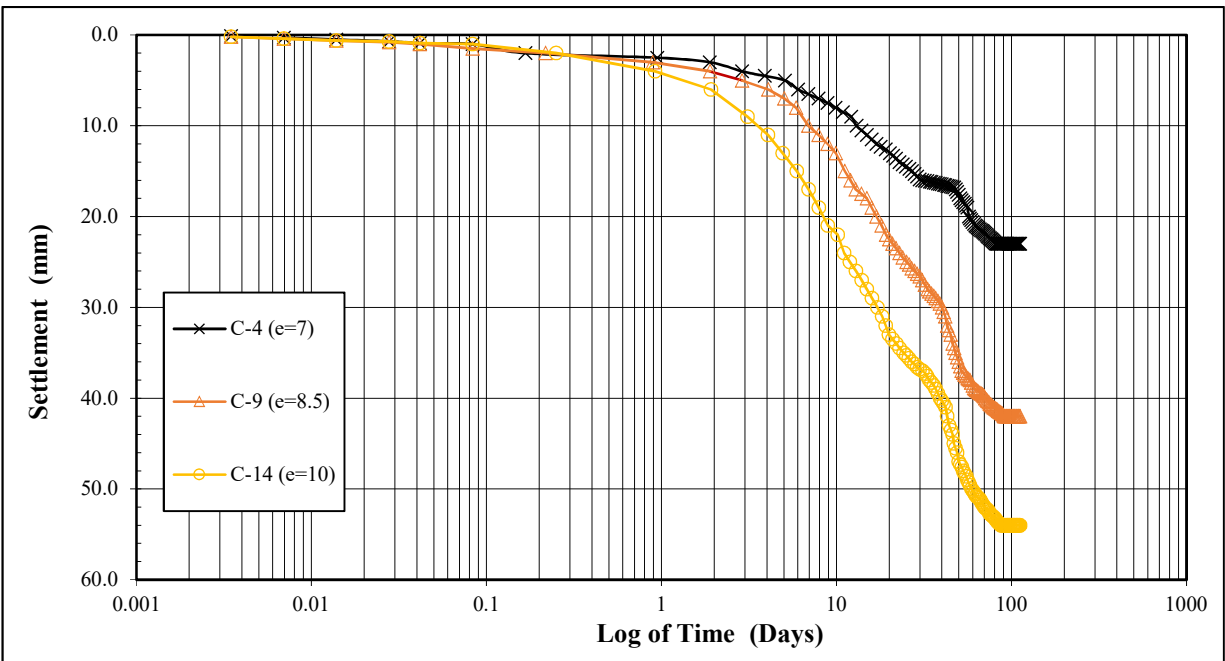
Figure 4.4: Settlement vs. Time Measurements for 16 Week Samples

72

4.1.2   Void Ratio vs. Effective stress

Void ratio vs. effective stress profiles were plotted for each group on a semi-logarithmic scale, to study the effect of the initial void ratio as it pertains to the effective stresses developed in different layers of each test with time. Individual points in each figure represent roughly ½ inch thick layers of slurry sampled from the test cylinder at increasing depth. Void ratio/effective stress curves for samples dismounted at four weeks, figure 4.5, show that for each test specimen the void ratio varies greatly at the same effective stress, for any given layer. Additionally, the first layer of each test is almost still at the tests initial void ratio, this could be attributed to the fact that the top layer of each sample underwent the least amount of self-weight consolidation due to the weight of solids being the lowest at these points at the time of sampling. Although it must be noted, as mentioned in section 3.3.2, the void ratios calculated for the very top layer of each sample may be inaccurate since it is nearly impossible to completely decant the topmost layer of all expelled water without disturbing the actual slurry layer.

Effective stresses for all tests were calculated based on the buoyant weight of the solids present in each layer. When comparing the changes in effective stress with time in any given layer, it can be seen that for the same effective stress, void ratio reduces with time for samples with the same initial void ratios. This can be attributed to the fact that the pore water is continuously being expelled from the soil matrix with time, thus reducing the average void ratio in each test cylinder, making the test sample denser, causing smaller void ratios in each layer with time. Since the volume of solids available in a specimen at any given time does not change, the average effective stress in a layer remains relatively constant while the void ratio continues to

reduce. As the solids in each layer are pushed together and become denser, layers begin to exhibit smaller void ratios while showing slightly larger values of effective stresses.

All test samples were filled to roughly the same height in the testing cylinders, making it such that specimens with higher initial void ratios contained less volume of solids in the overall test cylinder. By studying the curves, it can be seen that samples with the same initial void ratios all exhibit the same effective stress at the very bottom layer, regardless of the time of sampling. Thus, suggesting that the testing method used was successful in terms of repeatability and sample homogeneity.

Figure 4.8 shows clearly shows the test curves converging for 16 weeks samples (C-4, C-9, and C-14). This suggests that each test will eventually arrive at the same void ratio, for a given effective stress. Additionally, when comparing the effects of time using figures 4.5, 4.6, 4.7, and 4.8, it can be seen that the distance between individual curves continues to decrease with time, again suggesting that all test samples will eventually approach the same void ratio for a given effective stress. Gibson et al. (1981) & Cargill (1982) mention that in order for finite strain theory of consolidation to be applicable, there is assumed to be a unique relationship between void ratio and effective stress for soft, fine grained clays that exhibit large strains. The data presented clearly shows that with time void ratios approach the same effective stress ranges. Therefore, it is theorized, based on the literature, that eventually, for any initial void ratio, a given effective stress will correspond to a unique void ratio value in a homogenous test sample. However, the effective stresses developed in these tests, especially in the top layers, may not be adequate to consolidate the sample to a point where these curves would fall onto one another. To

test this hypothesis, it is recommended that these test procedures be repeated in taller cylinders where multiple layers can be incrementally added overtime, thus facilitating consolidation by adding more load.
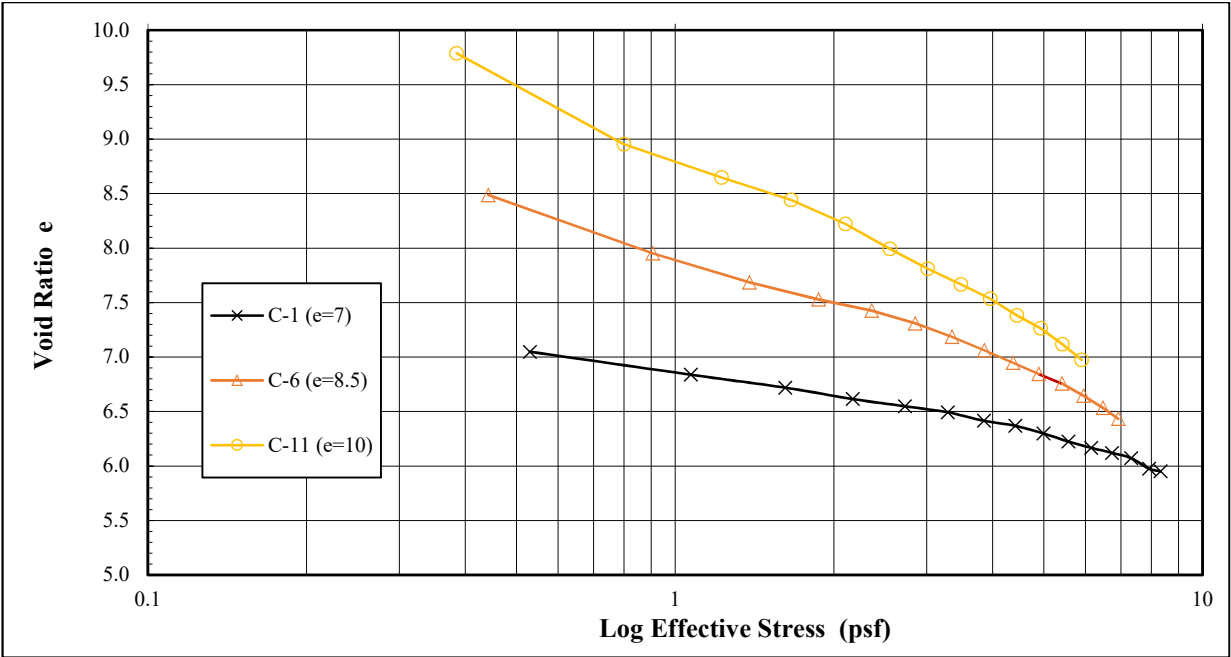
Figure 4.5: Void Ratio vs. Effective Stress for 4 Week Samples
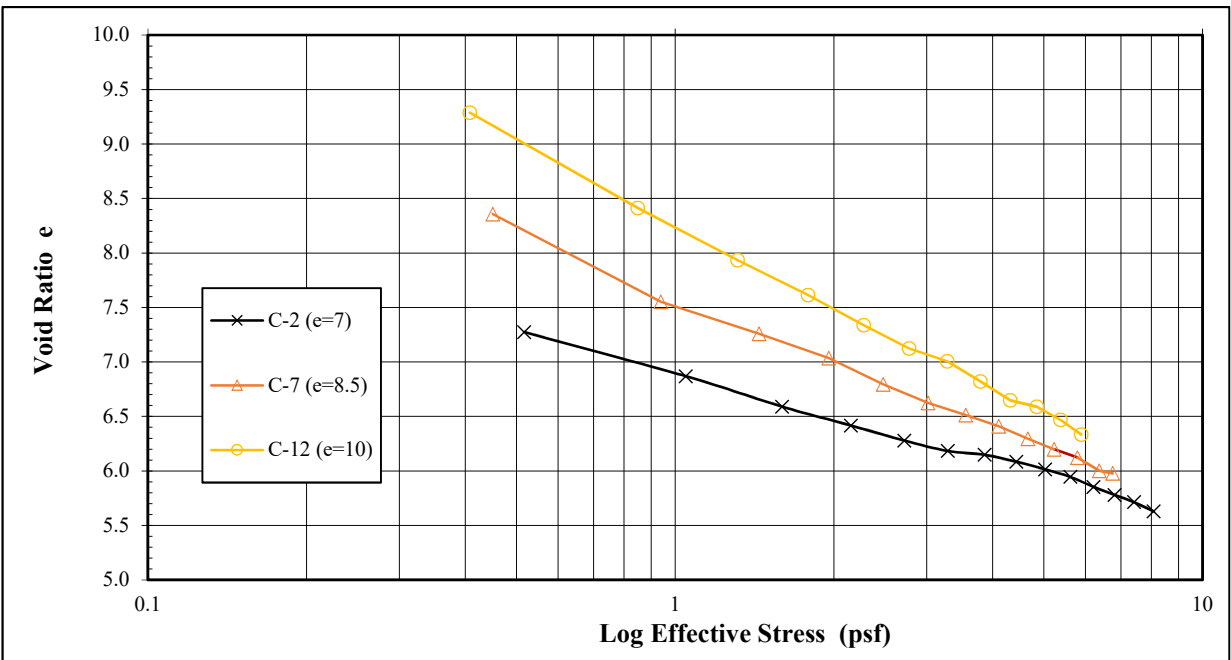
Figure 4.6: Void Ratio vs. Effective Stress for 8 Week Samples

76
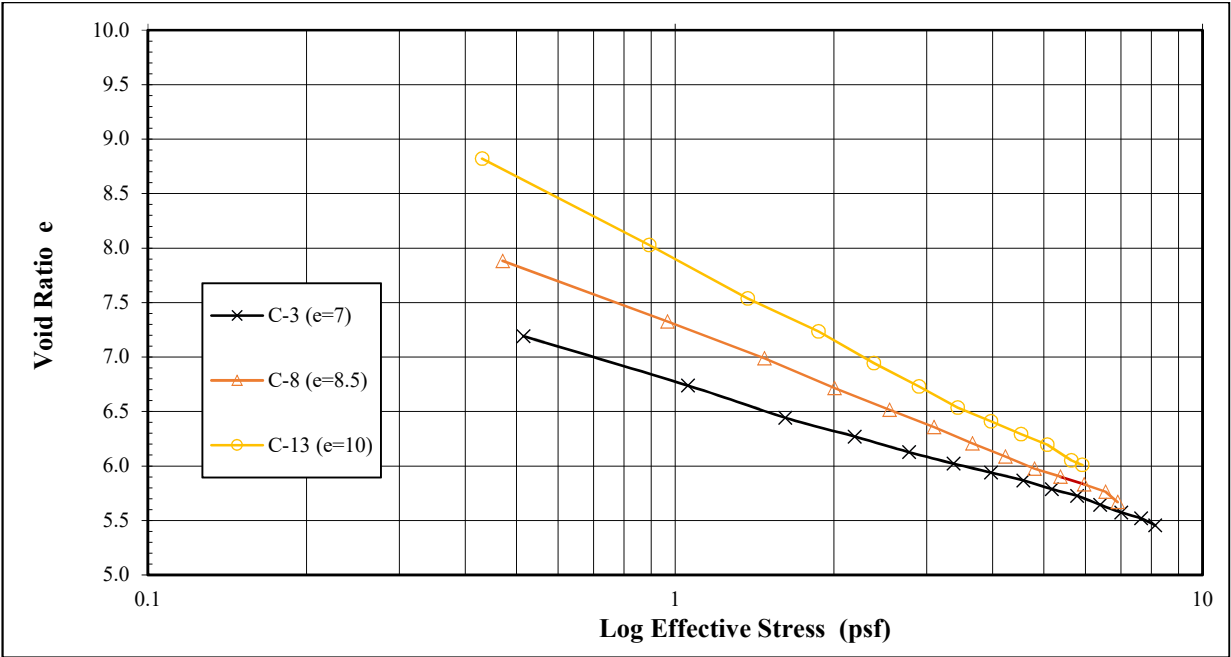
Figure 4.7: Void Ratio vs. Effective Stress for 12 Week Samples
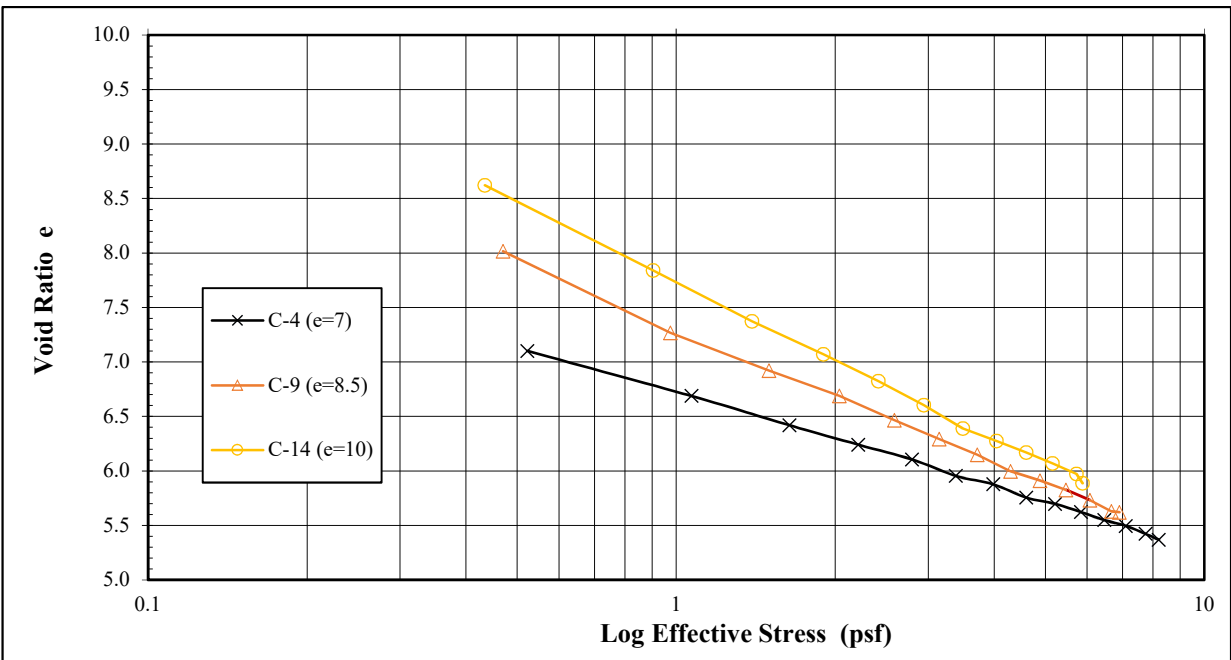
Figure 4.8: Void Ratio vs. Effective Stress for 16 Week Samples

77

4.1.3   Strain vs. Time

Each void ratio group was plotted as a single curve, where each test represents a single point, to illustrate the amount of strain each initial void ratio will undergo with time. The curve containing tests C-1, C-2, C-3, and C-4, the lowest initial void ratio group of 7.0, showed the least amount of total strain. Additionally, almost no additional strain was seen from test C-3 to test C-4, which suggests that for initial void ratios of 7.0, a three-month testing program is acceptable to obtain a majority of the potential consolidation for the test methods provided. The void ratio group containing samples C-6, C-7, C-8, and C-9, initial void ratios of 8.5, exhibit a sharper slope than the previous group and an overall large degree of strain. The rate of strain appears to become less after the second month, C-7, and shows a relatively constant rate thereafter. The void ratio group containing samples C-11, C-12, C-13, and C-14, initial void ratios of 10.0 exhibits a constant rate of strain until three months, where the magnitude of strain becomes much less between C-13 and C-14. All tests exhibit no more than roughly one percent strain from month three to month four, suggesting that four months, for the self-weight consolidation tests outlined in this research paper, is an adequate amount of time to obtain close to full consolidation.
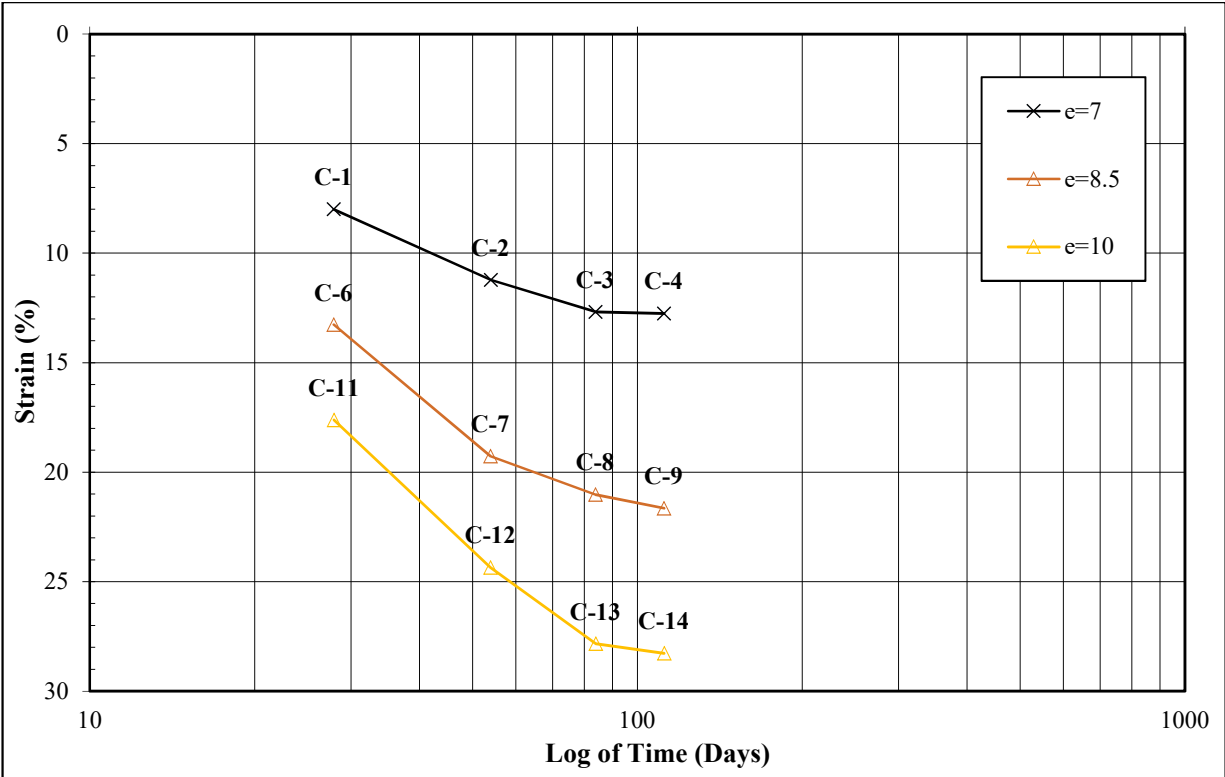
Figure 4.9: Samples with the Same Initial Void Ratios Plotted as Overall Strain Against Log-Time.

4.1.4   Exponential Void Ratio/Effective Stress Curves

Curves for the exponential void ratio/effective stress relationships used to in all subsequent calculations are provided in Appendix A. The curves are plotted using the same data from section 4.1.2, however, are plotted on a linear scale to determine the best apparent fit curve using equation 2.29.

4.1.5   Using USACE Method to Calculate Ultimate Settlement

To determine the validity of the testing methods described, each tests settlement was calculated using laboratory data with methods outlined in section 2.2.3.3 and compared to final measured settlements. Although, the primary purpose is to predict the settlement of a large deposited layer of dredged material exhibiting a range of void ratios, the procedure was applied to the test samples used in this research paper to find any inconsistencies or deviations between values measured in the laboratory and values calculated using laboratory data. Comparisons were favorable, indicating that the testing procedures and calculation methods are suitable. Table 4.1 shows the final measured height of each test and the final calculated height using the finite strain method as outlined by the USACE. Tabulated calculations can be found in Appendix A.

Sample Number	Void ratio	Initial Measured Height	Final Measured Height	Final Calculated Height Using USACE Method	Length of Test
(-)	(-)	(inches)	(inches)	(inches)	(days)
C1	7	7.87	7.24	7.28	28
C2	7	7.72	6.85	6.81	53
C3	7	7.76	6.77	6.77	84
C4	7	7.72	6.73	6.73	112
C6	8.5	7.72	6.69	6.61	28
C7	8.5	7.56	6.10	6.10	53
C8	8.5	7.68	6.06	5.98	84
C9	8.5	7.64	5.98	5.91	112
C11	10	7.60	6.22	6.22	28
C12	10	7.60	5.75	5.67	53
C13	10	7.64	5.51	5.55	84
C14	10	7.52	5.39	5.35	112

Table 4.1: Final Measured Height and Final Calculated Height for Each Test Sample

4.1.6   Permeability

Using the coefficient of consolidation g, calculated from laboratory data, the permeability

k of each test specimen was calculated at different degrees of consolidation, to establish a

81

relationship between void ratio and permeability at low effective stresses. This data can be used to estimate the time rate of consolidation for a layer of dredged material at low effective stresses. Figures 4.10, 4.11, and 4.12 plot permeability against average void ratio for 20, 50, 90 percent consolidation, for each test sample. Each point on a single curve represents a different degree of consolidation, 20, 50, & 90 percent from top to bottom, respectively. Samples tested for the shortest amount of time (C-1, C-6, C-11) show large deviations in permeability from the samples all other sample that were tested at the same initial void ratio for longer periods of time. All test results obtained at 8 weeks and later, show relatively similar values for permeability at any given void ratio. This is especially true after 50 percent consolidation (the middle point in the curve). This observation may be able to be explained by the idea put forth by Monte and Krizek (1976) that the coefficient of permeability in soft clays will depend on whether the pore fluid passes through a fixed matrix of solids or is squeezed through a deforming matrix of solids. The soil matrix in the first month of testing may not have been deformed to the same degree as later tests, thus providing less consistent values of permeability. Additionally, consolidation at 20 percent (top most point), was certainly less deformed than higher degrees of consolidation, which may be able to explain the inconsistent nature of the top most points.

The test results suggest that the procedure used can provide relatively consistent values of permeability k for a given void ratio e, but it is recommended to only use values obtained once 50 percent consolidation is complete for samples tested for at least 8 weeks. All results indicate that permeability decreases with time and void ratio. Appendix A provides all tabulated calculations for permeability.
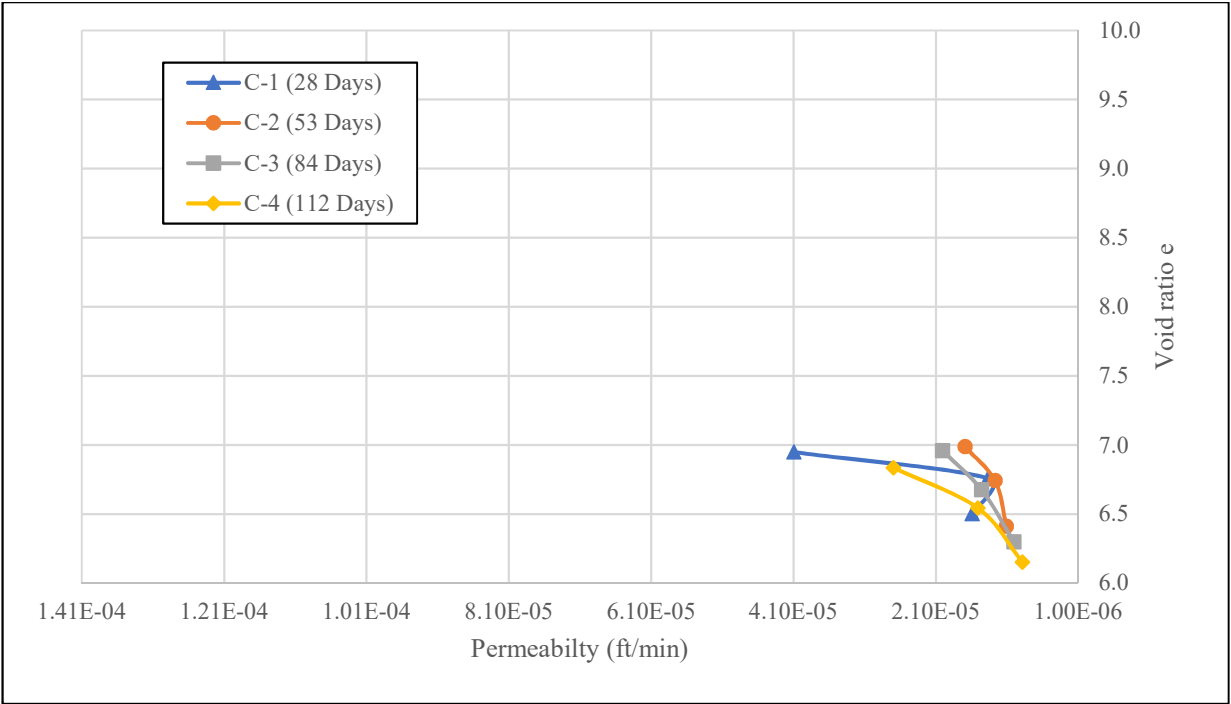
Figure 4.10: Average Void Ratio Plotted Against Permeability, for Different Degrees of Consolidation for

Samples with Initial Void ratios of 7.0
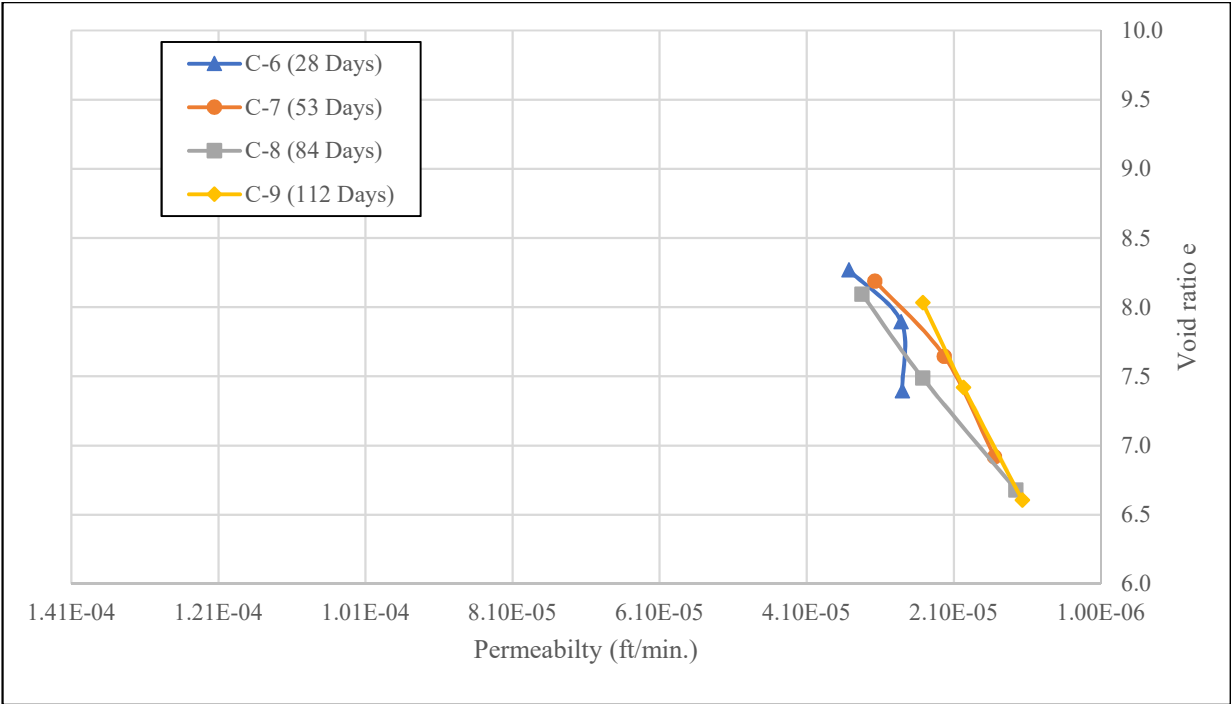
Figure 4.11: Average Void Ratio Plotted Against Permeability, for Different Degrees of Consolidation for

Samples with Initial Void ratios of 8.5
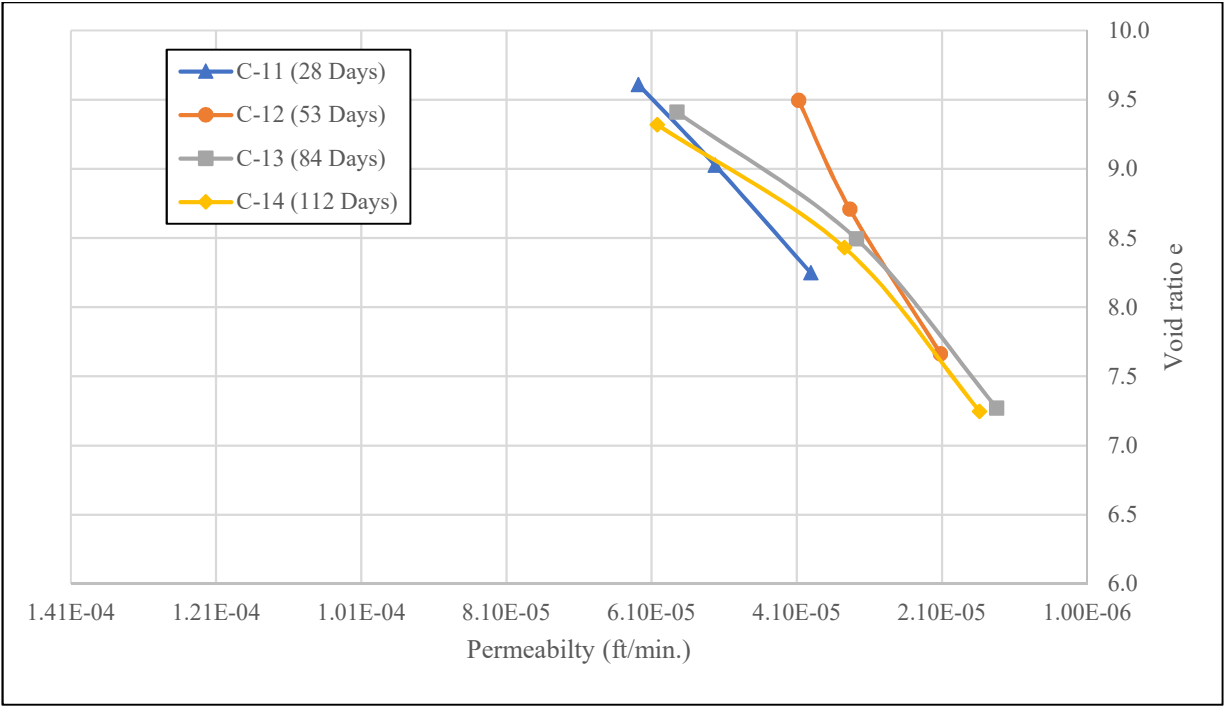
Figure 4.12: Average Void Ratio Plotted Against Permeability, for Different Degrees of Consolidation for

Samples with Initial Void ratios of 10.0

5. Conclusion

5.1 Concluding Remarks

The following conclusions can be made for the testing of dredged material from the Savannah Harbor that is allowed to consolidate under its own weight using the prescribed methods outlined in this research project:

1. Using test methods presented, a reliable relationship between void ratio and effective stress can be established using one-dimensional finite strain consolidation principles. This is confirmed by using laboratory data from the self-weight consolidation tests to calculate ultimate settlement using methods suggested by the USACE, which provided very agreeable values to those measured in the laboratory.

2. A reliable relationship between void ratio and permeability can be obtained from the test methods described. However, it is recommended that tests be allowed to consolidate for at least two months before attempting to define such a relationship.

3. A three to four-month period is a satisfactory amount of time to obtain near 100 percent primary consolidation for materials with initial void ratios of 7.0 to 10.0.

4. As consolidation advances, void ratios appear to approach the same values of effective stress over time, indicating a unique void ratio/effective stress relationship exists for the material tested.

5. All tests with the same initial void ratios exhibit approximately equal values of total effective stress developed, suggesting that the test method used is repeatable and can produce homogenous samples.

5.2 Recommendations for Future Work

Based on the research done in this project the following recommendations are made for any continued work regarding self-weight consolidation properties of dredged material:

1. Each test showed a small hump when plotted for settlement vs time in the middle of the settlement curve, it is theorized that the density and side wall friction of the cylinder played a role in this observation. Future work may consider using cylinders with a larger internal diameter to see if this effect is diminished.

2. The scope of the research presented in this paper focuses solely on self-weight consolidation of dredged slurry. Initial void ratios were selected such that the samples would immediately be in the consolidation phase once placed in the test cylinder. However, in real world applications dredged material experiences multiple stages of settlement before the soil matrix becomes a single consolidating mass. It is recommended that samples with higher initial void ratios be tested using the described methods to identify different stages of settlements and compare results.

3. The real-world disposal of dredged slurry involves incrementally depositing multiple layers of slurry over time as more volume in the disposal facility is recovered. It is recommended that the testing procedures described in this report are repeated in taller

cylinders so that multiple layers can be deposited over time. This would simulate what happens in the field and would also provide a larger range of effective stress since the material would not only consolidate under its own weight, but also would experience a surcharge load that would facilitate consolidation. Moreover, this additional loading would further consolidate the original layer to see if the effective stresses approach the same values of void ratio with additional load.

4. It is recommended that these testing procedures be used to analyze different materials from locations other than the one used in this study.

5. Values of permeability were estimated from the void ratio/effective stress curves measured in the laboratory. It is suggested that more advanced equipment (i.e. cylinders with piezometers attached) be used to obtain permeability values. As described in section 2.2.3.5 of the literature review, Li et al. (2013) used cylinders with piezometer attachments to obtain values for hydraulic gradient and fluid flow velocity. These parameters would provide more accurate values of permeability, if needed. Additionally, the ability to measure excess pore water pressure at any given time would provide a better understanding of when primary consolidation is complete in a test cylinder.

References

Bartos, M. J. (1977). *Classification and Engineering Properties of Dredged Material.* Technical Report D-77-18, U.S. Army Engineer Waterways Experiment Station, CE: Vicksburg, Miss.

Been, K., & Sills, G. C. (1981). Self-Weight Consolidation of Soft Soils: An Experimental and Theoretical Study. *Geotechnique, 31*(4), 519-535.

Cargill, K. W. (1982). *Consolidation of Soft Layers by Finite Strain Analysis.* Technical Report GL-82-3, U.S. Army Engineer Waterways Experiment Station, CE: Vicksburg, Miss.

Cargill, K. W. (1983). *Procedures for Prediction of Consolidation in Soft, Fine-Grained Dredged Material.* Technical Report D-83-1, U. S. Army Engineer Waterways Experiment Station, CE: Vicksburg, Miss.

Cargill, K. W. (1986). *The Large Strain, Controlled Rate of Strain (LSCRS) Device for Consolidation Testing of Soft Fine-Grained Soils.* Technical Report GL-86-13, U. S. Army Engineer Waterways Experiment Station, CE: Vicksburg, Miss.

Carrier, W. I., & Keshian, B. J. (1979). Measurement and Prediction of Consolidation of Dredged Material. *12th Annual Dredging Seminar.* Texas A&M University.

Coe, H. S., & Clevenger, G. H. (1916). Methods for Determining the Capacities of Slime-Settling Tanks. *American Institute of Mining Engineers Transactions, 55*(9), 356-384.

Gao, Y. F., Zhang, Y., Zhou, Y., & Li, D. Y. (2016). Effects of Column Diameter on Setting

    Behavior of Dredged Slurry in Sedimentation Experiments. *Marine Georesources and*

    Geotechnology, 34, 431-439.

Gibson, R. E., England, G. L., & Hussey, M. L. (1967). The Theory of One-Dimensional

    Consolidation of Saturated Clays. I. Finite Non-Linear Consolidation of Thin

    Homogeneous Layers. *Geotechnique, 17*(3), 261-273.

Gibson, R. E., Schiffman, R. L., & Cargill, K. W. (1981). The Theory of One-Dimensional

    Consolidation of Saturated Clays. II. Finite Non-Linear Consolidation of Thick

    Homogeneous Layers. *Canadian Geotechnical Journal, 18*(2), 280-293.

Imai, G. (1980). A New In-Laboratory Method to Make Homogenous Clayey Samples and Their

    Mechanical Properties. *Soils and Foundations, 34*(2), 87-93.

Imai, G. (1980). Settling Behavior of Clay Suspension. *Soils and Foundations, 20*(2), 61-77.

Katagiri, M., & Imai, G. (1980). A New In-Laboratory Method to Make Homogenous Clayey

    Samples and Their Mechanical Properties. *Soils and Foundations, 34*(2), 87-93.

Lacasse, S. E., Lambe, T. W., & Marr, W. A. (1977). *Sizing of Containment Areas for Dredged*

    Material. Technical Report D-77-21, U.S. Army Engineer Waterways Experiment

    Station, CE: Vicksburg, Miss.

Lee, K., & Sills, G. C. (1981). The Consolidation of a Soil Stratum, Including Self-Weight

    Effects and Large Strains. *International Journal for Numerical and Analytical Methods in*

    Geomechanics, 5, 405-428.

Li, L., Alvarez, I. C., & Aubertin, J. D. (2013). Self-Weight Consolidation of Slurried

    Deposition: Tests and Interpretation. *International Journal of Geotechnical Engineering,*

    7(2), 205-213.

Lin, T. W. (1983). Sedimentation and Self Weight Consolidation of Dredge Spoil. *Retrospective*

    Theses and Dissertations. 7643.

McCarthy, D. F. (1977). *Essentials of Soil Mechanics and Foundations.* Reston, Virginia: Reston

    Publishing Company.

Mikasa, M. (1965). The Consolidation of Soft Clay, a New Consolidation Theory and Its

    Application. *Japanese Society of Civil Engineers*, 21-26.

Monte, J. L., & Krizek, R. J. (1975). One-Dimensional Mathematical Model for Large-Strain

    Consolidation. *Geotechnique, 26*(3), 495-510.

Montgomery, R. L. (1978). *Methodology for Design of Fine-Grained Deredged Material*

    Containment Areas for Solids Retention. Technical RepTechnical Report D-78-56, U.S.

    Army Engineer Waterways Experiment Station, CE: Vicksburg, Miss.

National Oceanic and Atmospheric Administration. (2018, June 25). *What is dredging?*

    Retrieved from www.oceanservice.noaa.gov:

    https://oceanservice.noaa.gov/facts/dredging.html

Palermo, M. R., Montgomery, R. L., & Poindexter, M. E. (1978). *Guidelines for Designing,*

    Operating, and Managing Dredged Material Containment Areas. Technical Report DS-

    78-10, U.S. Army Engineer Waterways Experiment Station, CE: Vicksburg, Miss.

Sridharan, A., & Prakash, K. (2003). Self Weight Consolidation: Compressibility Behavior of

    Segregated and Homogeneous Fine-Grained Sediments. *Marine Georesources and*

    Geotechnology, 21, 73-80.

Stark, T. D., Choi, H., & Schroeder, P. R. (2005). Settlement of Dredged and Contaminated

    Material Placement Areas. I: Theory and Use of Primary Consolidation, Secondary

    Compression, and Desiccation of Dredged Fill. *Journal of Waterway, Port, Coastal, and*

    Ocean Engineering, 131(2), 43-51.

Thackston, E. L., Palermo, M. R., & Schroeder, P. R. (1988). *Environmental Effects of*

    Dredging. Technical Report EEDP-02-5, U. S. Army Engineer Waterways Experiment

    Station, CE: Vicksburg, Miss.

U.S. Army Corps of Engineers. (1987). Confined Disposal of Dredged Material. *Engineer*

    Manual 1110-2-5027. Washington, DC: U.S. Army Corps of Engineers.

U.S. Army Corps of Engineers. (2012). *Savannah Harbor Expansion Project - Final GRR.*

    Retrieved from

    http://www.sas.usace.army.mil/Portals/61/docs/SHEP/reports/GRR/SHEP_GRR_Exec_S

    umm_JUL_2012.pdf

U.S. Army Corps of Engineers. (2012). *Savannah Harbor Expansion Project Dredged Material*

    Management Plan Update. Retrieved from

    http://www.sas.usace.army.mil/Portals/61/docs/SHEP/Reports/GRR/39%20SHEP%20Dr

    edged%20Material%20Management%20Plan%20January%202012.pdf

U.S. Army Corps of Engineers. (2015). Dredging and Dredged Material Management. *Engineer Manual 1110-2-5025*. Washington, DC: U.S. Army Corps of Engineers.

U.S. Army Corps of Engineers. (2017). *Savannah Harbor Expansion Frequently Asked Questions.* Retrieved from

http://www.sas.usace.army.mil/Portals/61/SHEP%20FAQs%20-

%2007%20April%202017.pdf

Appendix A: Data Tables & Figures

Table A-1: Calculations of Void ratio and Effective Stress from Laboratory Data for Test C-1.

Layer	Tare Wt.	Moist Wt. + Tare	Dry Wt. + Tare	Net Moist Wt.	Moisture Content	Weight of Solids	Weight of Water	Volume of Solids	Volume of Water	Total Volume	Height of Layer	Note 1	Note 2	Void Ratio of Layer	Height of Solids	Bouyant Weight of Solids	Effective Stress at Layer Bottom	Effective Stress at Layer Bottom	Linear Finite Strain Void
(-)	(gr)	(gr)	(gr)	(gr)	(%)	(gr)	(gr)	(cc)	(cc)	(cc)	(cm)	(cm)	(cm)	(-)	(cm)	(gr)	(gr/cm^2)	(psf)	(-)
1	8.4	278.8	82.1	270.4	266.89	73.7	196.7	27.91	196.70	224.61	1.27	1.27	0.63	7.05	0.158	0.259	0.259	0.530	7.049
2	8.5	278.4	83.7	269.9	258.91	75.2	194.7	28.47	194.70	223.17	1.26	2.53	1.90	6.84	0.161	0.264	0.523	1.071	6.911
3	8.6	278.3	84.7	269.7	254.40	76.1	193.6	28.81	193.60	222.41	1.26	3.79	3.16	6.72	0.163	0.267	0.790	1.618	6.785
4	8.6	278.1	85.5	269.5	250.46	76.9	192.6	29.12	192.60	221.72	1.25	5.04	4.41	6.61	0.165	0.270	1.060	2.171	6.672
5	8.4	278.4	86.0	270.0	247.94	77.6	192.4	29.38	192.40	221.78	1.25	6.29	5.67	6.55	0.166	0.272	1.332	2.729	6.569
6	8.4	278.5	86.5	270.1	245.84	78.1	192.0	29.57	192.00	221.57	1.25	7.54	6.92	6.49	0.167	0.274	1.606	3.290	6.477
7	8.5	277.0	86.8	268.5	242.91	78.3	190.2	29.65	190.20	219.85	1.24	8.79	8.16	6.42	0.168	0.275	1.881	3.853	6.394
8	8.3	274.4	86.3	266.1	241.15	78.0	188.1	29.53	188.10	217.63	1.23	10.02	9.40	6.37	0.167	0.274	2.155	4.414	6.320
9	8.4	280.2	88.7	271.8	238.48	80.3	191.5	30.41	191.50	221.91	1.25	11.27	10.64	6.30	0.172	0.282	2.437	4.991	6.253
10	8.5	278.4	88.9	269.9	235.70	80.4	189.5	30.44	189.50	219.94	1.24	12.51	11.89	6.22	0.172	0.282	2.719	5.570	6.192
11	8.8	278.6	89.7	269.8	233.50	80.9	188.9	30.63	188.90	219.53	1.24	13.75	13.13	6.17	0.173	0.284	3.003	6.151	6.138
12	8.5	278.2	89.8	269.7	231.73	81.3	188.4	30.78	188.40	219.18	1.24	14.99	14.37	6.12	0.174	0.285	3.289	6.736	6.090
13	8.6	277.8	90.2	269.2	229.90	81.6	187.6	30.90	187.60	218.50	1.23	16.22	15.61	6.07	0.175	0.286	3.575	7.322	6.047
14	8.4	276.9	90.7	268.5	226.25	82.3	186.2	31.16	186.20	217.36	1.23	17.45	16.84	5.98	0.176	0.289	3.864	7.914	6.008
15	8.4	193.5	65.3	185.1	225.31	56.9	128.2	21.54	128.20	149.74	0.85	18.30	17.88	5.95	0.122	0.200	4.064	8.323	5.984

Note1: Distance from the bottom of each layer to the top of sediment surface at the end of self weight consolidation.
Note 2: Distance from the middle of each layer to the top of sediment surface at the end of self weight consolidation.

Table A-2: Calculations of Void ratio and Effective Stress from Laboratory Data for Test C-2.

Layer	Tare Wt.	Moist Wt. + Tare	Dry Wt. + Tare	Net Moist Wt.	Moisture Content	Weight of Solids	Weight of Water	Volume of Solids	Volume of Water	Total Volume	Height of Layer	Note 1	Note 2	Void Ratio of Layer	Height of Solids	Bouyant Weight of Solids	Effective Stress at Layer Bottom	Effective Stress at Layer Bottom	Linear Finite Strain Void
(-)	(gr)	(gr)	(gr)	(gr)	(%)	(gr)	(gr)	(cc)	(cc)	(cc)	(cm)	(cm)	(cm)	(-)	(cm)	(gr)	(gr/cm^2)	(psf)	(-)
1	8.7	279.0	80.7	270.3	275.42	72.0	198.3	27.26	198.30	225.56	1.27	1.27	0.64	7.27	0.154	0.253	0.253	0.517	7.217
2	8.6	274.0	82.3	265.4	260.11	73.7	191.7	27.91	191.70	219.61	1.24	2.51	1.89	6.87	0.158	0.259	0.511	1.047	6.966
3	8.5	274.5	84.6	266.0	249.54	76.1	189.9	28.81	189.90	218.71	1.23	3.75	3.13	6.59	0.163	0.267	0.778	1.594	6.744
4	8.4	274.9	86.1	266.5	242.99	77.7	188.8	29.42	188.80	218.22	1.23	4.98	4.36	6.42	0.166	0.273	1.051	2.152	6.549
5	8.5	274.3	87.2	265.8	237.74	78.7	187.1	29.80	187.10	216.90	1.22	6.21	5.59	6.28	0.168	0.276	1.327	2.718	6.381
6	8.6	272.9	87.7	264.3	234.13	79.1	185.2	29.95	185.20	215.15	1.21	7.42	6.81	6.18	0.169	0.278	1.604	3.286	6.237
7	9.0	275.9	89.2	266.9	232.79	80.2	186.7	30.37	186.70	217.07	1.23	8.65	8.03	6.15	0.171	0.281	1.886	3.863	6.112
8	9.0	273.3	89.0	264.3	230.38	80.0	184.3	30.29	184.30	214.59	1.21	9.86	9.25	6.08	0.171	0.281	2.166	4.437	6.006
9	8.8	277.2	90.7	268.4	227.72	81.9	186.5	31.01	186.50	217.51	1.23	11.09	10.47	6.01	0.175	0.287	2.454	5.026	5.914
10	8.8	274.1	90.4	265.3	225.12	81.6	183.7	30.90	183.70	214.60	1.21	12.30	11.69	5.95	0.174	0.286	2.740	5.612	5.836
11	8.8	278.0	92.5	269.2	221.62	83.7	185.5	31.69	185.50	217.19	1.23	13.52	12.91	5.85	0.179	0.294	3.034	6.214	5.769
12	9.0	274.9	92.4	265.9	218.82	83.4	182.5	31.58	182.50	214.08	1.21	14.73	14.13	5.78	0.178	0.293	3.326	6.813	5.712
13	9.0	274.7	93.0	265.7	216.31	84.0	181.7	31.81	181.70	213.51	1.21	15.94	15.34	5.71	0.180	0.295	3.621	7.417	5.663
14	8.6	297.3	100.8	288.7	213.12	92.2	196.5	34.91	196.50	231.41	1.31	17.25	16.59	5.63	0.197	0.323	3.945	8.079	5.619

Note1: Distance from the bottom of each layer to the top of sediment surface at the end of self weight consolidation.
Note 2: Distance from the middle of each layer to the top of sediment surface at the end of self weight consolidation.

Table A-3: Calculations of Void ratio and Effective Stress from Laboratory Data for Test C-3.

Layer	Tare Wt.	Moist Wt.+Tare	Dry Wt.+Tare	Net Moist Wt.	Moisture Content	Weight of Solids	Weight of Water	Volume of Solids	Volume of Water	Total Volume	Height of Layer	Note 1	Note 2	Void Ratio of Layer	Height of Solids	Bouyant Weight of Solids	Effective Stress at Layer Bottom (gr/cm^2)	Effective Stress at Layer Bottom (psf)	Linear Finite Strain Void
(-)	(gr)	(gr)	(gr)	(gr)	(%)	(gr)	(gr)	(cc)	(cc)	(cc)	(cm)	(cm)	(cm)	(-)	(cm)	(gr)	(gr/cm^2)	(psf)	(-)
1	8.4	273.5	79.6	265.1	272.33	71.2	193.9	26.96	193.90	220.86	1.25	1.25	0.62	7.19	0.153	0.252	0.252	0.515	7.104
2	8.7	274.7	83.6	266.0	255.14	74.9	191.1	28.36	191.10	219.46	1.24	2.49	1.87	6.74	0.161	0.265	0.516	1.058	6.836
3	8.3	274.5	85.7	266.2	243.93	77.4	188.8	29.31	188.80	218.11	1.23	3.72	3.10	6.44	0.167	0.274	0.790	1.618	6.599
4	8.4	275.3	87.5	266.9	237.42	79.1	187.8	29.95	187.80	217.75	1.23	4.95	4.34	6.27	0.170	0.280	1.070	2.191	6.391
5	8.2	276.8	89.1	268.6	232.01	80.9	187.7	30.63	187.70	218.33	1.23	6.18	5.57	6.13	0.174	0.286	1.355	2.776	6.211
6	8.5	279.1	91.0	270.6	228.00	82.5	188.1	31.24	188.10	219.34	1.24	7.42	6.80	6.02	0.178	0.292	1.647	3.373	6.055
7	8.3	277.3	91.1	269.0	224.88	82.8	186.2	31.35	186.20	217.55	1.23	8.65	8.04	5.94	0.178	0.293	1.940	3.973	5.923
8	8.4	275.8	91.4	267.4	222.17	83.0	184.4	31.43	184.40	215.83	1.22	9.87	9.26	5.87	0.179	0.293	2.233	4.574	5.811
9	8.4	275.2	92.0	266.8	219.14	83.6	183.2	31.65	183.20	214.85	1.21	11.09	10.48	5.79	0.180	0.295	2.529	5.179	5.716
10	8.5	274.0	92.3	265.5	216.83	83.8	181.7	31.73	181.70	213.43	1.21	12.29	11.69	5.73	0.180	0.296	2.825	5.786	5.635
11	8.3	274.0	93.0	265.7	213.70	84.7	181.0	32.07	181.00	213.07	1.20	13.49	12.89	5.64	0.182	0.299	3.124	6.399	5.567
12	8.4	273.7	93.7	265.3	211.02	85.3	180.0	32.30	180.00	212.30	1.20	14.69	14.09	5.57	0.184	0.301	3.426	7.016	5.508
13	8.3	276.5	95.1	268.2	208.99	86.8	181.4	32.87	181.40	214.27	1.21	15.90	15.30	5.52	0.187	0.307	3.732	7.645	5.459
14	8.5	213.3	75.3	204.8	206.59	66.8	138.0	25.29	138.00	163.29	0.92	16.83	16.37	5.46	0.144	0.236	3.968	8.128	5.426

Note1: Distance from the bottom of each layer to the top of sediment surface at the end of self weight consolidation.
Note 2: Distance from the middle of each layer to the top of sediment surface at the end of self weight consolidation.

Table A-4: Calculations of Void ratio and Effective Stress from Laboratory Data for Test C-4.

Layer	Tare Wt.	Moist Wt.+Tare	Dry Wt.+Tare	Net Moist Wt.	Moisture Content	Weight of Solids	Weight of Water	Volume of Solids	Volume of Water	Total Volume	Height of Layer	Note 1	Note 2	Void Ratio of Layer	Height of Solids	Bouyant Weight of Solids	Effective Stress at Layer Bottom (gr/cm^2)	Effective Stress at Layer Bottom (psf)	Linear Finite Strain Void
(-)	(gr)	(gr)	(gr)	(gr)	(%)	(gr)	(gr)	(cc)	(cc)	(cc)	(cm)	(cm)	(cm)	(-)	(cm)	(gr)	(gr/cm^2)	(psf)	(-)
1	8.1	275.9	80.7	267.8	268.87	72.6	195.2	27.49	195.20	222.69	1.26	1.26	0.63	7.10	0.155	0.255	0.255	0.523	7.116
2	8.2	276.3	84.1	268.1	253.23	75.9	192.2	28.74	192.20	220.94	1.25	2.51	1.88	6.69	0.163	0.267	0.522	1.069	6.819
3	8.2	279.9	87.4	271.7	243.06	79.2	192.5	29.99	192.50	222.49	1.26	3.76	3.13	6.42	0.170	0.278	0.800	1.639	6.557
4	8.2	275.9	87.8	267.7	236.31	79.6	188.1	30.14	188.10	218.24	1.23	5.00	4.38	6.24	0.170	0.280	1.080	2.212	6.334
5	8.2	277.1	89.4	268.9	231.16	81.2	187.7	30.75	187.70	218.45	1.23	6.23	5.61	6.10	0.174	0.285	1.365	2.797	6.144
6	8.4	274.3	90.1	265.9	225.46	81.7	184.2	30.94	184.20	215.14	1.22	7.45	6.84	5.95	0.175	0.287	1.652	3.385	5.983
7	8.4	277.4	91.8	269.0	222.54	83.4	185.6	31.58	185.60	217.18	1.23	8.67	8.06	5.88	0.179	0.293	1.946	3.985	5.846
8	8.4	279.9	93.8	271.5	217.92	85.4	186.1	32.34	186.10	218.44	1.23	9.91	9.29	5.76	0.183	0.300	2.246	4.600	5.729
9	8.5	279.4	94.3	270.9	215.73	85.8	185.1	32.49	185.10	217.59	1.23	11.14	10.52	5.70	0.184	0.302	2.547	5.217	5.631
10	8.2	280.7	95.3	272.5	212.86	87.1	185.4	32.98	185.40	218.38	1.23	12.37	11.75	5.62	0.187	0.306	2.853	5.844	5.548
11	8.1	277.6	95.0	269.5	210.13	86.9	182.6	32.90	182.60	215.50	1.22	13.59	12.98	5.55	0.186	0.305	3.159	6.470	5.480
12	8.3	279.7	96.4	271.4	208.06	88.1	183.3	33.36	183.30	216.66	1.22	14.81	14.20	5.49	0.189	0.310	3.468	7.104	5.423
13	8.1	278.0	96.5	269.9	205.32	88.4	181.5	33.47	181.50	214.97	1.21	16.03	15.42	5.42	0.189	0.311	3.779	7.740	5.376
14	8.2	203.2	72.5	195.0	203.27	64.3	130.7	24.35	130.70	155.05	0.88	16.90	16.46	5.37	0.138	0.226	4.005	8.203	5.346

Note1: Distance from the bottom of each layer to the top of sediment surface at the end of self weight consolidation.
Note 2: Distance from the middle of each layer to the top of sediment surface at the end of self weight consolidation.

Table A-5: Calculations of Void ratio and Effective Stress from Laboratory Data for Test C-6.

Layer	Tare Wt.	Moist Wt.+Tare	Dry Wt.+Tare	Net Moist Wt.	Moisture Content	Weight of Solids	Weight of Water	Volume of Solids	Volume of Water	Total Volume	Height of Layer	Note 1	Note 2	Void Ratio of Layer	Height of Solids	Bouyant Weight of Solids	Effective Stress at Layer Bottom (gr/cm^2)	Effective Stress at Layer Bottom (psf)	Linear Finite Strain Void
(-)	(gr)	(gr)	(gr)	(gr)	(%)	(gr)	(gr)	(cc)	(cc)	(cc)	(cm)	(cm)	(cm)	(-)	(cm)	(gr)	(gr/cm^2)	(psf)	(-)
1	8.5	268.9	70.3	260.4	321.36	61.8	198.6	23.40	198.60	222.00	11.10	11.10	5.55	8.49	0.1	0.22	0.216	0.442	8.328
2	8.4	269.1	73.4	260.7	301.08	65.0	195.7	24.61	195.70	220.31	11.02	22.12	16.61	7.95	0.1	0.23	0.443	0.907	8.072
3	8.4	268.8	75.0	260.4	290.99	66.6	193.8	25.22	193.80	219.02	10.95	33.07	27.59	7.69	0.1	0.23	0.675	1.384	7.840
4	8.4	269.9	76.3	261.5	285.13	67.9	193.6	25.71	193.60	219.31	10.97	44.03	38.55	7.53	0.1	0.24	0.913	1.869	7.629
5	8.5	268.1	76.6	259.6	281.20	68.1	191.5	25.79	191.50	217.29	10.86	54.90	49.46	7.43	0.1	0.24	1.151	2.356	7.443
6	8.5	269.6	77.8	261.1	276.77	69.3	191.8	26.24	191.80	218.04	10.90	65.80	60.35	7.31	0.1	0.24	1.393	2.852	7.274
7	8.6	267.2	78.1	258.6	272.09	69.5	189.1	26.32	189.10	215.42	10.77	76.57	71.18	7.19	0.1	0.24	1.635	3.349	7.125
8	8.3	269.9	79.5	261.6	267.42	71.2	190.4	26.96	190.40	217.36	10.87	87.44	82.00	7.06	0.2	0.25	1.884	3.859	6.991
9	8.3	269.3	80.2	261.0	263.00	71.9	189.1	27.22	189.10	216.32	10.82	98.25	92.85	6.95	0.2	0.25	2.135	4.373	6.871
10	8.7	268.7	81.1	260.0	259.12	72.4	187.6	27.41	187.60	215.01	10.75	109.00	103.63	6.84	0.2	0.25	2.388	4.891	6.765
11	8.5	269.3	81.8	260.8	255.80	73.3	187.5	27.75	187.50	215.25	10.76	119.77	114.39	6.76	0.2	0.26	2.644	5.415	6.671
12	8.7	268.5	82.6	259.8	251.56	73.9	185.9	27.98	185.90	213.88	10.69	130.46	125.11	6.64	0.2	0.26	2.902	5.944	6.588
13	8.9	268.7	83.7	259.8	247.33	74.8	185.0	28.32	185.00	213.32	10.67	141.13	135.79	6.53	0.2	0.26	3.163	6.479	6.515
14	8.8	220.8	70.5	212.0	243.60	61.7	150.3	23.36	150.30	173.66	8.68	149.81	145.47	6.43	0.1	0.22	3.379	6.921	6.461

Note1: Distance from the bottom of each layer to the top of sediment surface at the end of self weight consolidation.
Note 2: Distance from the middle of each layer to the top of sediment surface at the end of self weight consolidation.

Table A-6: Calculations of Void ratio and Effective Stress from Laboratory Data for Test C-7.

Layer	Tare Wt.	Moist Wt. +Tare	Dry Wt. +Tare	Net Moist Wt.	Moisture Content	Weight of Solids	Weight of Water	Volume of Solids	Volume of Water	Total Volume	Height of Layer	Note 1	Note 2	Void Ratio of Layer	Height of Solids	Bouyant Weight of Solids	Effective Stress at Layer Bottom (gr/cm²)	Effective Stress at Layer Bottom (psf)	Linear Finite Strain Void
(-)	(gr)	(gr)	(gr)	(gr)	(%)	(gr)	(gr)	(cc)	(cc)	(cc)	(cm)	(cm)	(cm)	(-)	(cm)	(gr)	(gr/cm²)	(psf)	(-)
1	8.5	268.8	71.0	260.3	316.48	62.5	197.8	23.67	197.80	221.47	11.07	11.07	5.54	8.36	0.134	0.220	0.220	0.451	8.158
2	8.3	269.6	76.0	261.3	285.97	67.7	193.6	25.63	193.60	219.23	10.96	22.03	16.55	7.55	0.145	0.238	0.459	0.939	7.754
3	8.4	269.3	78.0	260.9	274.86	69.6	191.3	26.35	191.30	217.65	10.88	32.92	27.48	7.26	0.149	0.245	0.704	1.441	7.406
4	8.4	269.3	79.6	260.9	266.43	71.2	189.7	26.96	189.70	216.66	10.83	43.75	38.33	7.04	0.153	0.251	0.955	1.955	7.109
5	8.3	268.8	81.2	260.5	257.34	72.9	187.6	27.60	187.60	215.20	10.76	54.51	49.13	6.80	0.156	0.257	1.211	2.481	6.858
6	8.3	268.3	82.4	260.0	250.88	74.1	185.9	28.06	185.90	213.96	10.70	65.21	59.86	6.63	0.159	0.261	1.472	3.016	6.646
7	8.3	268.6	83.4	260.3	246.60	75.1	185.2	28.44	185.20	213.64	10.68	75.89	70.55	6.51	0.161	0.265	1.737	3.558	6.470
8	8.4	269.9	84.7	261.5	242.73	76.3	185.2	28.89	185.20	214.09	10.70	86.60	81.24	6.41	0.164	0.269	2.006	4.108	6.322
9	8.4	270.0	85.7	261.6	238.42	77.3	184.3	29.27	184.30	213.57	10.68	97.27	91.93	6.30	0.166	0.272	2.278	4.666	6.200
10	8.5	268.6	86.2	260.1	234.75	77.7	182.4	29.42	182.40	211.82	10.59	107.86	102.57	6.20	0.167	0.274	2.552	5.226	6.099
11	8.4	268.9	86.9	260.5	231.85	78.5	182.0	29.72	182.00	211.72	10.59	118.45	113.16	6.12	0.169	0.277	2.828	5.793	6.017
12	8.7	270.5	88.7	261.8	227.25	80.0	181.8	30.29	181.80	212.09	10.60	129.06	123.75	6.00	0.172	0.282	3.110	6.370	5.948
13	8.4	183.0	61.9	174.6	226.36	53.5	121.1	20.26	121.10	141.36	7.07	136.12	132.59	5.98	0.115	0.188	3.298	6.756	5.909

Note1: Distance from the bottom of each layer to the top of sediment surface at the end of self weight consolidation.
Note 2: Distance from the middle of each layer to the top of sediment surface at the end of self weight consolidation.

Table A-7: Calculations of Void ratio and Effective Stress from Laboratory Data for Test C-8.

Layer	Tare Wt.	Moist Wt. +Tare	Dry Wt. +Tare	Net Moist Wt.	Moisture Content	Weight of Solids	Weight of Water	Volume of Solids	Volume of Water	Total Volume	Height of Layer	Note 1	Note 2	Void Ratio of Layer	Height of Solids	Bouyant Weight of Solids	Effective Stress at Layer Bottom (gr/cm²)	Effective Stress at Layer Bottom (psf)	Linear Finite Strain Void
(-)	(gr)	(gr)	(gr)	(gr)	(%)	(gr)	(gr)	(cc)	(cc)	(cc)	(cm)	(cm)	(cm)	(-)	(cm)	(gr)	(gr/cm²)	(psf)	(-)
1	8.3	268.1	73.5	259.8	298.47	65.2	194.6	24.69	194.60	219.29	1.24	1.24	0.62	7.88	0.140	0.230	0.230	0.471	7.935
2	8.6	267.9	77.3	259.3	277.44	68.7	190.6	26.01	190.60	216.61	1.23	2.47	1.86	7.33	0.148	0.242	0.472	0.967	7.488
3	8.3	266.1	79.0	257.8	264.64	70.7	187.1	26.77	187.10	213.87	1.21	3.69	3.08	6.99	0.152	0.249	0.721	1.477	7.112
4	8.4	267.7	81.6	259.3	254.23	73.2	186.1	27.72	186.10	213.82	1.21	4.90	4.29	6.71	0.157	0.258	0.979	2.005	6.795
5	8.4	269.5	83.7	261.1	246.75	75.3	185.8	28.51	185.80	214.31	1.22	6.11	5.51	6.52	0.162	0.265	1.244	2.549	6.532
6	8.5	267.1	84.4	258.6	240.71	75.9	182.7	28.74	182.70	211.44	1.20	7.31	6.71	6.36	0.163	0.268	1.512	3.097	6.319
7	8.5	269.8	86.5	261.3	235.00	78.0	183.3	29.53	183.30	212.83	1.21	8.52	7.92	6.21	0.168	0.275	1.787	3.660	6.144
8	8.6	268.7	87.3	260.1	230.50	78.7	181.4	29.80	181.40	211.20	1.20	9.72	9.12	6.09	0.169	0.277	2.064	4.228	6.003
9	8.3	266.4	87.4	258.1	226.30	79.1	179.0	29.95	179.00	208.95	1.19	10.90	10.31	5.98	0.170	0.279	2.343	4.799	5.890
10	8.5	268.2	88.8	259.7	223.41	80.3	179.4	30.41	179.40	209.81	1.19	12.09	11.50	5.90	0.172	0.283	2.626	5.379	5.799
11	8.4	268.6	89.5	260.2	220.84	81.1	179.1	30.71	179.10	209.81	1.19	13.28	12.69	5.83	0.174	0.286	2.912	5.964	5.726
12	8.6	267.3	89.9	258.7	218.20	81.3	177.4	30.78	177.40	208.18	1.18	14.46	13.87	5.76	0.175	0.287	3.198	6.551	5.668
13	8.5	161.1	57.0	152.6	214.64	48.5	104.1	18.36	104.10	122.46	0.69	15.16	14.81	5.67	0.104	0.171	3.369	6.901	5.640

Note1: Distance from the bottom of each layer to the top of sediment surface at the end of self weight consolidation.
Note 2: Distance from the middle of each layer to the top of sediment surface at the end of self weight consolidation.

Table A-8: Calculations of Void ratio and Effective Stress from Laboratory Data for Test C-9.

Layer	Tare Wt.	Moist Wt. +Tare	Dry Wt. +Tare	Net Moist Wt.	Moisture Content	Weight of Solids	Weight of Water	Volume of Solids	Volume of Water	Total Volume	Height of Layer	Note 1	Note 2	Void Ratio of Layer	Height of Solids	Bouyant Weight of Solids	Effective Stress at Layer Bottom (gr/cm²)	Effective Stress at Layer Bottom (psf)	Linear Finite Strain Void
(-)	(gr)	(gr)	(gr)	(gr)	(%)	(gr)	(gr)	(cc)	(cc)	(cc)	(cm)	(cm)	(cm)	(-)	(cm)	(gr)	(gr/cm²)	(psf)	(-)
1	8.4	271.5	73.6	263.1	303.53	65.2	197.9	24.69	197.90	222.59	1.26	1.26	0.63	8.02	0.140	0.229	0.229	0.470	7.948
2	8.3	271.3	78.4	263.0	275.18	70.1	192.9	26.54	192.90	219.44	1.24	2.50	1.88	7.27	0.150	0.247	0.476	0.975	7.465
3	8.4	270.9	80.9	262.5	262.07	72.5	190.0	27.45	190.00	217.45	1.23	3.73	3.12	6.92	0.155	0.255	0.731	1.498	7.062
4	8.4	272.3	83.1	263.9	253.28	74.7	189.2	28.28	189.20	217.48	1.23	4.97	4.35	6.69	0.160	0.263	0.994	2.036	6.730
5	8.4	272.9	85.1	264.5	244.85	76.7	187.8	29.04	187.80	216.84	1.23	6.19	5.58	6.47	0.164	0.270	1.264	2.589	6.458
6	8.4	271.2	86.1	262.8	238.22	77.7	185.1	29.42	185.10	214.52	1.21	7.41	6.80	6.29	0.167	0.273	1.537	3.149	6.241
7	8.4	270.7	87.2	262.3	232.87	78.8	183.5	29.84	183.50	213.34	1.21	8.62	8.01	6.15	0.169	0.277	1.814	3.716	6.067
8	8.5	271.8	89.0	263.3	227.08	80.5	182.8	30.48	182.80	213.28	1.21	9.82	9.22	6.00	0.173	0.283	2.098	4.296	5.927
9	8.5	271.8	89.8	263.3	223.86	81.3	182.0	30.78	182.00	212.78	1.20	11.03	10.43	5.91	0.174	0.286	2.384	4.882	5.816
10	8.5	271.4	90.5	262.9	220.61	82.0	180.9	31.05	180.90	211.95	1.20	12.23	11.63	5.83	0.176	0.289	2.672	5.473	5.729
11	8.5	270.7	91.2	262.2	217.05	82.7	179.5	31.31	179.50	210.81	1.19	13.42	12.83	5.73	0.177	0.291	2.963	6.069	5.661
12	8.6	270.4	92.2	261.8	213.16	83.6	178.2	31.65	178.20	209.85	1.19	14.61	14.02	5.63	0.179	0.294	3.257	6.672	5.607
13	8.5	110.8	41.2	102.3	212.84	32.7	69.6	12.38	69.60	81.98	0.46	15.08	14.84	5.62	0.070	0.115	3.372	6.907	5.589

Note1: Distance from the bottom of each layer to the top of sediment surface at the end of self weight consolidation.
Note 2: Distance from the middle of each layer to the top of sediment surface at the end of self weight consolidation.

Table A-9: Calculations of Void ratio and Effective Stress from Laboratory Data for Test C-11.

Layer	Tare Wt.	Moist Wt. + Tare	Dry Wt. + Tare	Net Moist Wt.	Moisture Content	Weight of Solids	Weight of Water	Volume of Solids	Volume of Water	Total Volume	Height of Layer	Note 1	Note 2	Void Ratio of Layer	Height of Solids	Bouyant Weight of Solids	Effective Stress at Layer Bottom	Effective Stress at Layer Bottom	Linear Finite Strain Void
(-)	(gr)	(gr)	(gr)	(gr)	(%)	(gr)	(gr)	(cc)	(cc)	(cc)	(cm)	(cm)	(cm)	(-)	(cm)	(gr)	(gr/cm²)	(psf)	(-)
1	9.3	262.0	63.0	252.7	370.58	53.7	199.0	20.33	199.00	219.33	1.24	1.24	0.62	9.79	0.115	0.188	0.188	0.385	9.708
2	8.3	261.6	66.0	253.3	338.99	57.7	195.6	21.85	195.60	217.45	1.23	2.46	1.85	8.95	0.123	0.202	0.390	0.799	9.253
3	8.4	262.3	67.8	253.9	327.44	59.4	194.5	22.49	194.50	216.99	1.22	3.69	3.07	8.65	0.127	0.208	0.598	1.225	8.851
4	8.5	262.0	68.9	253.5	319.70	60.4	193.1	22.87	193.10	215.97	1.22	4.90	4.29	8.44	0.129	0.212	0.810	1.659	8.503
5	8.4	262.6	70.2	254.2	311.33	61.8	192.4	23.40	192.40	215.80	1.22	6.12	5.51	8.22	0.132	0.216	1.026	2.102	8.200
6	8.3	262.0	71.3	253.7	302.70	63.0	190.7	23.85	190.70	214.55	1.21	7.33	6.72	7.99	0.134	0.221	1.247	2.554	7.938
7	8.5	260.6	72.2	252.1	295.76	63.7	188.4	24.12	188.40	212.52	1.20	8.53	7.93	7.81	0.136	0.223	1.470	3.011	7.714
8	8.3	264.7	74.0	256.4	290.26	65.7	190.7	24.88	190.70	215.58	1.22	9.74	9.13	7.67	0.140	0.230	1.700	3.482	7.520
9	8.4	264.6	74.9	256.2	285.26	66.5	189.7	25.18	189.70	214.88	1.21	10.95	10.35	7.53	0.142	0.233	1.933	3.959	7.355
10	8.4	266.1	76.3	257.7	279.53	67.9	189.8	25.71	189.80	215.51	1.21	12.17	11.56	7.38	0.145	0.238	2.171	4.446	7.214
11	8.2	262.1	75.9	253.9	275.04	67.7	186.2	25.63	186.20	211.83	1.19	13.36	12.76	7.26	0.144	0.237	2.408	4.932	7.097
12	8.4	262.6	77.2	254.2	269.48	68.8	185.4	26.05	185.40	211.45	1.19	14.55	13.96	7.12	0.147	0.241	2.649	5.426	6.997
13	8.3	248.6	74.3	240.3	264.09	66.0	174.3	24.99	174.30	199.29	1.12	15.68	15.12	6.97	0.141	0.231	2.880	5.899	6.917

Note1: Distance from the bottom of each layer to the top of sediment surface at the end of self weight consolidation.
Note 2: Distance from the middle of each layer to the top of sediment surface at the end of self weight consolidation.

Table A-10: Calculations of Void ratio and Effective Stress from Laboratory Data for Test C-12.

Layer	Tare Wt.	Moist Wt. + Tare	Dry Wt. + Tare	Net Moist Wt.	Moisture Content	Weight of Solids	Weight of Water	Volume of Solids	Volume of Water	Total Volume	Height of Layer	Note 1	Note 2	Void Ratio of Layer	Height of Solids	Bouyant Weight of Solids	Effective Stress at Layer Bottom	Effective Stress at Layer Bottom	Linear Finite Strain Void
(-)	(gr)	(gr)	(gr)	(gr)	(%)	(gr)	(gr)	(cc)	(cc)	(cc)	(cm)	(cm)	(cm)	(-)	(cm)	(gr)	(gr/cm²)	(psf)	(-)
1	8.5	261.0	64.4	252.5	351.70	55.9	196.6	21.17	196.60	217.77	1.25	1.25	0.62	9.29	0.121	0.199	0.199	0.408	9.321
2	8.9	262.1	69.4	253.2	318.51	60.5	192.7	22.91	192.70	215.61	1.24	2.48	1.87	8.41	0.131	0.216	0.415	0.849	8.713
3	7.5	261.8	71.0	254.3	300.47	63.5	190.8	24.04	190.80	214.84	1.23	3.72	3.10	7.94	0.138	0.226	0.641	1.313	8.193
4	8.6	260.2	73.4	251.6	288.27	64.8	186.8	24.54	186.80	211.34	1.21	4.93	4.32	7.61	0.141	0.231	0.872	1.786	7.763
5	8.4	262.3	75.6	253.9	277.83	67.2	186.7	25.44	186.70	212.14	1.22	6.15	5.54	7.34	0.146	0.239	1.111	2.276	7.404
6	8.2	262.6	77.0	254.4	269.77	68.8	185.6	26.05	185.60	211.65	1.21	7.36	6.75	7.12	0.149	0.245	1.356	2.778	7.110
7	8.7	260.0	77.5	251.3	265.26	68.8	182.5	26.05	182.50	208.55	1.20	8.55	7.96	7.01	0.149	0.245	1.601	3.280	6.876
8	8.5	260.0	78.7	251.5	258.26	70.2	181.3	26.58	181.30	207.88	1.19	9.75	9.15	6.82	0.152	0.250	1.852	3.792	6.685
9	8.5	262.1	80.6	253.6	251.73	72.1	181.5	27.30	181.50	208.80	1.20	10.94	10.35	6.65	0.157	0.257	2.108	4.319	6.530
10	8.3	261.0	80.6	252.7	249.52	72.3	180.4	27.38	180.40	207.78	1.19	12.14	11.54	6.59	0.157	0.258	2.366	4.846	6.407
11	8.8	261.3	82.0	252.5	244.95	73.2	179.3	27.72	179.30	207.02	1.19	13.32	12.73	6.47	0.159	0.261	2.627	5.380	6.310
12	8.5	245.0	78.1	236.5	239.80	69.6	166.9	26.35	166.90	193.25	1.11	14.43	13.88	6.33	0.151	0.248	2.875	5.888	6.236

Note1: Distance from the bottom of each layer to the top of sediment surface at the end of self weight consolidation.
Note 2: Distance from the middle of each layer to the top of sediment surface at the end of self weight consolidation.

Table A-11: Calculations of Void ratio and Effective Stress from Laboratory Data for Test C-13.

Layer	Tare Wt.	Moist Wt. + Tare	Dry Wt. + Tare	Net Moist Wt.	Moisture Content	Weight of Solids	Weight of Water	Volume of Solids	Volume of Water	Total Volume	Height of Layer	Note 1	Note 2	Void Ratio of Layer	Height of Solids	Bouyant Weight of Solids	Effective Stress at Layer Bottom	Effective Stress at Layer Bottom	Linear Finite Strain Void
(-)	(gr)	(gr)	(gr)	(gr)	(%)	(gr)	(gr)	(cc)	(cc)	(cc)	(cm)	(cm)	(cm)	(-)	(cm)	(gr)	(gr/cm²)	(psf)	(-)
1	8.2	269.9	68.5	261.7	334.00	60.3	201.4	22.83	201.40	224.23	1.26	1.26	0.63	8.82	0.128	0.210	0.210	0.430	8.867
2	8.2	270.0	73.0	261.8	304.01	64.8	197.0	24.54	197.00	221.54	1.24	2.50	1.88	8.03	0.138	0.226	0.436	0.893	8.276
3	8.2	267.6	75.5	259.4	285.44	67.3	192.1	25.48	192.10	217.58	1.22	3.72	3.11	7.54	0.143	0.235	0.670	1.373	7.779
4	8.2	267.7	77.6	259.5	273.92	69.4	190.1	26.28	190.10	216.38	1.21	4.93	4.33	7.23	0.147	0.242	0.912	1.869	7.368
5	8.2	268.1	79.8	259.9	262.99	71.6	188.3	27.11	188.30	215.41	1.21	6.14	5.54	6.95	0.152	0.250	1.162	2.380	7.029
6	8.2	267.2	81.2	259.0	254.79	73.0	186.0	27.64	186.00	213.64	1.20	7.34	6.74	6.73	0.155	0.254	1.416	2.901	6.756
7	8.2	267.4	82.8	259.2	247.45	74.6	184.6	28.25	184.60	212.85	1.19	8.53	7.94	6.54	0.158	0.260	1.676	3.433	6.535
8	8.2	267.6	83.9	259.4	242.67	75.7	183.7	28.66	183.70	212.36	1.19	9.73	9.13	6.41	0.161	0.264	1.940	3.974	6.359
9	8.2	269.7	85.5	261.5	238.29	77.3	184.2	29.27	184.20	213.47	1.20	10.92	10.32	6.29	0.164	0.269	2.209	4.525	6.219
10	8.2	266.2	85.3	258.0	234.63	77.1	180.9	29.19	180.90	210.09	1.18	12.10	11.51	6.20	0.164	0.269	2.478	5.076	6.109
11	8.2	269.2	87.5	261.0	229.13	79.3	181.7	30.03	181.70	211.73	1.19	13.29	12.69	6.05	0.168	0.276	2.754	5.642	6.022
12	8.2	134.3	46.7	126.1	227.53	38.5	87.6	14.58	87.60	102.18	0.57	13.86	13.57	6.01	0.082	0.134	2.889	5.916	5.987

Note1: Distance from the bottom of each layer to the top of sediment surface at the end of self weight consolidation.
Note 2: Distance from the middle of each layer to the top of sediment surface at the end of self weight consolidation.

Table A-12: Calculations of Void ratio and Effective Stress from Laboratory Data for Test C-14.

Layer	Tare Wt.	Moist Wt. + Tare	Dry Wt. + Tare	Net Moist Wt.	Moisture Content	Weight of Solids	Weight of Water	Volume of Solids	Volume of Water	Total Volume	Height of Layer	Note 1	Note 2	Void Ratio of Layer	Height of Solids	Bouyant Weight of Solids	Effective Stress at Layer Bottom	Effective Stress at Layer Bottom	Linear Finite Strain Void
(-)	(gr)	(gr)	(gr)	(gr)	(%)	(gr)	(gr)	(cc)	(cc)	(cc)	(cm)	(cm)	(cm)	(-)	(cm)	(gr)	(gr/cm^2)	(psf)	(-)
1	8.2	261.5	67.6	253.3	326.43	59.4	193.9	22.49	193.90	216.39	1.24	1.24	0.62	8.62	0.129	0.212	0.212	0.434	8.648
2	8.2	263.4	72.5	255.2	296.89	64.3	190.9	24.35	190.90	215.25	1.24	2.48	1.86	7.84	0.140	0.229	0.441	0.904	8.069
3	8.2	261.1	74.9	252.9	279.16	66.7	186.2	25.26	186.20	211.46	1.21	3.69	3.09	7.37	0.145	0.238	0.680	1.392	7.583
4	8.2	263.8	77.7	255.6	267.77	69.5	186.1	26.32	186.10	212.42	1.22	4.91	4.30	7.07	0.151	0.248	0.928	1.900	7.176
5	8.2	260.5	78.6	252.3	258.38	70.4	181.9	26.66	181.90	208.56	1.20	6.11	5.51	6.82	0.153	0.251	1.179	2.414	6.846
6	8.3	261.4	80.6	253.1	250.07	72.3	180.8	27.38	180.80	208.18	1.20	7.31	6.71	6.60	0.157	0.258	1.437	2.943	6.577
7	8.1	264.2	83.0	256.1	241.92	74.9	181.2	28.36	181.20	209.56	1.20	8.51	7.91	6.39	0.163	0.267	1.704	3.490	6.357
8	8.2	261.4	83.2	253.2	237.60	75.0	178.2	28.40	178.20	206.60	1.19	9.70	9.10	6.28	0.163	0.268	1.972	4.039	6.184
9	8.2	263.7	84.8	255.5	233.55	76.6	178.9	29.00	178.90	207.90	1.19	10.89	10.29	6.17	0.167	0.273	2.245	4.599	6.046
10	8.1	261.1	84.8	253.0	229.86	76.7	176.3	29.04	176.30	205.34	1.18	12.07	11.48	6.07	0.167	0.274	2.519	5.159	5.937
11	8.2	261.9	86.0	253.7	226.09	77.8	175.9	29.46	175.90	205.36	1.18	13.25	12.66	5.97	0.169	0.278	2.797	5.728	5.852
12	8.1	77.2	29.4	69.1	224.41	21.3	47.8	8.07	47.80	55.87	0.32	13.57	13.41	5.93	0.046	0.076	2.873	5.884	5.832

Note1: Distance from the bottom of each layer to the top of sediment surface at the end of self weight consolidation.

Note 2: Distance from the middle of each layer to the top of sediment surface at the end of self weight consolidation.

Figure A-1: Laboratory Test Curve with Best Apparent Fit Curve Fitted Using Equation 2.29 for Test C-1.
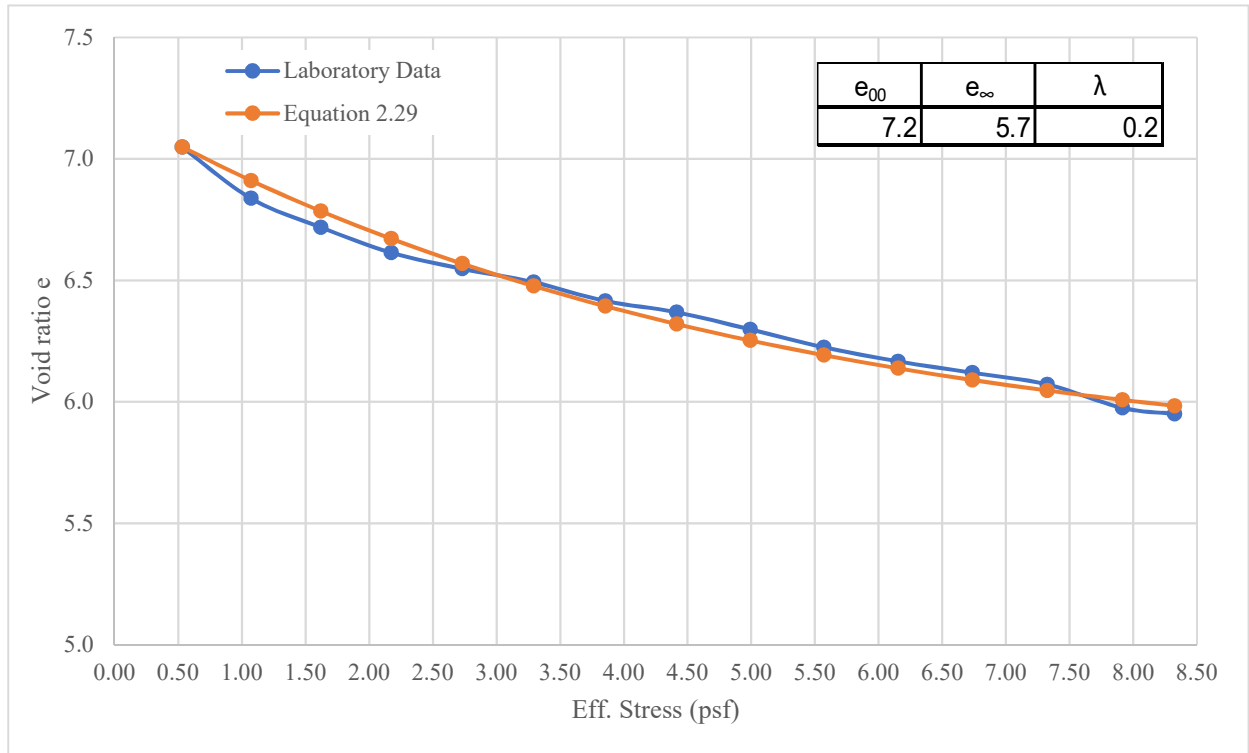
Figure A-2: Laboratory Test Curve with Best Apparent Fit Curve Fitted Using Equation 2.29 for Test C-2.
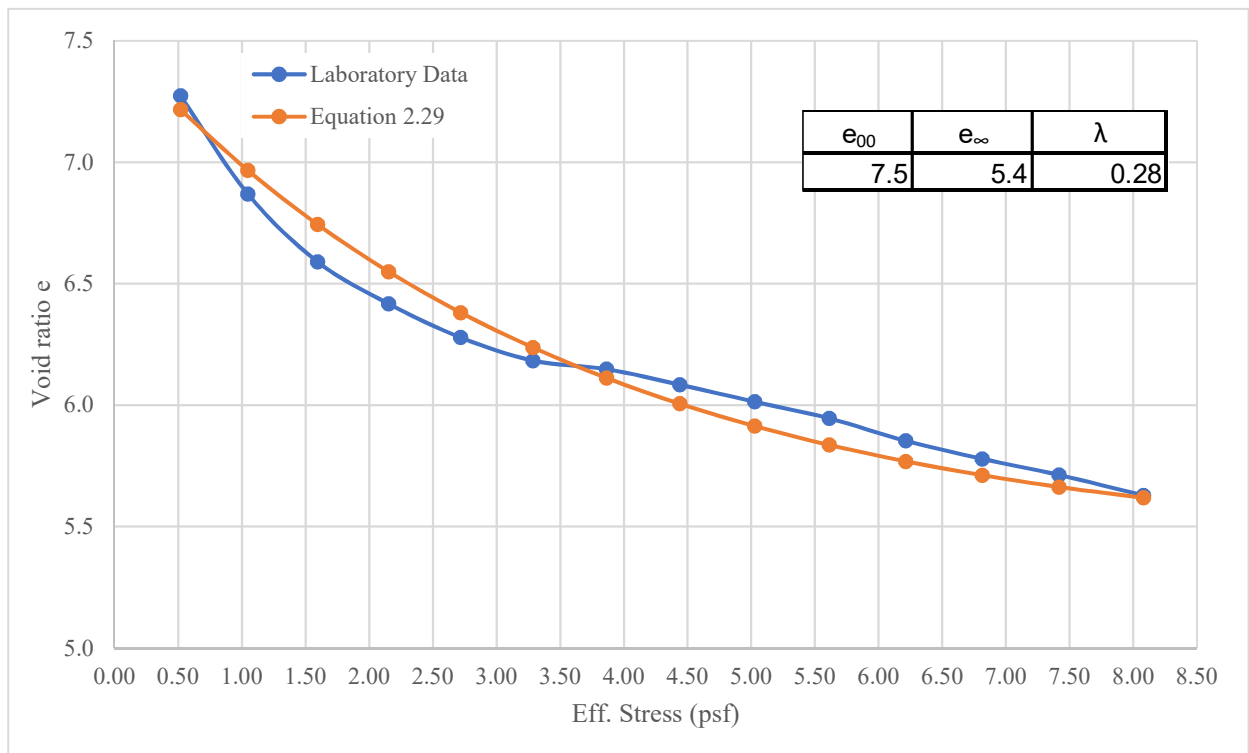
Figure A-3: Laboratory Test Curve with Best Apparent Fit Curve Fitted Using Equation 2.29 for Test C-3.

e_{00}	e_{∞}	λ
7.4	5.2	0.28
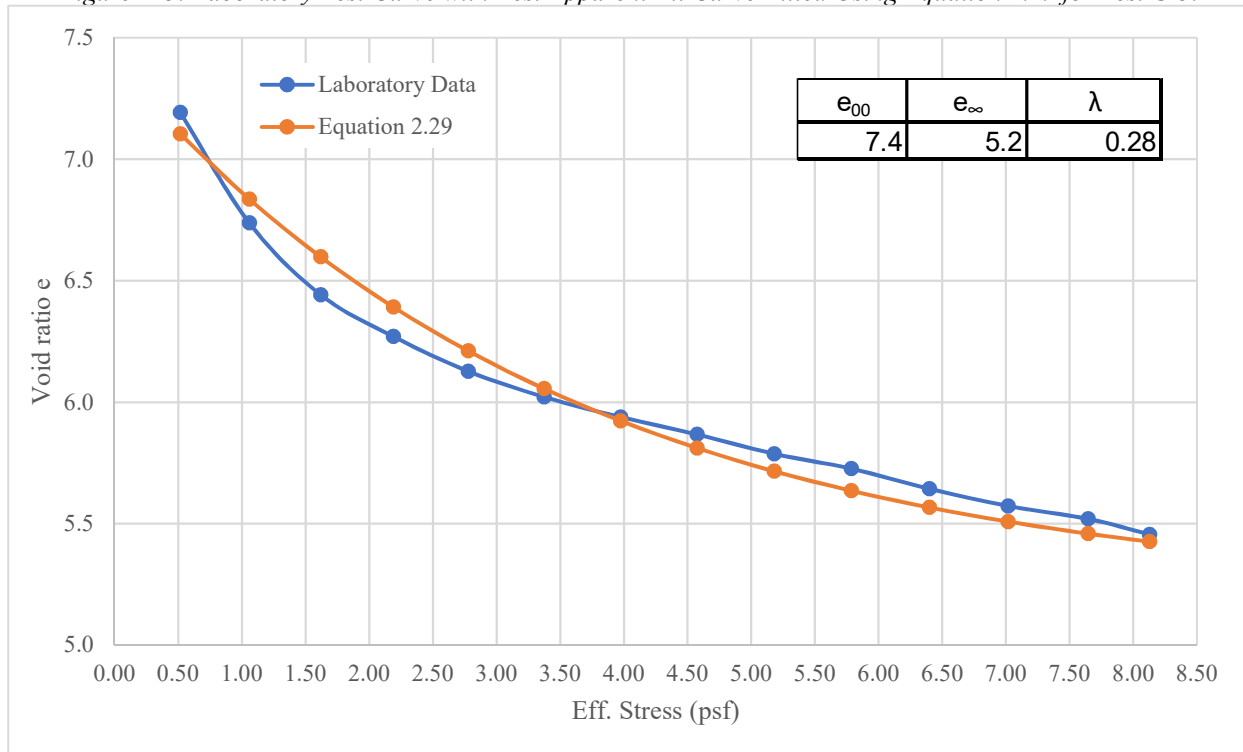
Figure A-4: Laboratory Test Curve with Best Apparent Fit Curve Fitted Using Equation 2.29 for Test C-4.

e_{00}	e_{∞}	λ
7.45	5.15	0.3

100
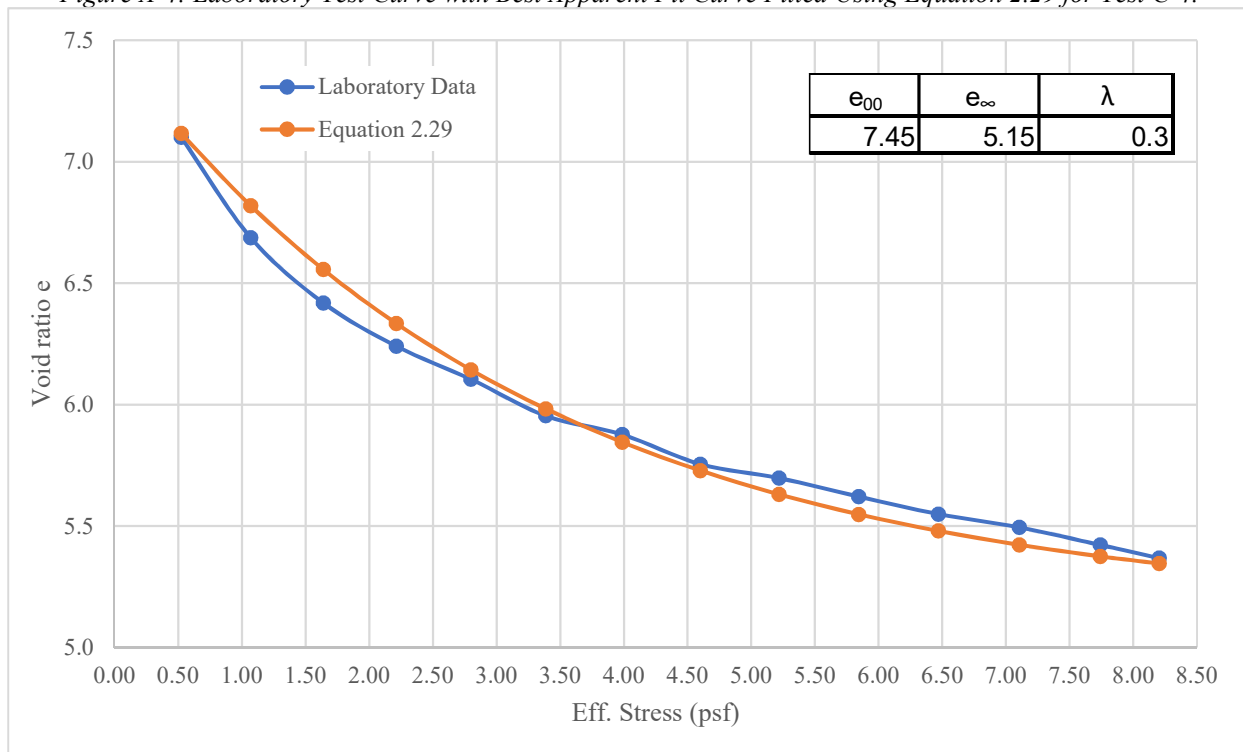
Figure A-5: Laboratory Test Curve with Best Apparent Fit Curve Fitted Using Equation 2.29 for Test C-6.

e_{00}	e_{∞}	λ
8.60	6.00	0.25
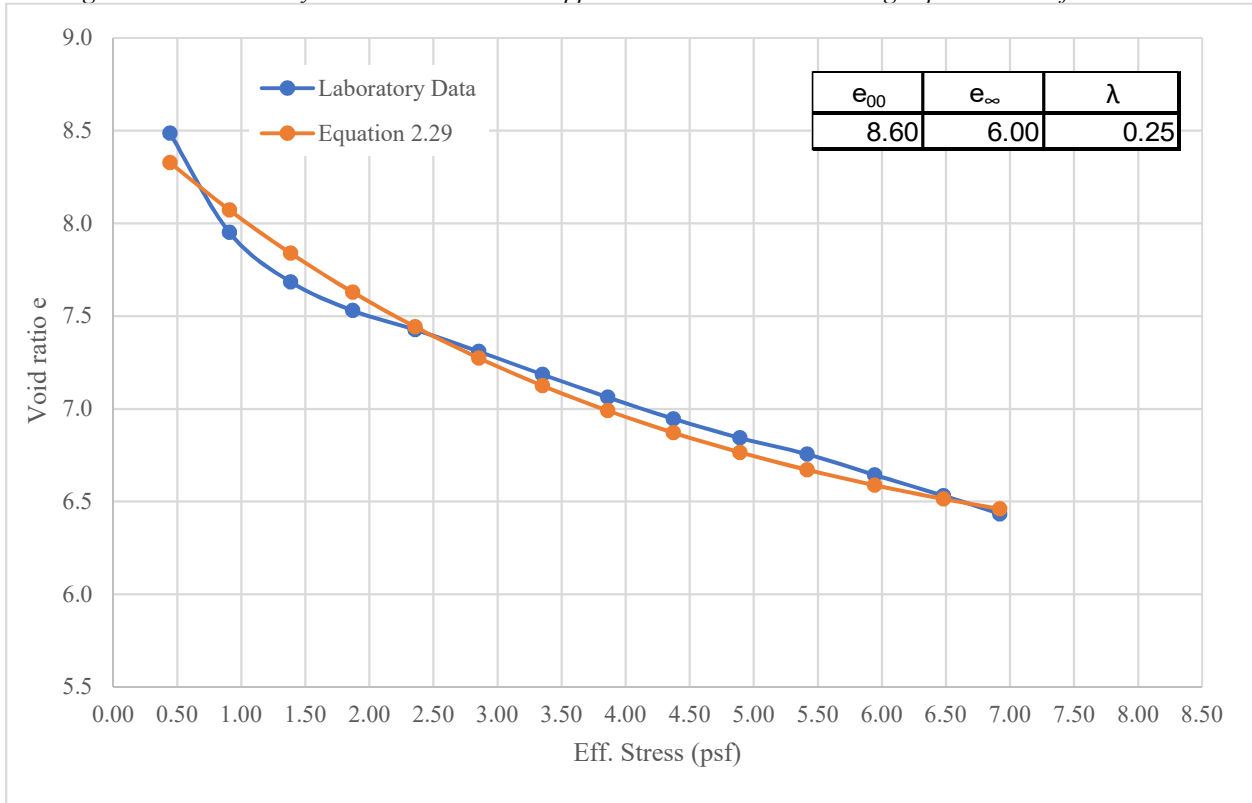
Figure A-6: Laboratory Test Curve with Best Apparent Fit Curve Fitted Using Equation 2.29 for Test C-7.

e_{00}	e_{∞}	λ
8.6	5.65	0.36
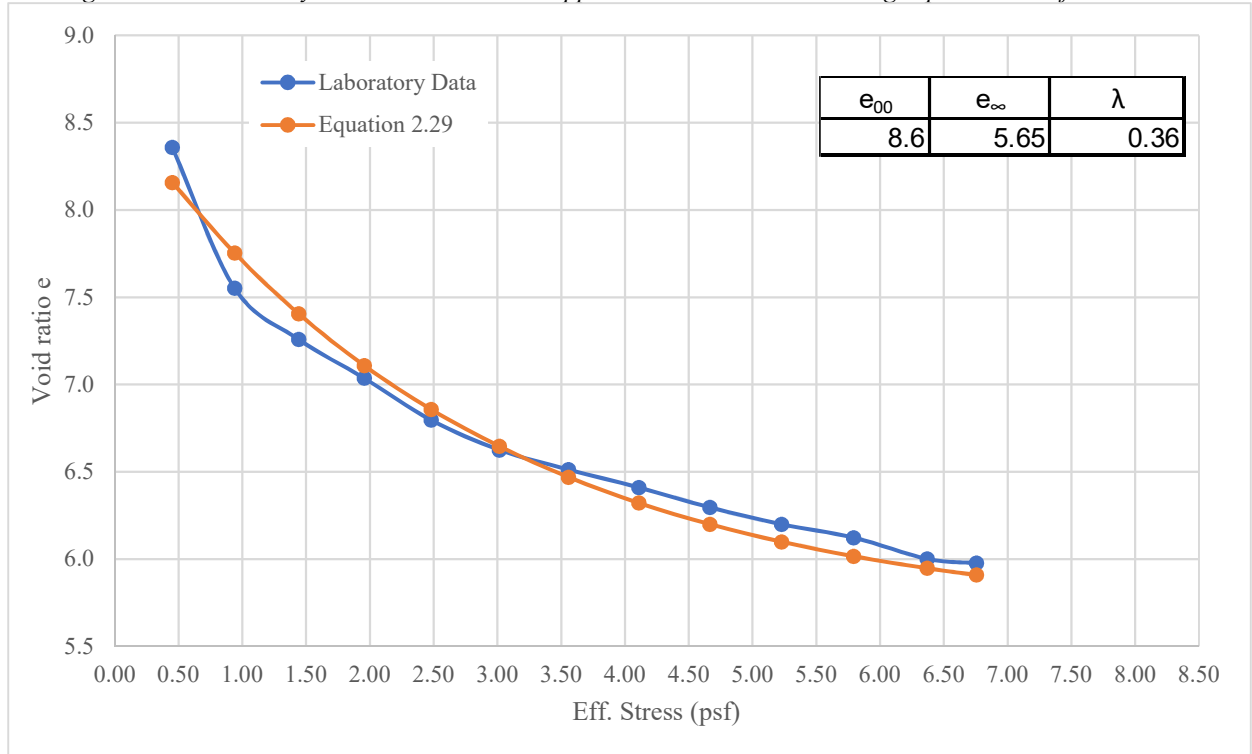
Figure A-7: Laboratory Test Curve with Best Apparent Fit Curve Fitted Using Equation 2.29 for Test C-8.

e_{00}	e_{∞}	λ
8.45	5.45	0.4
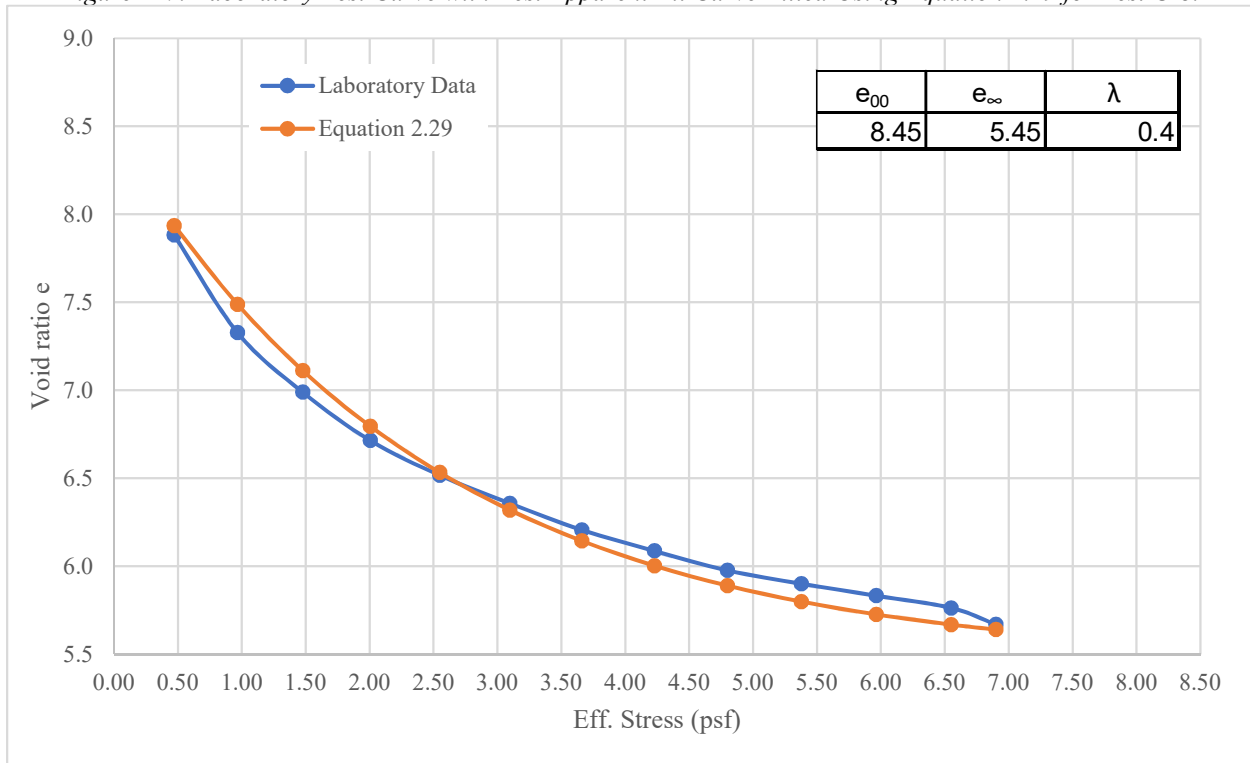
Figure A-8: Laboratory Test Curve with Best Apparent Fit Curve Fitted Using Equation 2.29 for Test C-9.

e_{00}	e_{∞}	λ
8.5	5.42	0.42
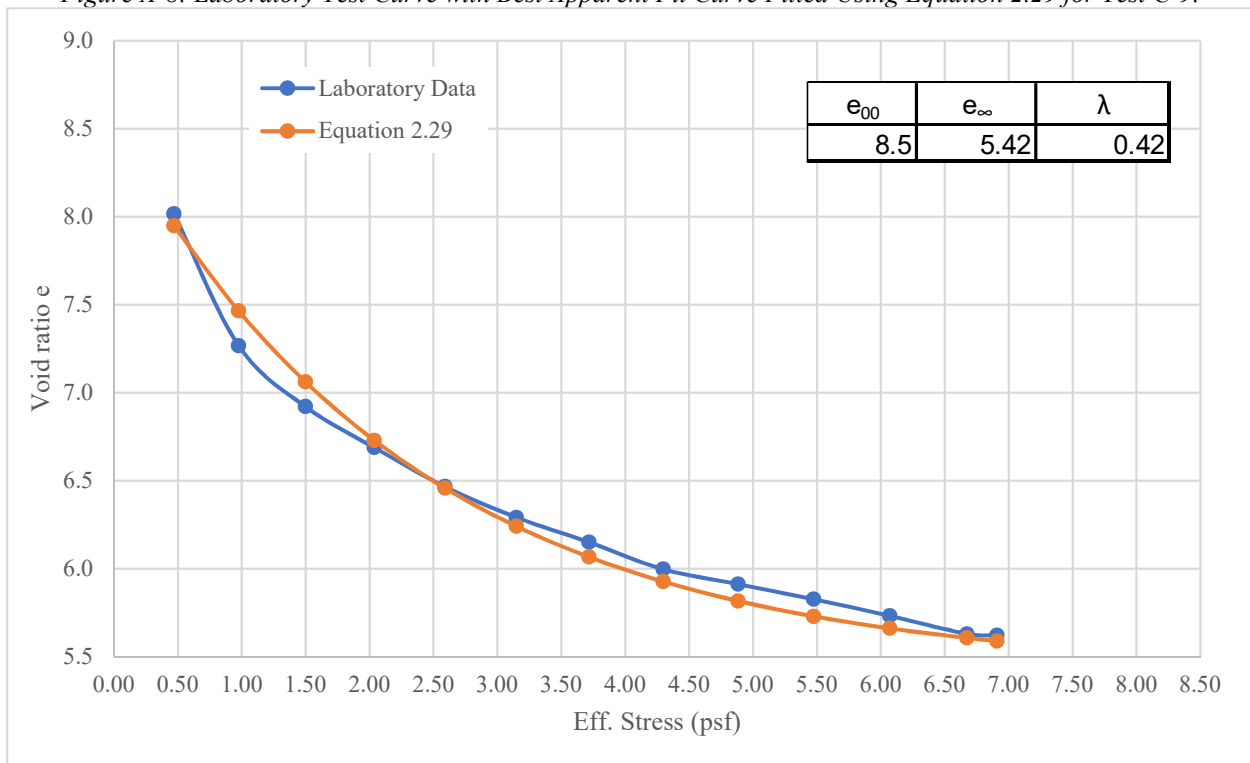
Figure A-9: Laboratory Test Curve with Best Apparent Fit Curve Fitted Using Equation 2.29 for Test C-11.
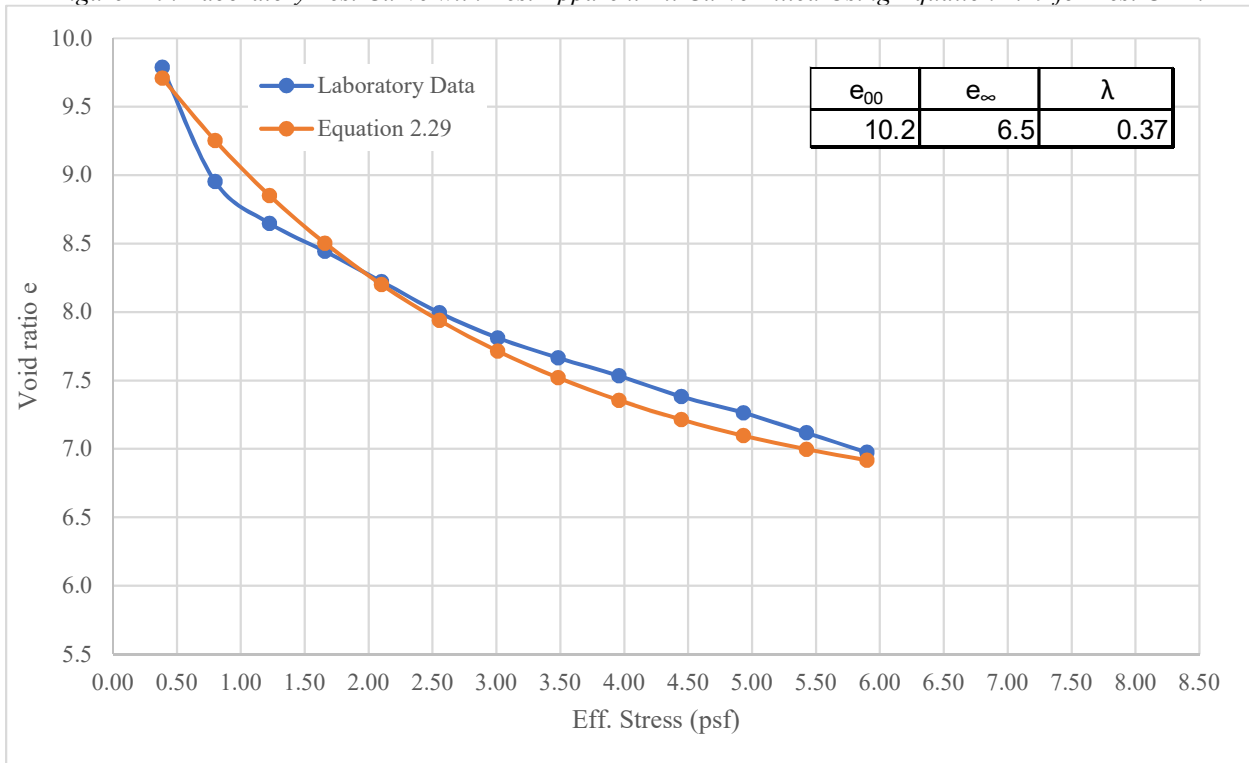
Figure A-10: Laboratory Test Curve with Best Apparent Fit Curve Fitted Using Equation 2.29 for Test C-12.
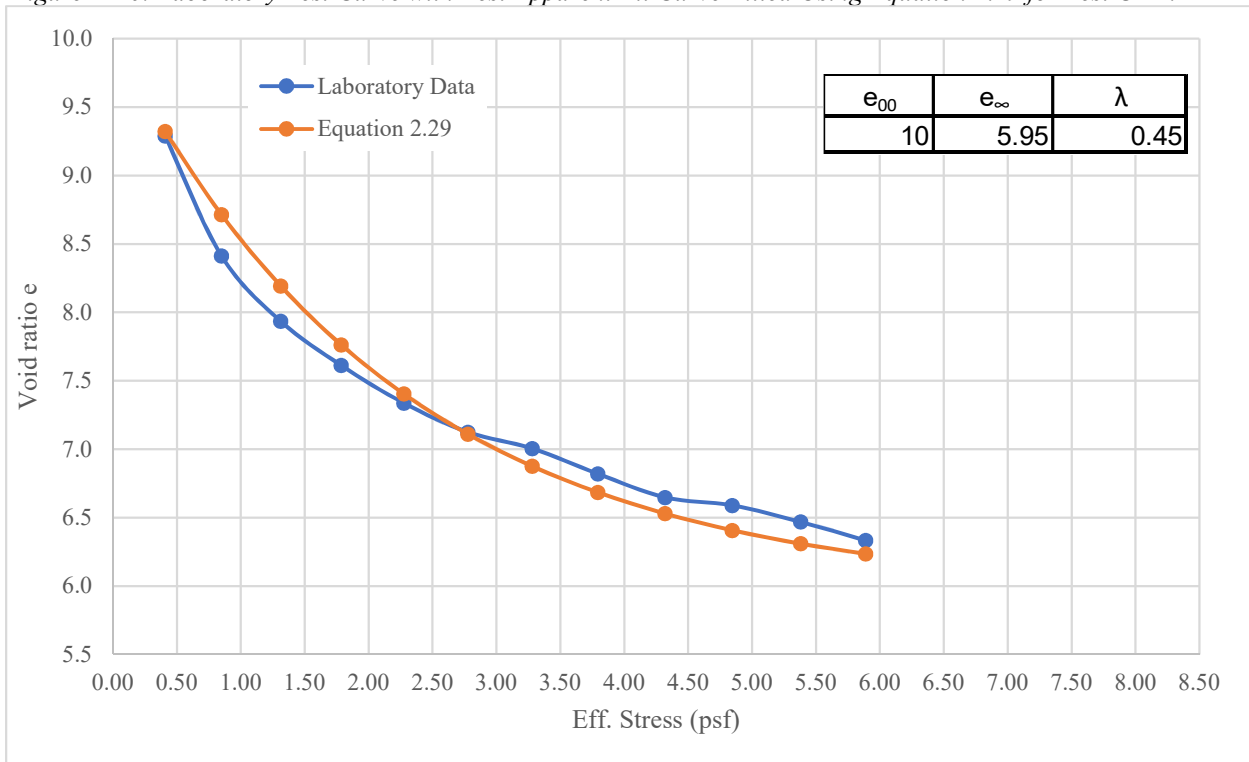
Figure A-11: Laboratory Test Curve with Best Apparent Fit Curve Fitted Using Equation 2.29 for Test C-13.

e_{00}	e_∞	λ
9.54	5.72	0.45
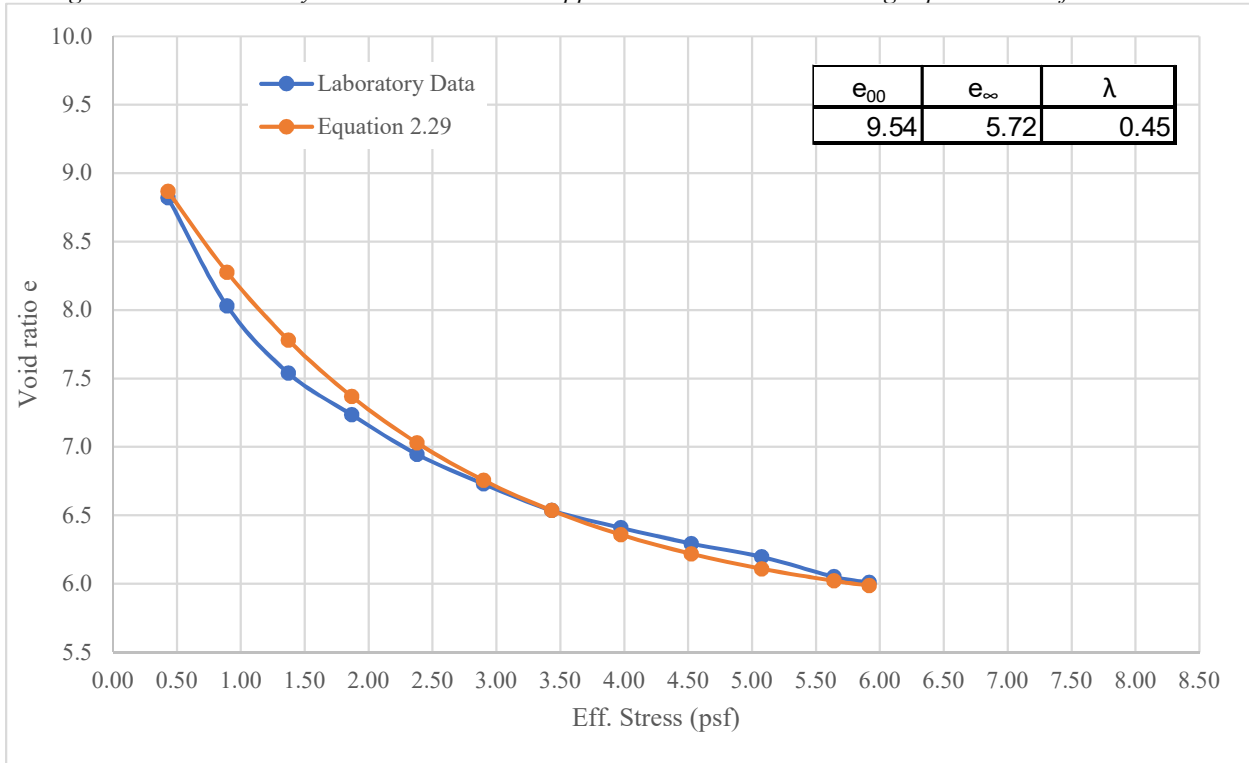
Figure A-12: Laboratory Test Curve with Best Apparent Fit Curve Fitted Using Equation 2.29 for Test C-14.

e_{00}	e_∞	λ
9.3	5.55	0.44
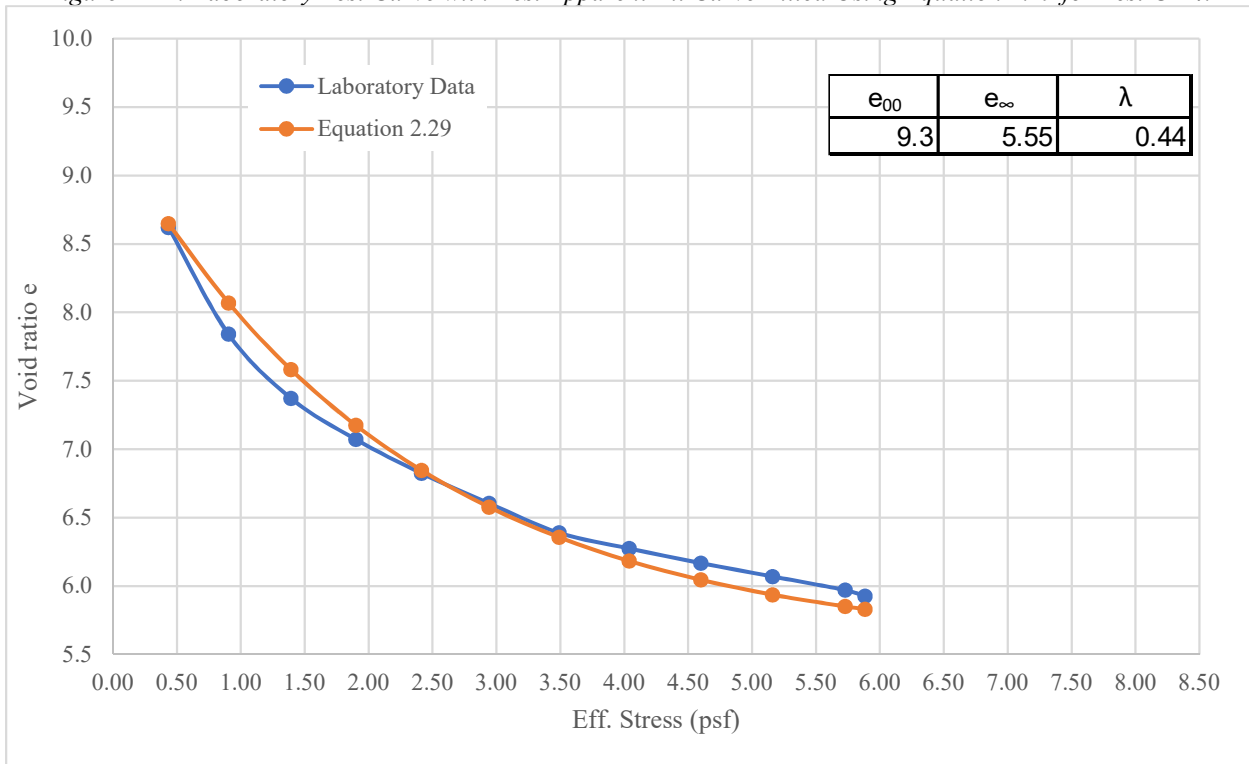
Figure A-13: Coefficient of Compression Plotted Against Void Ratio. Used to Calculate Permeability for Test C-1.
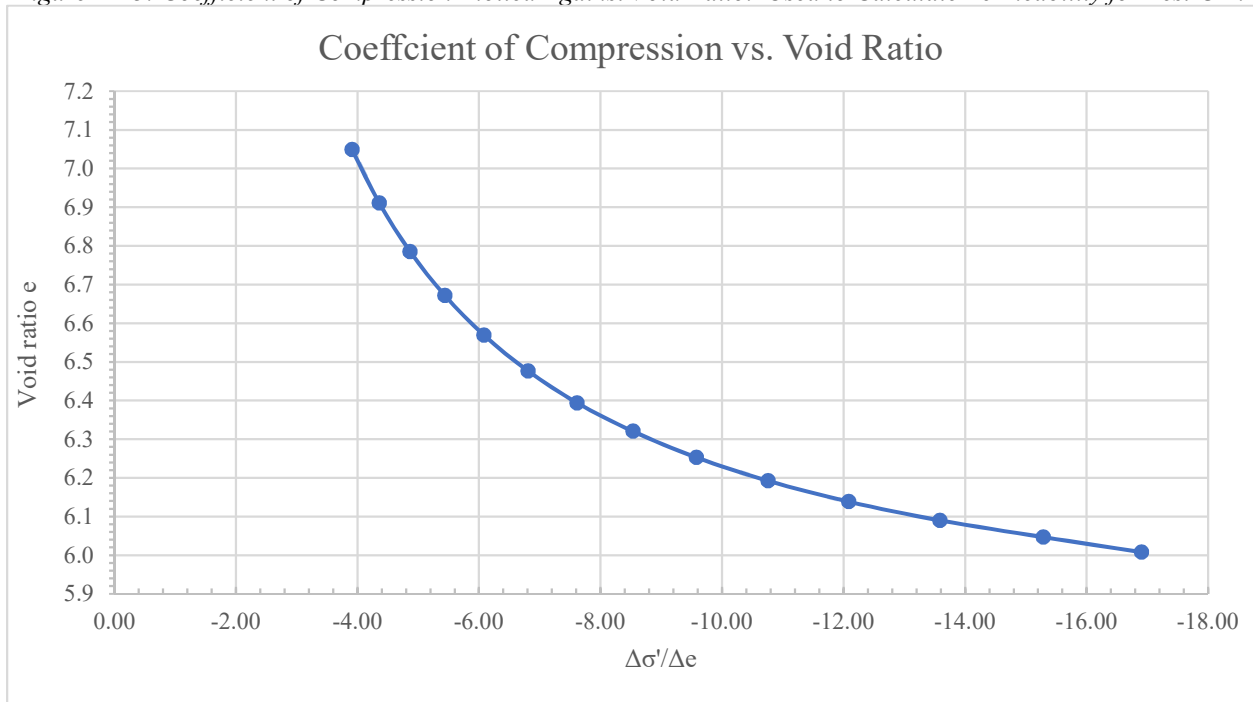
Figure A-14: Coefficient of Compression Plotted Against Void Ratio. Used to Calculate Permeability for Test C-2.
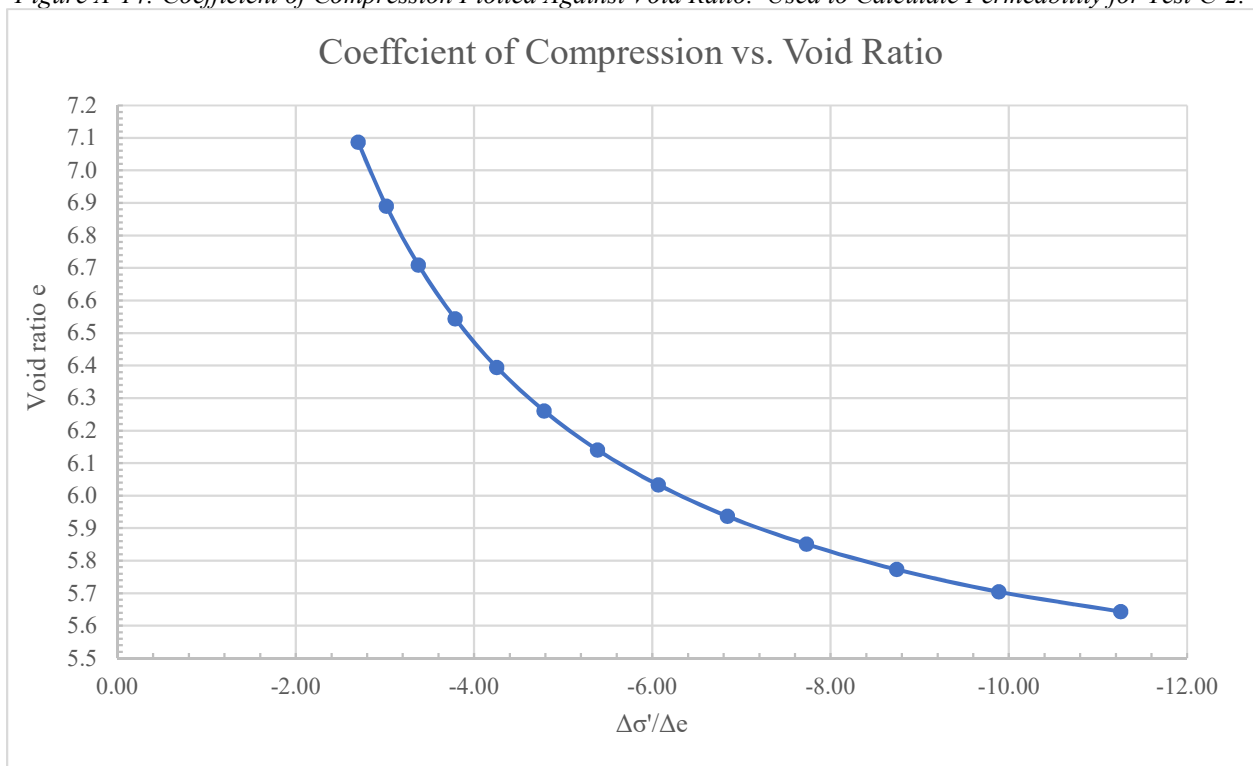
Figure A-15: Coefficient of Compression Plotted Against Void Ratio. Used to Calculate Permeability for Test C-3.

Coeffcient of Compression vs. Void Ratio
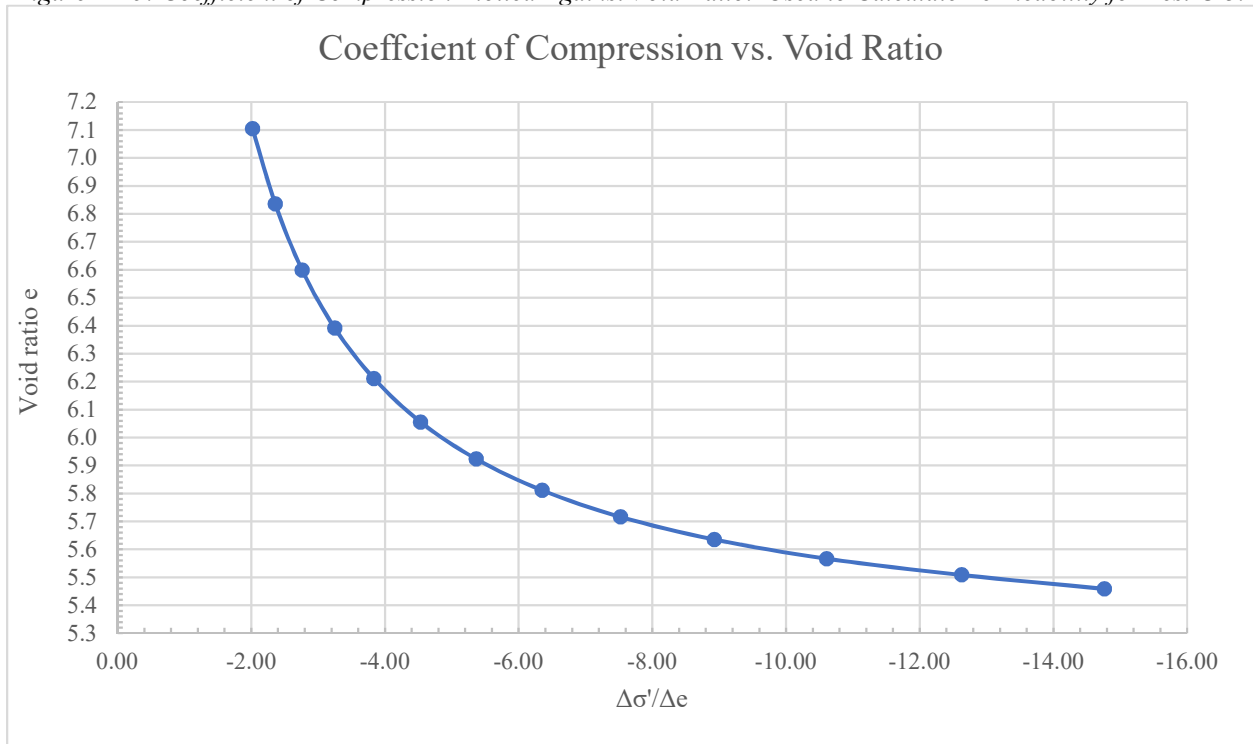
Figure A-16: Coefficient of Compression Plotted Against Void Ratio. Used to Calculate Permeability for Test C-4.

Coeffcient of Compression vs Void Ratio
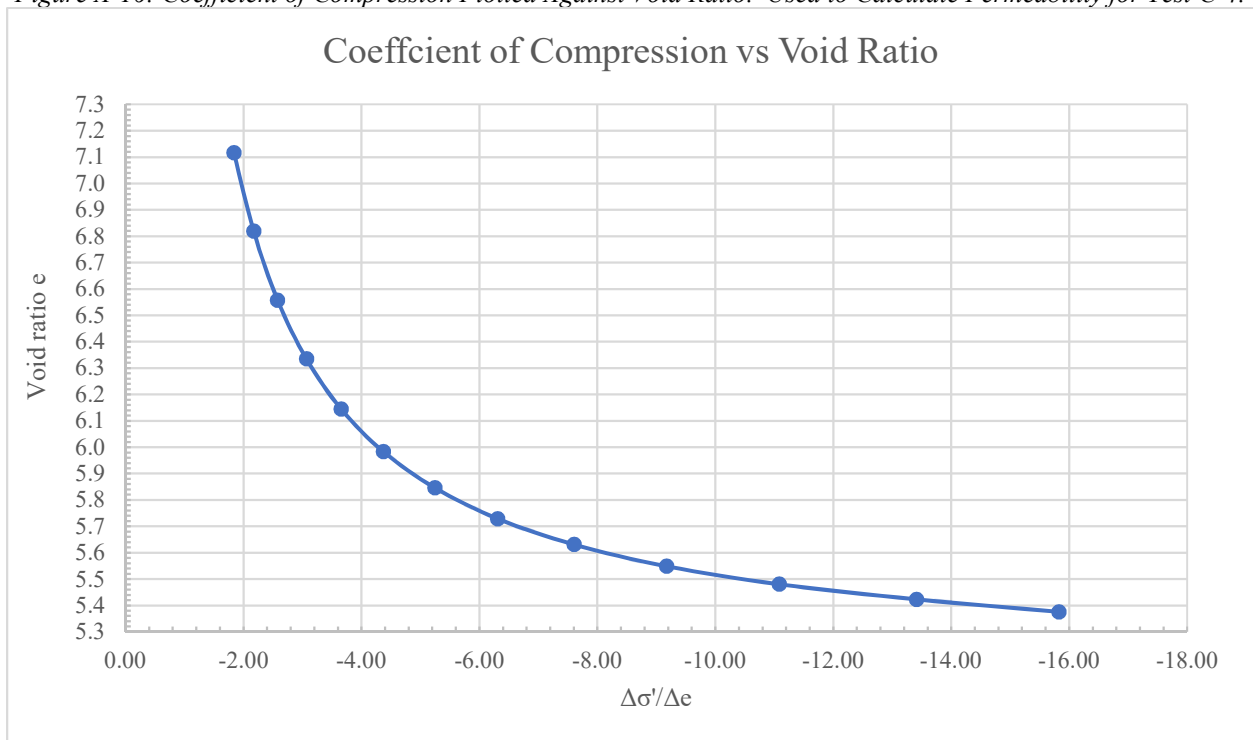
Figure A-17: Coefficient of Compression Plotted Against Void Ratio. Used to Calculate Permeability for Test C-6.
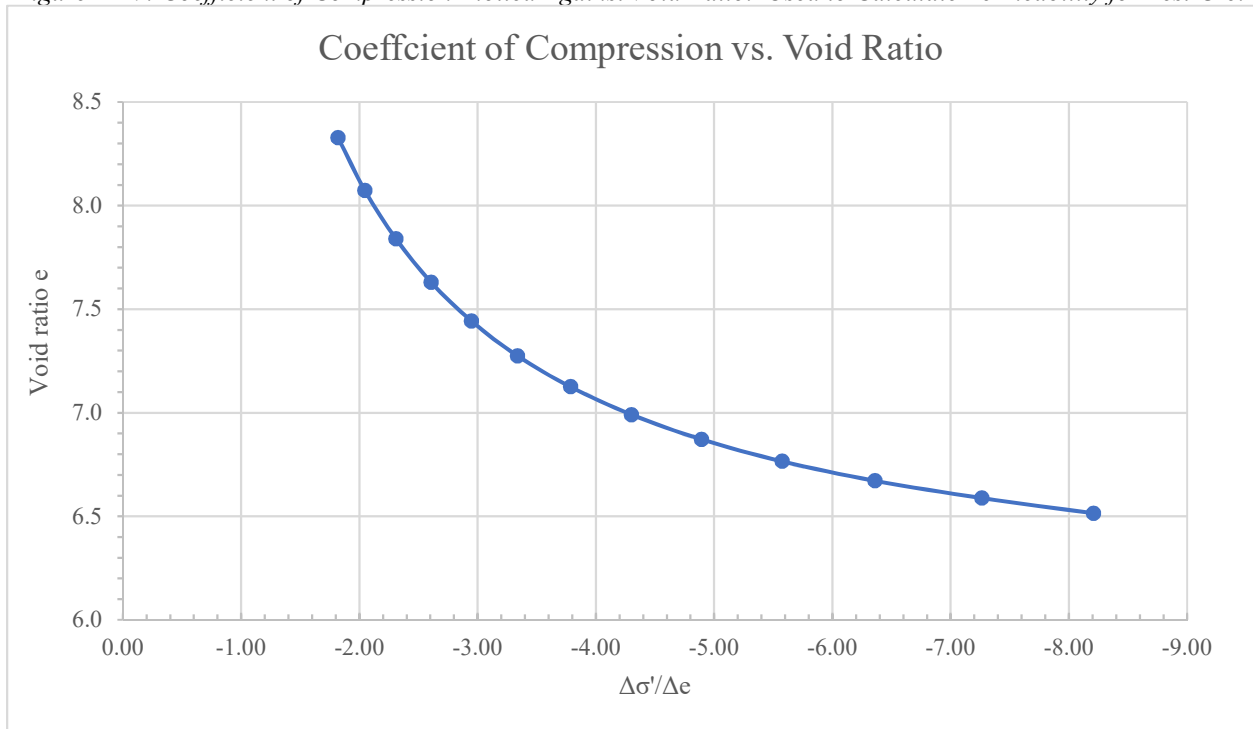
Figure A-18: Coefficient of Compression Plotted Against Void Ratio. Used to Calculate Permeability for Test C-7.
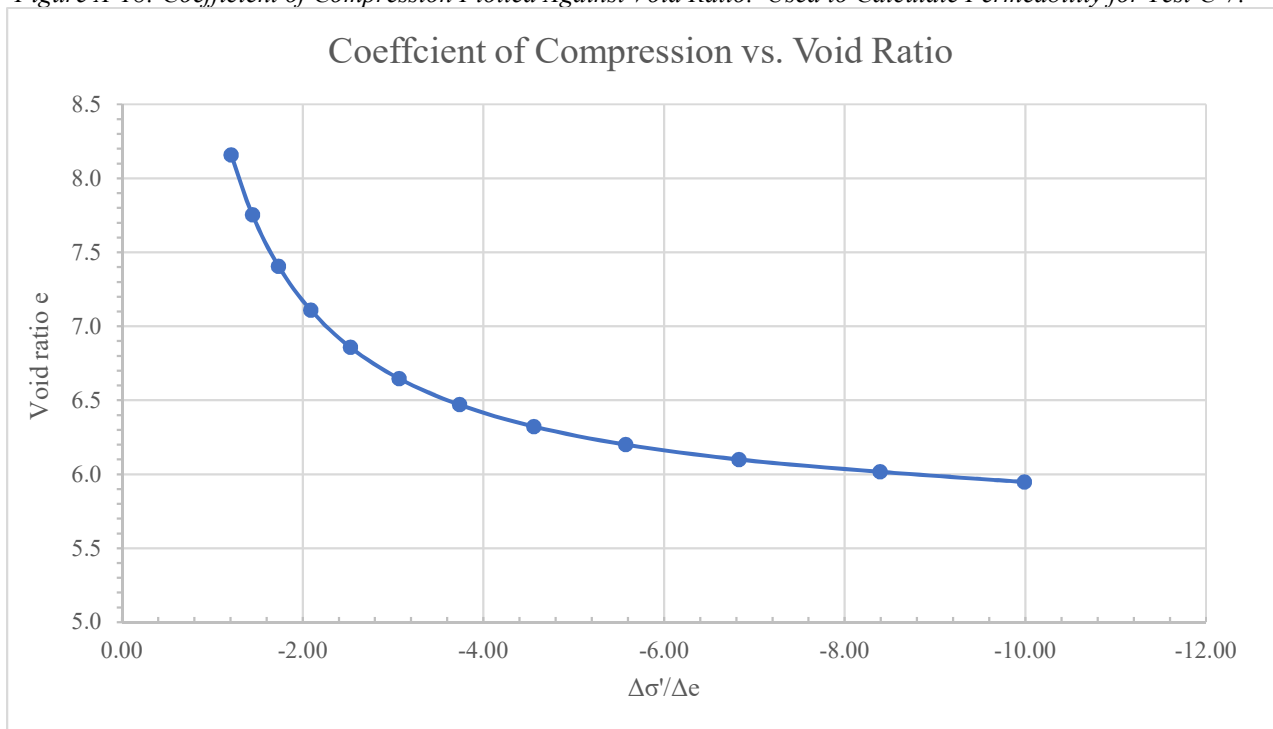
Figure A-19: Coefficient of Compression Plotted Against Void Ratio. Used to Calculate Permeability for Test C-8.
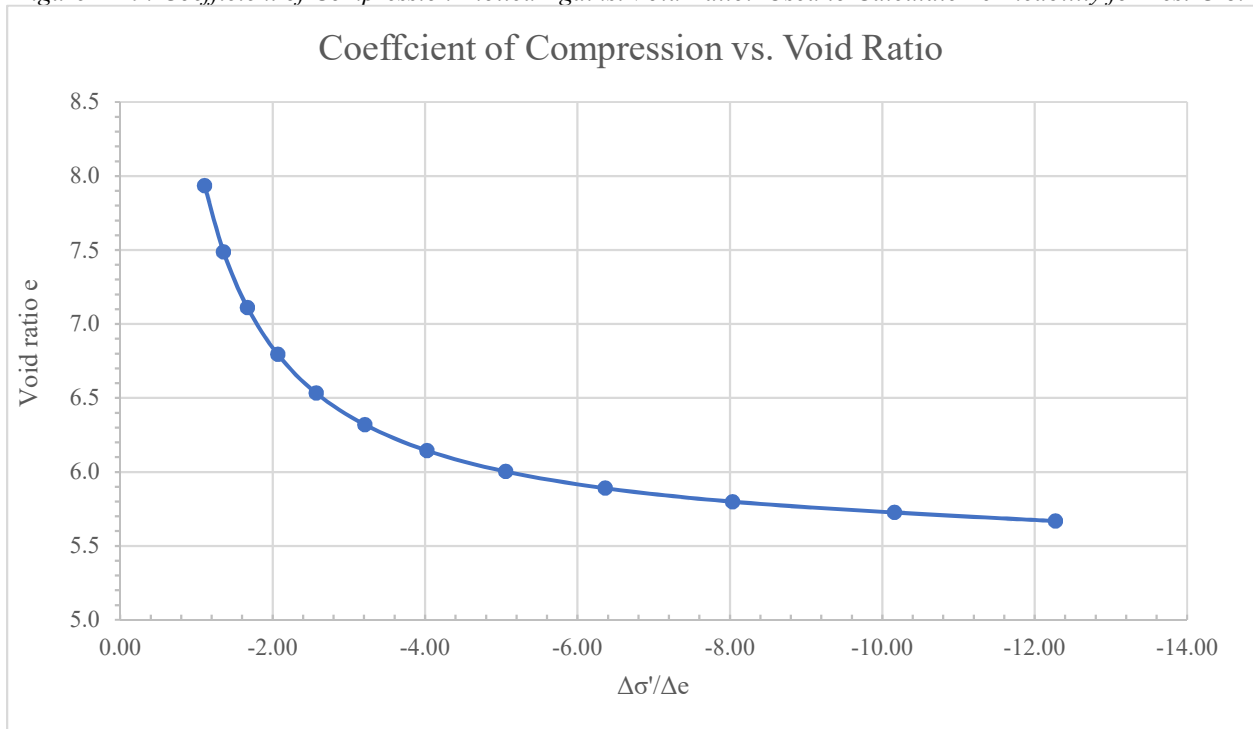
Figure A-20: Coefficient of Compression Plotted Against Void Ratio. Used to Calculate Permeability for Test C-9.
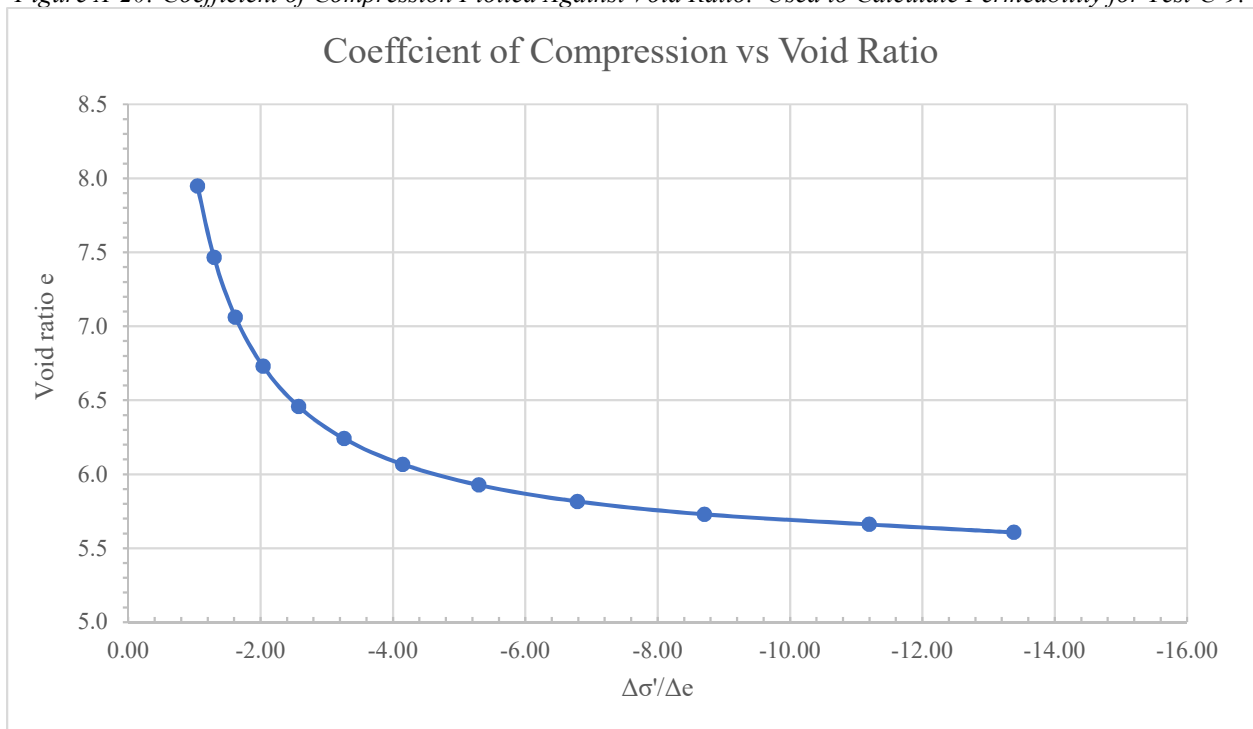
Figure A-21: Coefficient of Compression Plotted Against Void Ratio. Used to Calculate Permeability for Test C-11.
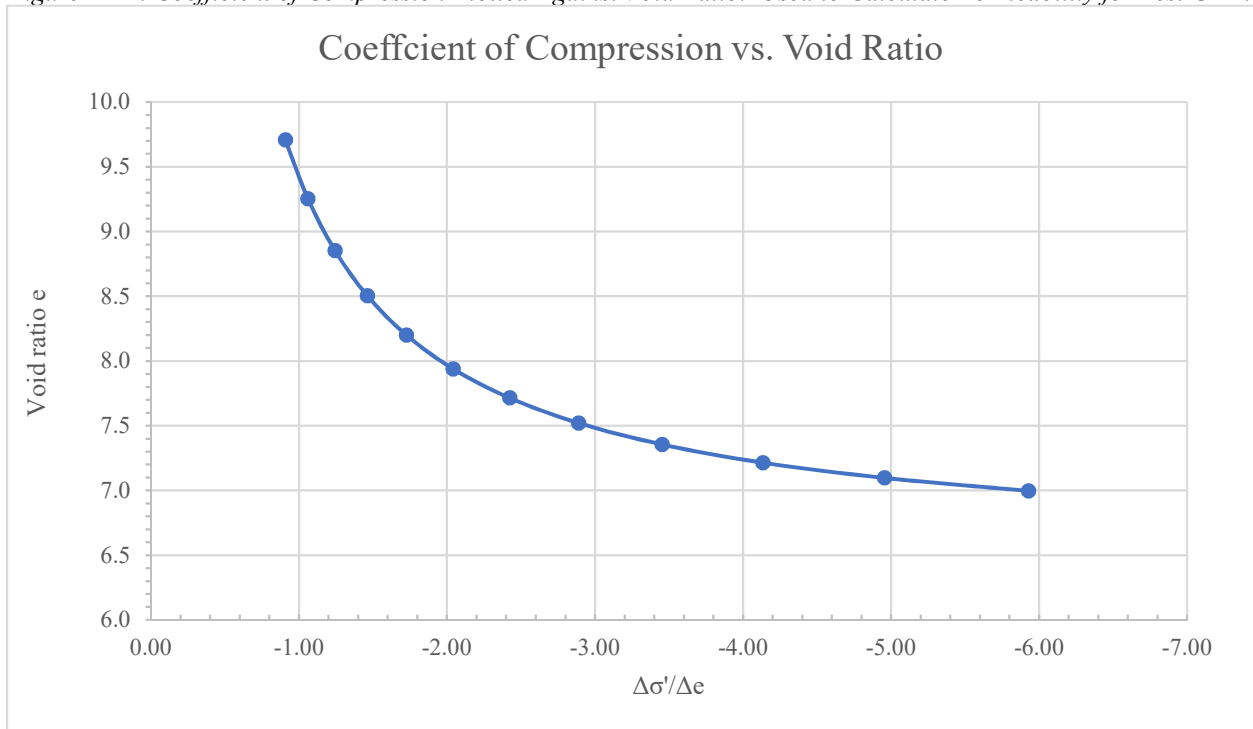
Figure A-22: Coefficient of Compression Plotted Against Void Ratio. Used to Calculate Permeability for Test C-12.
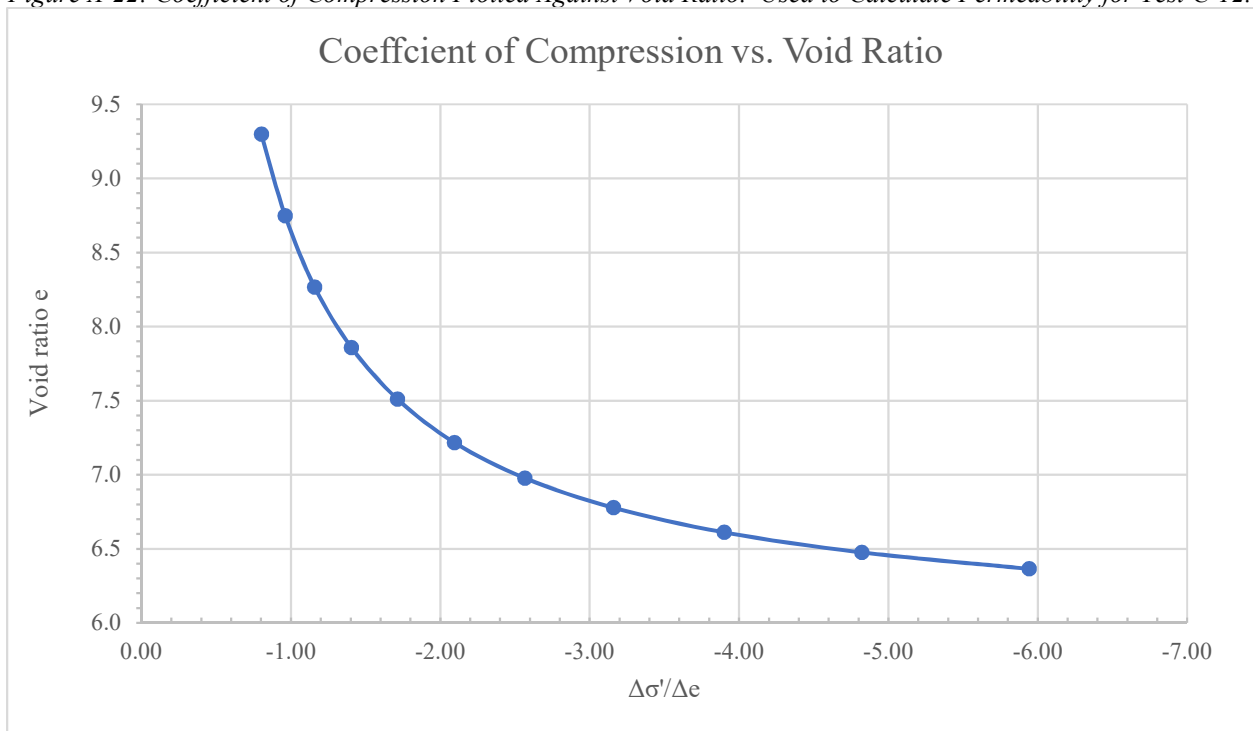
Figure A-23: Coefficient of Compression Plotted Against Void Ratio. Used to Calculate Permeability for Test C-13.
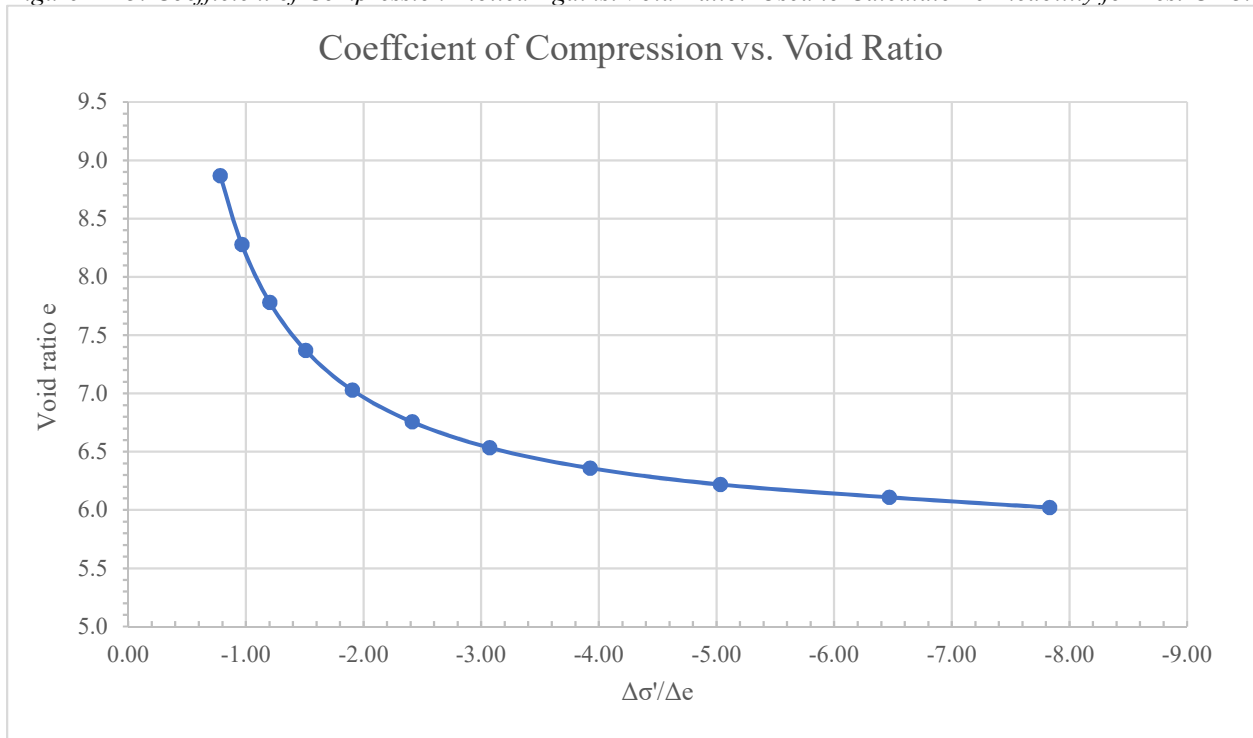
Figure A-24: Coefficient of Compression Plotted Against Void Ratio. Used to Calculate Permeability for Test C-14.
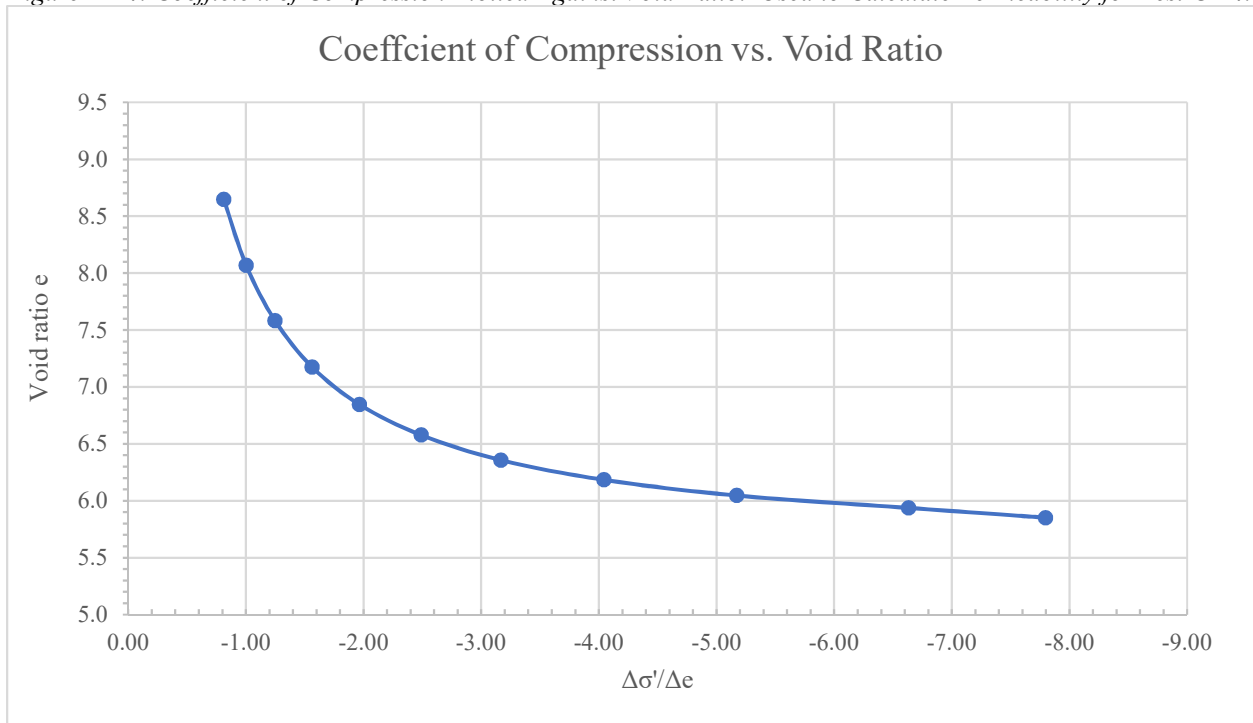
Table A-13: Permeability Calculations for Test C-1.

Initial Ht	20	cm	Degree of Consolidation	Time Factor	Deformation	Avg. Void Ratio	Height of Solids	Time	Coeff. of Compress. Inv.	Coeff. of Consol.	Permeability
Gs	2.641	(-)									
Ht Solids	0.081246	ft	(%)	(-)	(cm)	(-)	(ft)	(min)	(dσ'/de)	(ft/min.)	(ft/min.)
λ	0.2	(-)	20%	0.1	0.3160	6.949	0.08125	2000	-4	3.30E-07	4.09E-05
d100	1.58	cm	50%	0.3	0.7900	6.757	0.08125	14000	-5	1.41E-07	1.37E-05
N	0.026665	(-)	90%	1.0	1.4220	6.502	0.08125	29000	-6.7	2.28E-07	1.59E-05

Table A-14: Permeability Calculations for Test C-2.

Initial Ht	19.6	cm	Degree of Consolidation	Time Factor	Deformation	Avg. Void Ratio	Height of Solids	Time	Coeff. of Compress. Inv.	Coeff. of Consol.	Permeability
Gs	2.641	(-)									
Ht Solids	0.078864	ft	(%)	(-)	(cm)	(-)	(ft)	(min)	(dσ'/de)	(ft/min.)	(ft/min.)
λ	0.28	(-)	20%	0.1	0.3960	6.989	0.07886	6500	-2.82	9.57E-08	1.69E-05
d100	1.98	cm	50%	0.3	0.9900	6.742	0.07886	22000	-3.23	8.48E-08	1.27E-05
N	0.036237	(-)	90%	1.0	1.7820	6.412	0.07886	60000	-4.32	1.04E-07	1.11E-05

Table A-15: Permeability Calculations for Test C-3.

Initial Ht	19.7	cm	Degree of Consolidation	Time Factor	Deformation	Avg. Void Ratio	Height of Solids	Time	Coeff. of Compress. Inv.	Coeff. of Consol.	Permeability
Gs	2.641	(-)									
Ht Solids	0.079341	ft	(%)	(-)	(cm)	(-)	(ft)	(min)	(dσ'/de)	(ft/min.)	(ft/min.)
λ	0.28	(-)	20%	0.1	0.4560	6.958	0.07934	7000	-2.23	8.99E-08	2.00E-05
d100	2.28	cm	50%	0.3	1.1400	6.675	0.07934	23000	-2.7	8.21E-08	1.46E-05
N	0.036456	(-)	90%	1.0	2.0520	6.298	0.07934	80000	-3.58	7.87E-08	1.00E-05

Table A-16: Permeability Calculations for Test C-4.

Initial Ht	19.6	cm	Degree of Consolidation	Time Factor	Deformation	Avg. Void Ratio	Height of Solids	Time	Coeff. of Compress. Inv.	Coeff. of Consol.	Permeability
Gs	2.641	(-)									
Ht Solids	0.080073	ft	(%)	(-)	(cm)	(-)	(ft)	(min)	(dσ'/de)	(ft/min.)	(ft/min.)
λ	0.3	(-)	20%	0.1	0.4760	6.836	0.08007	5100	-2.28	1.26E-07	2.70E-05
d100	2.38	cm	50%	0.3	1.1900	6.543	0.08007	23000	-2.61	8.36E-08	1.51E-05
N	0.03942	(-)	90%	1.0	2.1420	6.153	0.08007	85000	-3.8	7.54E-08	8.86E-06

Table A-17: Permeability Calculations for Test C-6.

Initial Ht	19.6	cm	Degree of Consolidation	Time Factor	Deformation	Avg. Void Ratio	Height of Solids	Time	Coeff. of Compress. Inv.	Coeff. of Consol.	Permeability
Gs	2.641	(-)									
Ht Solids	0.067553	ft	(%)	(-)	(cm)	(-)	(ft)	(min)	(dσ'/de)	(ft/min.)	(ft/min.)
λ	0.25	(-)	20%	0.1	0.5140	8.269	0.06755	4050	-1.85	1.13E-07	3.52E-05
d100	2.57	cm	50%	0.3	1.2850	7.895	0.06755	12000	-2.25	1.14E-07	2.82E-05
N	0.027714	(-)	90%	1.0	2.3130	7.396	0.06755	28000	-3.05	1.63E-07	2.80E-05

Table A-18: Permeability Calculations for Test C-7.

Initial Ht	19.2	cm	Degree of Consolidation	Time Factor	Deformation	Avg. Void Ratio	Height of Solids	Time	Coeff. of Compress. Inv.	Coeff. of Consol.	Permeability
Gs	2.641	(-)									
Ht Solids	0.065945	ft	(%)	(-)	(cm)	(-)	(ft)	(min)	(dσ'/de)	(ft/min.)	(ft/min.)
λ	0.36	(-)	20%	0.1	0.7300	8.189	0.06594	6500	-1.21	6.69E-08	3.17E-05
d100	3.65	cm	50%	0.3	1.8250	7.644	0.06594	20000	-1.58	6.52E-08	2.23E-05
N	0.038957	(-)	90%	1.0	3.2850	6.918	0.06594	58000	-2.4	7.50E-08	1.54E-05

Table A-19: Permeability Calculations for Test C-8.

Initial Ht	19.5	cm	Degree of Consolidation	Time Factor	Deformation	Avg. Void Ratio	Height of Solids	Time	Coeff. of Compress. Inv.	Coeff. of Consol.	Permeability
Gs	2.641	(-)									
Ht Solids	0.067363	ft	(%)	(-)	(cm)	(-)	(ft)	(min)	(dσ'/de)	(ft/min.)	(ft/min.)
λ	0.4	(-)	20%	0.1	0.8300	8.093	0.06736	7000	-1.1	6.48E-08	3.35E-05
d100	4.15	cm	50%	0.3	2.0750	7.487	0.06736	22000	-1.3	6.19E-08	2.52E-05
N	0.044217	(-)	90%	1.0	3.7350	6.678	0.06736	73000	-2.38	6.22E-08	1.25E-05

Table A-20: Permeability Calculations for Test C-9.

Initial Ht	19.4	cm	Degree of Consolidation	Time Factor	Deformation	Avg. Void Ratio	Height of Solids	Time	Coeff. of Compress. Inv.	Coeff. of Consol.	Permeability
Gs	2.641	(-)									
Ht Solids	0.067425	ft	(%)	(-)	(cm)	(-)	(ft)	(min)	(dσ'/de)	(ft/min.)	(ft/min.)
λ	0.42	(-)	20%	0.1	0.8380	8.032	0.06742	9000	-1.13	5.05E-08	2.52E-05
d100	4.19	cm	50%	0.3	2.0950	7.421	0.06742	28000	-1.3	4.87E-08	1.97E-05
N	0.04647	(-)	90%	1.0	3.7710	6.605	0.06742	80000	-2.31	5.68E-08	1.17E-05

Table A-21: Permeability Calculations for Test C-11.

Initial Ht	19.3	cm	Degree of Consolidation	Time Factor	Deformation	Avg. Void Ratio	Height of Solids	Time	Coeff. of Compress. Inv.	Coeff. of Consol.	Permeability
Gs	2.641	(-)									
Ht Solids	0.057583	ft	(%)	(-)	(cm)	(-)	(ft)	(min)	(dσ'/de)	(ft/min.)	(ft/min.)
λ	0.37	(-)	20%	0.1	0.6820	9.608	0.05758	3800	-0.92	8.73E-08	6.28E-05
d100	3.41	cm	50%	0.3	1.7050	9.025	0.05758	10100	-1.18	9.85E-08	5.22E-05
N	0.034963	(-)	90%	1.0	3.0690	8.248	0.05758	28000	-1.75	1.18E-07	3.91E-05

Table A-22: Permeability Calculations for Test C-12.

Initial Ht	19.3	cm	Degree of Consolidation	Time Factor	Deformation	Avg. Void Ratio	Height of Solids	Time	Coeff. of Compress. Inv.	Coeff. of Consol.	Permeability
Gs	2.641	(-)									
Ht Solids	0.057476	ft	(%)	(-)	(cm)	(-)	(ft)	(min)	(dσ'/de)	(ft/min.)	(ft/min.)
λ	0.45	(-)	20%	0.1	0.9160	9.494	0.05748	5900	-0.9	5.60E-08	4.08E-05
d100	4.58	cm	50%	0.3	2.2900	8.710	0.05748	18000	-0.99	5.51E-08	3.37E-05
N	0.042443	(-)	90%	1.0	4.1220	7.664	0.05748	54000	-1.56	6.12E-08	2.12E-05

Table A-23: Permeability Calculations for Test C-13.

Initial Ht	19.4	cm	Degree of Consolidation	Time Factor	Deformation	Avg. Void Ratio	Height of Solids	Time	Coeff. of Compress. Inv.	Coeff. of Consol.	Permeability
Gs	2.641	(-)									
Ht Solids	0.057752	ft	(%)	(-)	(cm)	(-)	(ft)	(min)	(dσ'/de)	(ft/min.)	(ft/min.)
λ	0.45	(-)	20%	0.1	1.0760	9.410	0.05775	5800	-0.65	5.75E-08	5.75E-05
d100	5.38	cm	50%	0.3	2.6900	8.493	0.05775	20100	-0.9	4.98E-08	3.28E-05
N	0.042647	(-)	90%	1.0	4.8420	7.270	0.05775	79500	-1.61	4.20E-08	1.35E-05

Table A-24: Permeability Calculations for Test C-14.

Initial Ht	19.1	cm	Degree of Consolidation	Time Factor	Deformation	Avg. Void Ratio	Height of Solids	Time	Coeff. of Compress. Inv.	Coeff. of Consol.	Permeability
Gs	2.641	(-)									
Ht Solids	0.057433	ft	(%)	(-)	(cm)	(-)	(ft)	(min)	(dσ'/de)	(ft/min.)	(ft/min.)
λ	0.44	(-)	20%	0.1	1.0360	9.319	0.05743	5600	-0.63	5.89E-08	6.02E-05
d100	5.18	cm	50%	0.3	2.5900	8.431	0.05743	19000	-0.89	5.21E-08	3.45E-05
N	0.041469	(-)	90%	1.0	4.6620	7.248	0.05743	72000	-1.49	4.58E-08	1.58E-05

Table A-25: Calculations of Ultimate Settlement Based on USACE Method for Test C-1.

Layer	Height of Sublayer	Sublayer in Reduced Coordinates	Cumulative Sublayer in Reduced Coordinates	Mid Point of Sublayer in Redu. Coor.	Initial Effective Stress	Initial Void Ratio	Final Effective Stress	Final Void Ratio	Δe_∞	Final Height of Layer	Settlement of layer		
i	h_i	l	l	l_m	$\sigma'_{i,o}$	e_{io}	$\sigma'_{i,\infty}$	e_∞		$h_{i,\infty}$	$\delta_{i,\infty}$		
(-)	(ft)	(ft)	(ft)	(ft)	(psf)	(-)	(psf)	(-)		(ft)	(ft)		
1	0.044	0.0054	0.005	0.003	0.0	7.03	0.28	7.00	-	0.044	0.0002		
2	0.044	0.0054	0.011	0.008	0.0	7.0	0.84	6.96	0.040	0.043	0.0004		
3	0.044	0.0054	0.016	0.014	0.0	7.0	1.39	6.84	0.120	0.043	0.0010		
4	0.044	0.0054	0.022	0.019	0.0	7.0	1.95	6.71	0.130	0.042	0.0017		
5	0.044	0.0054	0.027	0.025	0.0	7.0	2.51	6.60	0.110	0.041	0.0023		
6	0.044	0.0054	0.033	0.030	0.0	7.0	3.07	6.51	0.090	0.041	0.0028		
7	0.044	0.0054	0.038	0.035	0.0	7.0	3.63	6.41	0.100	0.040	0.0034		
8	0.044	0.0054	0.044	0.041	0.0	7.0	4.18	6.32	0.090	0.040	0.0039		
9	0.044	0.0054	0.049	0.046	0.0	7.0	4.74	6.28	0.040	0.040	0.0041		
10	0.044	0.0054	0.054	0.052	0.0	7.0	5.30	6.21	0.070	0.039	0.0045		
11	0.044	0.0054	0.060	0.057	0.0	7.0	5.86	6.18	0.030	0.039	0.0046		
12	0.044	0.0054	0.065	0.063	0.0	7.0	6.42	6.11	0.070	0.039	0.0050		
13	0.044	0.0054	0.071	0.068	0.0	7.0	6.97	6.08	0.030	0.039	0.0052		
14	0.044	0.0054	0.076	0.074	0.0	7.0	7.53	6.02	0.060	0.038	0.0055		
15	0.044	0.0054	0.082	0.079	0.0	7.0	8.09	5.98	0.040	0.038	0.0057		
											0.050	ft	
											1.53	cm	
											18.5	Final Ht of Slurry	

Table A-26: Calculations of Ultimate Settlement Based on USACE Method for Test C-2.

Layer	Height of Sublayer	Sublayer in Reduced Coordinates	Cumulative Sublayer in Reduced Coordinates	Mid Point of Sublayer in Redu. Coor.	Initial Effective Stress	Initial Void Ratio	Final Effective Stress	Final Void Ratio	Δe_∞	Final Height of Layer	Settlement of layer		
i	h_i	l	l	l_m	$\sigma'_{i,o}$	e_{io}	$\sigma'_{i,\infty}$	e_∞		$h_{i,\infty}$	$\delta_{i,\infty}$		
(-)	(ft)	(ft)	(ft)	(ft)	(psf)	(-)	(psf)	(-)		(ft)	(ft)		
1	0.045	0.0057	0.006	0.003	0.0	7.03	0.29	7.00	-	0.045	0.0002		
2	0.045	0.0057	0.011	0.008	0.0	7.0	0.87	6.95	0.050	0.045	0.0005		
3	0.045	0.0057	0.017	0.014	0.0	7.0	1.45	6.77	0.180	0.044	0.0015		
4	0.045	0.0057	0.023	0.020	0.0	7.0	2.03	6.57	0.200	0.043	0.0026		
5	0.045	0.0057	0.028	0.025	0.0	7.0	2.61	6.40	0.170	0.042	0.0036		
6	0.045	0.0057	0.034	0.031	0.0	7.0	3.19	6.27	0.130	0.041	0.0043		
7	0.045	0.0057	0.040	0.037	0.0	7.0	3.77	6.12	0.150	0.040	0.0052		
8	0.045	0.0057	0.045	0.042	0.0	7.0	4.35	6.02	0.100	0.040	0.0057		
9	0.045	0.0057	0.051	0.048	0.0	7.0	4.93	5.91	0.110	0.039	0.0063		
10	0.045	0.0057	0.057	0.054	0.0	7.0	5.51	5.82	0.090	0.039	0.0069		
11	0.045	0.0057	0.062	0.059	0.0	7.0	6.09	5.75	0.070	0.038	0.0072		
12	0.045	0.0057	0.068	0.065	0.0	7.0	6.67	5.68	0.070	0.038	0.0076		
13	0.045	0.0057	0.074	0.071	0.0	7.0	7.25	5.61	0.070	0.037	0.0080		
14	0.045	0.0057	0.079	0.076	0.0	7.0	7.83	5.55	0.060	0.037	0.0084		
											0.068	ft	
											2.07	cm	
											17.3	Final Ht of Slurry	

113

Table A-27: Calculations of Ultimate Settlement Based on USACE Method for Test C-3.

Layer	Height of Sublayer	Sublayer in Reduced Coordinates	Cumulative Sublayer in Reduced Coordinates	Mid Point of Sublayer in Redu. Coor.	Initial Effective Stress	Initial Void Ratio	Final Effective Stress	Final Void Ratio	Δe_∞	Final Height of Layer	Settlement of layer		
i	h_i	l	l	l_m	$\sigma'_{i,o}$	e_{io}	$\sigma'_{i,\infty}$	e_∞		$h_{i,\infty}$	$\delta_{i,\infty}$		
(-)	(ft)	(ft)	(ft)	(ft)	(psf)	(-)	(psf)	(-)		(ft)	(ft)		
1	0.046	0.0057	0.006	0.003	0.0	7.03	0.29	7.00	-	0.046	0.0002		
2	0.046	0.0057	0.011	0.009	0.0	7.0	0.88	6.79	0.210	0.045	0.0014		
3	0.046	0.0057	0.017	0.014	0.0	7.0	1.47	6.57	0.220	0.044	0.0026		
4	0.046	0.0057	0.023	0.020	0.0	7.0	2.06	6.38	0.190	0.042	0.0037		
5	0.046	0.0057	0.029	0.026	0.0	7.0	2.65	6.20	0.180	0.041	0.0048		
6	0.046	0.0057	0.034	0.032	0.0	7.0	3.24	6.07	0.130	0.041	0.0055		
7	0.046	0.0057	0.040	0.037	0.0	7.0	3.83	5.93	0.140	0.040	0.0063		
8	0.046	0.0057	0.046	0.043	0.0	7.0	4.42	5.84	0.090	0.039	0.0068		
9	0.046	0.0057	0.052	0.049	0.0	7.0	5.00	5.76	0.080	0.039	0.0073		
10	0.046	0.0057	0.057	0.055	0.0	7.0	5.59	5.68	0.080	0.038	0.0078		
11	0.046	0.0057	0.063	0.060	0.0	7.0	6.18	5.61	0.070	0.038	0.0082		
12	0.046	0.0057	0.069	0.066	0.0	7.0	6.77	5.57	0.040	0.038	0.0084		
13	0.046	0.0057	0.075	0.072	0.0	7.0	7.36	5.52	0.050	0.037	0.0087		
14	0.046	0.0057	0.080	0.078	0.0	7.0	7.95	5.48	0.040	0.037	0.0089		
											0.081	ft	
											2.46	cm	
											17.2	Final Ht of Slurry	

Table A-28: Calculations of Ultimate Settlement Based on USACE Method for Test C-4.

Layer	Height of Sublayer	Sublayer in Reduced Coordinates	Cumulative Sublayer in Reduced Coordinates	Mid Point of Sublayer in Redu. Coor.	Initial Effective Stress	Initial Void Ratio	Final Effective Stress	Final Void Ratio	Δe_∞	Final Height of Layer	Settlement of layer		
i	h_i	l	l	l_m	$\sigma'_{i,o}$	e_{io}	$\sigma'_{i,\infty}$	e_∞		$h_{i,\infty}$	$\delta_{i,\infty}$		
(-)	(ft)	(ft)	(ft)	(ft)	(psf)	(-)	(psf)	(-)		(ft)	(ft)		
1	0.046	0.0057	0.006	0.003	0.0	7.03	0.29	7.00	-	0.046	0.0002		
2	0.046	0.0057	0.011	0.009	0.0	7.0	0.88	6.88	0.120	0.045	0.0009		
3	0.046	0.0057	0.017	0.014	0.0	7.0	1.46	6.63	0.250	0.044	0.0023		
4	0.046	0.0057	0.023	0.020	0.0	7.0	2.05	6.39	0.240	0.042	0.0037		
5	0.046	0.0057	0.029	0.026	0.0	7.0	2.64	6.20	0.190	0.041	0.0047		
6	0.046	0.0057	0.034	0.031	0.0	7.0	3.22	6.03	0.170	0.040	0.0057		
7	0.046	0.0057	0.040	0.037	0.0	7.0	3.81	5.89	0.140	0.039	0.0065		
8	0.046	0.0057	0.046	0.043	0.0	7.0	4.39	5.78	0.110	0.039	0.0072		
9	0.046	0.0057	0.051	0.049	0.0	7.0	4.98	5.67	0.110	0.038	0.0078		
10	0.046	0.0057	0.057	0.054	0.0	7.0	5.56	5.59	0.080	0.038	0.0082		
11	0.046	0.0057	0.063	0.060	0.0	7.0	6.15	5.52	0.070	0.037	0.0086		
12	0.046	0.0057	0.069	0.066	0.0	7.0	6.74	5.47	0.050	0.037	0.0089		
13	0.046	0.0057	0.074	0.072	0.0	7.0	7.32	5.40	0.070	0.037	0.0093		
14	0.046	0.0057	0.080	0.077	0.0	7.0	7.91	5.37	0.030	0.036	0.0095		
											0.084	ft	
											2.55	cm	
											17.1	Final Ht of Slurry	

Table A-29: Calculations of Ultimate Settlement Based on USACE Method for Test C-6.

Layer	Height of Sublayer	Sublayer in Reduced Coordinates	Cumulative Sublayer in Reduced Coordinates	Mid Point of Sublayer in Redu. Coor.	Initial Effective Stress	Initial Void Ratio	Final Effective Stress	Final Void Ratio	Δe_∞	Final Height of Layer	Settlement of layer		
i	h_i	l	l	l_m	$\sigma'_{i,o}$	e_{io}	$\sigma'_{i,\infty}$	e_∞		$h_{i,\infty}$	$\delta_{i,\infty}$		
(-)	(ft)	(ft)	(ft)	(ft)	(psf)	(-)	(psf)	(-)		(ft)	(ft)		
1	0.046	0.0048	0.005	0.002	0.0	8.63	0.24	8.50	-	0.045	0.0006		
2	0.046	0.0048	0.010	0.007	0.0	8.6	0.73	8.16	0.340	0.044	0.0022		
3	0.046	0.0048	0.014	0.012	0.0	8.6	1.22	7.91	0.250	0.042	0.0034		
4	0.046	0.0048	0.019	0.017	0.0	8.6	1.71	7.69	0.220	0.041	0.0045		
5	0.046	0.0048	0.024	0.021	0.0	8.6	2.20	7.50	0.190	0.041	0.0054		
6	0.046	0.0048	0.029	0.026	0.0	8.6	2.69	7.31	0.190	0.040	0.0063		
7	0.046	0.0048	0.033	0.031	0.0	8.6	3.17	7.16	0.150	0.039	0.0070		
8	0.046	0.0048	0.038	0.036	0.0	8.6	3.66	7.03	0.130	0.038	0.0076		
9	0.046	0.0048	0.043	0.041	0.0	8.6	4.15	6.91	0.120	0.038	0.0082		
10	0.046	0.0048	0.048	0.045	0.0	8.6	4.64	6.80	0.110	0.037	0.0087		
11	0.046	0.0048	0.052	0.050	0.0	8.6	5.13	6.71	0.090	0.037	0.0092		
12	0.046	0.0048	0.057	0.055	0.0	8.6	5.62	6.61	0.100	0.036	0.0096		
13	0.046	0.0048	0.062	0.060	0.0	8.6	6.11	6.55	0.060	0.036	0.0099		
14	0.046	0.0048	0.067	0.064	0.0	8.6	6.59	6.49	0.060	0.036	0.0102		
											0.093	ft	
											2.83	cm	
											16.8	Final Ht of Slurry	

Table A-30: Calculations of Ultimate Settlement Based on USACE Method for Test C-7.

Layer	Height of Sublayer	Sublayer in Reduced Coordinates	Cumulative Sublayer in Reduced Coordinates	Mid Point of Sublayer in Redu. Coor.	Initial Effective Stress	Initial Void Ratio	Final Effective Stress	Final Void Ratio	Δe_∞	Final Height of Layer	Settlement of layer		
i	h_i	l	l	l_m	$\sigma'_{i,o}$	e_{io}	$\sigma'_{i,\infty}$	e_∞		$h_{i,\infty}$	$\delta_{i,\infty}$		
(-)	(ft)	(ft)	(ft)	(ft)	(psf)	(-)	(psf)	(-)		(ft)	(ft)		
1	0.046	0.0048	0.005	0.002	0.0	8.63	0.24	8.50	-	0.045	0.0006		
2	0.046	0.0048	0.010	0.007	0.0	8.6	0.73	8.16	0.340	0.044	0.0022		
3	0.046	0.0048	0.014	0.012	0.0	8.6	1.22	7.91	0.250	0.042	0.0034		
4	0.046	0.0048	0.019	0.017	0.0	8.6	1.71	7.69	0.220	0.041	0.0045		
5	0.046	0.0048	0.024	0.021	0.0	8.6	2.20	7.50	0.190	0.041	0.0054		
6	0.046	0.0048	0.029	0.026	0.0	8.6	2.69	7.31	0.190	0.040	0.0063		
7	0.046	0.0048	0.033	0.031	0.0	8.6	3.17	7.16	0.150	0.039	0.0070		
8	0.046	0.0048	0.038	0.036	0.0	8.6	3.66	7.03	0.130	0.038	0.0076		
9	0.046	0.0048	0.043	0.041	0.0	8.6	4.15	6.91	0.120	0.038	0.0082		
10	0.046	0.0048	0.048	0.045	0.0	8.6	4.64	6.80	0.110	0.037	0.0087		
11	0.046	0.0048	0.052	0.050	0.0	8.6	5.13	6.71	0.090	0.037	0.0092		
12	0.046	0.0048	0.057	0.055	0.0	8.6	5.62	6.61	0.100	0.036	0.0096		
13	0.046	0.0048	0.062	0.060	0.0	8.6	6.11	6.55	0.060	0.036	0.0099		
											0.122	ft	
											3.72	cm	
											15.5	Final Ht of Slurry	

Table A-31: Calculations of Ultimate Settlement Based on USACE Method for Test C-8.

Layer	Height of Sublayer	Sublayer in Reduced Coordinates	Cumulative Sublayer in Reduced Coordinates	Mid Point of Sublayer in Redu. Coor.	Initial Effective Stress	Initial Void Ratio	Final Effective Stress	Final Void Ratio	Δe_∞	Final Height of Layer	Settlement of layer		
i	h_i	l	l	l_m	$\sigma'_{i,o}$	e_{io}	$\sigma'_{i,\infty}$	e_∞		$h_{i,\infty}$	$\delta_{i,\infty}$		
(-)	(ft)	(ft)	(ft)	(ft)	(psf)	(-)	(psf)	(-)		(ft)	(ft)		
1	0.049	0.0051	0.005	0.003	0.0	8.63	0.26	8.50	-	0.049	0.0007		
2	0.049	0.0051	0.010	0.008	0.0	8.6	0.78	7.61	0.890	0.044	0.0052		
3	0.049	0.0051	0.015	0.013	0.0	8.6	1.31	7.20	0.410	0.042	0.0073		
4	0.049	0.0051	0.020	0.018	0.0	8.6	1.83	6.89	0.310	0.040	0.0089		
5	0.049	0.0051	0.026	0.023	0.0	8.6	2.35	6.61	0.280	0.039	0.0103		
6	0.049	0.0051	0.031	0.028	0.0	8.6	2.88	6.39	0.220	0.038	0.0114		
7	0.049	0.0051	0.036	0.033	0.0	8.6	3.40	6.20	0.190	0.037	0.0124		
8	0.049	0.0051	0.041	0.038	0.0	8.6	3.92	6.07	0.130	0.036	0.0131		
9	0.049	0.0051	0.046	0.043	0.0	8.6	4.45	5.93	0.140	0.035	0.0138		
10	0.049	0.0051	0.051	0.049	0.0	8.6	4.97	5.85	0.080	0.035	0.0142		
11	0.049	0.0051	0.056	0.054	0.0	8.6	5.49	5.78	0.070	0.035	0.0146		
12	0.049	0.0051	0.061	0.059	0.0	8.6	6.02	5.70	0.080	0.034	0.0150		
13	0.049	0.0051	0.066	0.064	0.0	8.6	6.54	5.65	0.050	0.034	0.0152		
											0.142	ft	
											4.33	cm	
											15.2	Final Ht of Slurry	

Table A-32: Calculations of Ultimate Settlement Based on USACE Method for Test C-9.

Layer	Height of Sublayer	Sublayer in Reduced Coordinates	Cumulative Sublayer in Reduced Coordinates	Mid Point of Sublayer in Redu. Coor.	Initial Effective Stress	Initial Void Ratio	Final Effective Stress	Final Void Ratio	Δe_∞	Final Height of Layer	Settlement of layer		
i	h_i	l	l	l_m	$\sigma'_{i,o}$	e_{io}	$\sigma'_{i,\infty}$	e_∞		$h_{i,\infty}$	$\delta_{i,\infty}$		
(-)	(ft)	(ft)	(ft)	(ft)	(psf)	(-)	(psf)	(-)		(ft)	(ft)		
1	0.049	0.0051	0.005	0.003	0.0	8.63	0.26	8.10	-	0.046	0.0027		
2	0.049	0.0051	0.010	0.008	0.0	8.6	0.78	7.67	0.430	0.044	0.0049		
3	0.049	0.0051	0.015	0.013	0.0	8.6	1.30	7.21	0.460	0.042	0.0072		
4	0.049	0.0051	0.020	0.018	0.0	8.6	1.82	6.85	0.360	0.040	0.0090		
5	0.049	0.0051	0.025	0.023	0.0	8.6	2.34	6.59	0.260	0.039	0.0104		
6	0.049	0.0051	0.031	0.028	0.0	8.6	2.86	6.31	0.280	0.037	0.0118		
7	0.049	0.0051	0.036	0.033	0.0	8.6	3.38	6.17	0.140	0.036	0.0125		
8	0.049	0.0051	0.041	0.038	0.0	8.6	3.90	6.02	0.150	0.036	0.0133		
9	0.049	0.0051	0.046	0.043	0.0	8.6	4.43	5.90	0.120	0.035	0.0139		
10	0.049	0.0051	0.051	0.048	0.0	8.6	4.95	5.80	0.100	0.035	0.0144		
11	0.049	0.0051	0.056	0.053	0.0	8.6	5.47	5.72	0.080	0.034	0.0148		
12	0.049	0.0051	0.061	0.058	0.0	8.6	5.99	5.67	0.050	0.034	0.0150		
13	0.049	0.0051	0.066	0.064	0.0	8.6	6.51	5.61	0.060	0.034	0.0154		
											0.145	ft	
											4.43	cm	
											15.0	Final Ht of Slurry	

Table A-33: Calculations of Ultimate Settlement Based on USACE Method for Test C-11.

Layer	Height of Sublayer	Sublayer in Reduced Coordinates	Cumulative Sublayer in Reduced Coordinates	Mid Point of Sublayer in Redu. Coor.	Initial Effective Stress	Initial Void Ratio	Final Effective Stress	Final Void Ratio	Δe∞	Final Height of Layer	Settlement of layer		
i	h_i	l	l	l_m	$\sigma'_{i,o}$	e_{io}	$\sigma'_{i,\infty}$	e_∞		$h_{i,\infty}$	$\delta_{i,\infty}$		
(-)	(ft)	(ft)	(ft)	(ft)	(psf)	(-)	(psf)	(-)		(ft)	(ft)		
1	0.049	0.0044	0.004	0.002	0.0	10.00	0.23	9.56	-	0.047	0.0019		
2	0.049	0.0044	0.009	0.007	0.0	10.0	0.68	9.23	0.330	0.045	0.0034		
3	0.049	0.0044	0.013	0.011	0.0	10.0	1.13	8.82	0.410	0.043	0.0052		
4	0.049	0.0044	0.018	0.015	0.0	10.0	1.59	8.55	0.270	0.042	0.0064		
5	0.049	0.0044	0.022	0.020	0.0	10.0	2.04	8.31	0.240	0.041	0.0075		
6	0.049	0.0044	0.027	0.024	0.0	10.0	2.49	8.02	0.290	0.040	0.0088		
7	0.049	0.0044	0.031	0.029	0.0	10.0	2.95	7.81	0.210	0.039	0.0097		
8	0.049	0.0044	0.035	0.033	0.0	10.0	3.40	7.65	0.160	0.038	0.0104		
9	0.049	0.0044	0.040	0.038	0.0	10.0	3.85	7.48	0.170	0.038	0.0112		
10	0.049	0.0044	0.044	0.042	0.0	10.0	4.31	7.33	0.150	0.037	0.0118		
11	0.049	0.0044	0.049	0.046	0.0	10.0	4.76	7.29	0.040	0.037	0.0120		
12	0.049	0.0044	0.053	0.051	0.0	10.0	5.21	7.19	0.100	0.036	0.0124		
13	0.049	0.0044	0.058	0.055	0.0	10.0	5.67	7.12	0.070	0.036	0.0128		
											0.114	ft	
											3.46	cm	
											15.8	Final Ht of Slurry	

Table A-34: Calculations of Ultimate Settlement Based on USACE Method for Test C-12.

Layer	Height of Sublayer	Sublayer in Reduced Coordinates	Cumulative Sublayer in Reduced Coordinates	Mid Point of Sublayer in Redu. Coor.	Initial Effective Stress	Initial Void Ratio	Final Effective Stress	Final Void Ratio	Δe∞	Final Height of Layer	Settlement of layer		
i	h_i	l	l	l_m	$\sigma'_{i,o}$	e_{io}	$\sigma'_{i,\infty}$	e_∞		$h_{i,\infty}$	$\delta_{i,\infty}$		
(-)	(ft)	(ft)	(ft)	(ft)	(psf)	(-)	(psf)	(-)		(ft)	(ft)		
1	0.053	0.0048	0.005	0.002	0.0	10.10	0.24	9.50	-	0.050	0.0029		
2	0.053	0.0048	0.010	0.007	0.0	10.1	0.73	8.91	0.590	0.047	0.0057		
3	0.053	0.0048	0.014	0.012	0.0	10.1	1.22	8.30	0.610	0.044	0.0086		
4	0.053	0.0048	0.019	0.017	0.0	10.1	1.70	7.86	0.440	0.042	0.0106		
5	0.053	0.0048	0.024	0.021	0.0	10.1	2.19	7.50	0.360	0.040	0.0124		
6	0.053	0.0048	0.029	0.026	0.0	10.1	2.68	7.18	0.320	0.039	0.0139		
7	0.053	0.0048	0.033	0.031	0.0	10.1	3.16	6.96	0.220	0.038	0.0149		
8	0.053	0.0048	0.038	0.036	0.0	10.1	3.65	6.75	0.210	0.037	0.0159		
9	0.053	0.0048	0.043	0.040	0.0	10.1	4.14	5.59	1.160	0.031	0.0214		
10	0.053	0.0048	0.048	0.045	0.0	10.1	4.62	6.45	-0.860	0.035	0.0174		
11	0.053	0.0048	0.052	0.050	0.0	10.1	5.11	6.39	0.060	0.035	0.0176		
12	0.053	0.0048	0.057	0.055	0.0	10.1	5.60	6.29	0.100	0.035	0.0181		
											0.159	ft	
											4.86	cm	
											14.4	Final Ht of Slurry	

Table A-35: Calculations of Ultimate Settlement Based on USACE Method for Test C-13.

Layer	Height of Sublayer	Sublayer in Reduced Coordinates	Cumulative Sublayer in Reduced Coordinates	Mid Point of Sublayer in Redu. Coor.	Initial Effective Stress	Initial Void Ratio	Final Effective Stress	Final Void Ratio	Δe_∞	Final Height of Layer	Settlement of layer		
i	h_i	l	l	l_m	$\sigma'_{i,o}$	e_{io}	$\sigma'_{i,\infty}$	e_∞		$h_{i,\infty}$	$\delta_{i,\infty}$		
(-)	(ft)	(ft)	(ft)	(ft)	(psf)	(-)	(psf)	(-)		(ft)	(ft)		
1	0.053	0.0048	0.005	0.002	0.0	10.10	0.24	9.09	-	0.048	0.0048		
2	0.053	0.0048	0.010	0.007	0.0	10.1	0.73	8.55	0.540	0.046	0.0074		
3	0.053	0.0048	0.014	0.012	0.0	10.1	1.22	7.95	0.600	0.043	0.0103		
4	0.053	0.0048	0.019	0.017	0.0	10.1	1.71	7.53	0.420	0.041	0.0123		
5	0.053	0.0048	0.024	0.022	0.0	10.1	2.20	7.17	0.360	0.039	0.0140		
6	0.053	0.0048	0.029	0.026	0.0	10.1	2.69	6.90	0.270	0.038	0.0153		
7	0.053	0.0048	0.033	0.031	0.0	10.1	3.18	6.66	0.240	0.037	0.0164		
8	0.053	0.0048	0.038	0.036	0.0	10.1	3.67	6.48	0.180	0.036	0.0173		
9	0.053	0.0048	0.043	0.041	0.0	10.1	4.16	6.31	0.170	0.035	0.0181		
10	0.053	0.0048	0.048	0.045	0.0	10.1	4.65	6.19	0.120	0.034	0.0187		
11	0.053	0.0048	0.053	0.050	0.0	10.1	5.14	6.10	0.090	0.034	0.0191		
12	0.053	0.0048	0.057	0.055	0.0	10.1	5.63	6.00	0.100	0.033	0.0196		
											0.173	ft	
											5.28	cm	
											14.1	Final Ht of Slurry	

Table A-36: Calculations of Ultimate Settlement Based on USACE Method for Test C-14.

Layer	Height of Sublayer	Sublayer in Reduced Coordinates	Cumulative Sublayer in Reduced Coordinates	Mid Point of Sublayer in Redu. Coor.	Initial Effective Stress	Initial Void Ratio	Final Effective Stress	Final Void Ratio	Δe_∞	Final Height of Layer	Settlement of layer		
i	h_i	l	l	l_m	$\sigma'_{i,o}$	e_{io}	$\sigma'_{i,\infty}$	e_∞		$h_{i,\infty}$	$\delta_{i,\infty}$		
(-)	(ft)	(ft)	(ft)	(ft)	(psf)	(-)	(psf)	(-)		(ft)	(ft)		
1	0.052	0.0047	0.005	0.002	0.0	10.10	0.24	8.80	-	0.046	0.0061		
2	0.052	0.0047	0.009	0.007	0.0	10.1	0.72	8.39	0.410	0.044	0.0080		
3	0.052	0.0047	0.014	0.012	0.0	10.1	1.20	7.79	0.600	0.041	0.0109		
4	0.052	0.0047	0.019	0.016	0.0	10.1	1.69	7.38	0.410	0.039	0.0128		
5	0.052	0.0047	0.024	0.021	0.0	10.1	2.17	7.04	0.340	0.038	0.0144		
6	0.052	0.0047	0.028	0.026	0.0	10.1	2.65	6.71	0.330	0.036	0.0159		
7	0.052	0.0047	0.033	0.031	0.0	10.1	3.13	6.50	0.210	0.035	0.0169		
8	0.052	0.0047	0.038	0.035	0.0	10.1	3.61	6.31	0.190	0.034	0.0178		
9	0.052	0.0047	0.042	0.040	0.0	10.1	4.09	6.18	0.130	0.034	0.0184		
10	0.052	0.0047	0.047	0.045	0.0	10.1	4.58	6.08	0.100	0.033	0.0189		
11	0.052	0.0047	0.052	0.049	0.0	10.1	5.06	5.95	0.130	0.033	0.0195		
12	0.052	0.0047	0.056	0.054	0.0	10.1	5.54	5.89	0.060	0.032	0.0198		
											0.180	ft	
											5.47	cm	
											13.6	Final Ht of Slurry	